Title
Mechanisms Underlying Disorders of Consciousness: Insights from Anatomical Connectivity

Author
Zheng, Zhong Sheng

Publication Date
2018

Peer reviewed|Thesis/dissertation

UNIVERSITY OF CALIFORNIA

Los Angeles

Mechanisms Underlying Disorders of Consciousness:

Insights from Anatomical Connectivity

A dissertation submitted in partial satisfaction of the requirements

for the degree of Doctor of Philosophy in Psychology

by

Zhong Sheng Zheng

2018

ABSTRACT OF THE DISSERTATION

Mechanisms Underlying Disorders of Consciousness:

Insights from Anatomical Connectivity

by

Zhong Sheng Zheng

Doctor of Philosophy in Psychology

University of California, Los Angeles, 2018

Professor Martin M. Monti, Chair

Disorders of consciousness (DOC) resulting from severe brain injury that disrupt arousal and awareness systems (main components of consciousness) bear one of the most complex patterns of neuropathology, often widespread and variable across patients. This makes it difficult to both unveil the mechanisms contributing to the pathological states of consciousness and develop reliable biomarkers to assist in the accurate diagnosis of patients with varying levels of residual awareness. To better address these issues, I present four studies aiming at elucidating the mechanisms underlying DOC using diffusing imaging techniques to assess anatomical connectivity in

patient and healthy populations. Study 1 examines the relationship between thalamo-cortical connectivity and variations in consciousness impairment. Study 2 replicates and expands upon Study 1 in a separate, larger cohort of patients, while additionally investigating thalamo-basal ganglia connectivity. Findings that replicated included a general pattern of decreased thalamo-prefrontal and increased thalamo-occipital connectivities in patients on the lower end of the consciousness spectrum compared to the higher end. The thalamo-prefrontal system is critical for maintaining conscious behavior and consistently implicated in DOC. The paradoxical increase in thalamo-occipital connectivity presents a novel finding and could underlie the brain's compensatory mechanism counteracting the loss of activity in more severely injured higher-order fronto-parietal-temporal cortices. Moreover, to enhance diagnostic accuracy, multivariate classifications were also carried out in both studies to identify neural markers that successfully distinguished among the patients. Study 3 and 4 focus on uncovering the multifaceted roles of an underappreciate structure, the external globus pallidus (GPe), and discuss its potential influence in the context of DOC. We found GPe to contain limbic, associative, and sensorimotor territories and direct prefrontal and thalamic connections, potential routes for impacting arousal and awareness. Addressing the limitations of the most widely accepted model, *The Mesocircuit Hypothesis*, in explaining the mechanisms underlying DOC, I propose a new working model with incorporation of GPe to help disentangle the pallidal circuits that differentially contribute to aspects of consciousness and motor behavior. These studies provide vital insights into the mechanisms associated with loss and recovery of consciousness, and may also facilitate important clinical and ethical implications.

The dissertation of Zhong Sheng Zheng is approved.

Nader Pouratian

Jesse A. Rissman

Adriana Galván

Martin M. Monti, Committee Chair

University of California, Los Angeles

2018

DEDICATION

To all those conscious and unconscious who have in one way or another contributed to this research.

TABLE OF CONTENTS

LIST OF FIGURES

LIST OF TABLES

ACKNOWLEDGMENTS

No research is done in isolation. I owe an enormous debt of gratitude to those who have empowered me to complete the work in this dissertation, including collaborators, committee members, and friends and family. In particular, I would like to thank my previous mentor, Nader Pouratian, for shaping me into a persevering scientist, my current mentor, Martin Monti, for the enthusiasm, encouragement, and support he has continually shown throughout my graduate career, and my husband and collaborator, Nicco Reggente, for inspiring me to step out of my comfort zone to engage in new experiences and broaden my perspectives.

Support from the following funding sources has enabled me to dedicate more time to my graduate research: National Science Foundation Graduate Research Fellowship, Dissertation Year Fellowship, Dean's Scholarship, Distinguished University Fellowship, Liu Yunghuo Bei-Qiu Memorial Fund, and Mautner Fellowship.

Valuable patient data were provided by our collaborators at University of Western Ontario and University of Liege, which contributed to studies 1 and 2, respectively. Healthy volunteer data used in studies 3 and 4 were obtained from the Human Connectome Project WU-Minn Consortium.

VITA

Education

2012−2016 **University of California, Los Angeles, CA | UCLA**

Ph.D. Candidate in Psychology—Cognitive Neuroscience

M.A. in Psychology—Cognitive Neuroscience

2005−2009 **Indiana University, Bloomington, IN | IUB**

B.S. in Psychology | Certificate in Neuroscience

Minors in Biology and Latin

Awards and Certifications

2016−2017 Dissertation Year Fellowship | Psychology, UCLA

Liu Yunghuo Bei-Qiu Memorial Fellowship | Psychology, UCLA

Mautner Fellowship | Life Sciences, UCLA

2014−2015 Neuroimaging Training Program | National Institute of Health

2013−2016 Graduate Research Fellowship | National Science Foundation

2012−2014 Dean's Scholarship | Psychology, UCLA

2012−2013 Distinguished University Fellowship | Psychology, UCLA

Teaching Experience

2017-2018, 2015 Teaching Assistant/Associate

Publications

Reggente, N., Cohen, M.S., **Zheng, Z**., Castel, A.D., Knowlton, B.J., Rissman, J. (2018). Memory recall for high reward value items correlates with individual differences in white matter pathways associated with reward processing and fronto-temporal communication. *In press at Frontiers in Human Neuroscience.*

Zheng Z., Reggente N., Lutkenhoff E., Owen A., Monti M. (2017). Disentangling disorders of consciousness: Insights from diffusion tensor imaging and machine learning. *Human Brain Mapping*. 38(1):431-443.

Zheng Z., Shemmassian S., Wijekoon C., Kim W., Bookheimer S., Pouratian N. (2014). DTI correlates of distinct cognitive impairments in Parkinson's disease. *Human Brain Mapping*. 35(4):1325-33.

Pouratian N., **Zheng Z**., Bari A., Behnke E., Elias J., DeSalles A. (2011). Multi-institutional evaluation of deep-brain stimulation targeting using probabilistic connectivity-based thalamic segmentation, *Journal of Neurosurgery*. 115(5):995-1004.

Elias J., **Zheng Z**., Domer P., Quigg M., Pouratian N. (2011). Validation of connectivity-based thalamic segmentation with direct electrophysiologic recordings from human thalamus, *Neuroimage*. 59(3), 2025-34.

Clelland C.D., **Zheng Z.**, Kim W., Pouratian N. (2014). Common cerebral networks associated with distinct deep brain stimulation targets for cluster headache. *Cephalalgia*. 34:224-30.

Bari A., **Zheng Z.**, DeSalles A., Pouratian N. 181 In---Vivo Segmentation of the Human Nucleus Accumbens Using Diffusion Tensor Imaging and Probabilistic Tractography. Neurosurgery. 71 (2), E570-E571.

Pouratian N., Genco A., Zemanyan A**., Zheng Z.**, DeSalles A., Dinov, I. Automated and reliable tractography-based thalamic segmentation for DBS surgery. *Journal of Neurosurgery.* 117 (2), A413-A413

Publications in Prep

Zheng Z., & Monti, M. Connectivity-based segmentation of the human external globus pallidus with high angular resolution diffusion imaging. *In prep*.

Zheng Z., & Monti, M. Characterization of direct pallidofugal connections with cortex and thalamus in humans. *In prep*.

Zheng Z., Reggente, N., Annen, J., Dell'Italia, J., Laureys, S., Monti, M. Generalizing findings using diffusion tensor imaging based methods to disentangle disorders of consciousness. *In prep*.

Background

Disorders of Consciousness

Consciousness in clinical neurology is defined by two main components: wakefulness/arousal (the level of consciousness) and awareness of the self or environment (the contents of consciousness) (Laureys, 2005). Individuals suffering from disorders of consciousness (DOC), either due to traumatic or non-traumatic causes (e.g. hypoxic-ischaemic injuries), often experience prolonged disturbances of consciousness after transitioning from a coma (a transient state of eyes-closed unconsciousness) into a vegetative or minimally conscious state (Bernat, 2006). Patients in a vegetative state (VS) are characterized by wakefulness without discernable signs of awareness (Jennett and Plum, 1972). Patients in a minimally conscious state (MCS) are able to show some signs of residual awareness, albeit intermittent (Giacino et al., 2002). Due to the variability of behaviors observed in minimally conscious patients, MCS can be further subdivided into MCS+ (patients exhibiting high-level behavioral responses such as command following, intelligible verbalizations, or yes/no responses) and MCS- (patients exhibiting low-level, non-reflexive responses such as visual pursuit, localization of noxious stimuli, or appropriate contingent behavior to emotional stimuli) (Bruno et al., 2011). Patients exhibiting functional recovery are said to be emerging from MCS (EMCS). DOC can be perceived to exist on a continuum, where patients may or may not transition sequentially through each state of consciousness.

Neuropathology

Traumatic versus non-traumatic Injury

Post-mortem studies revealed differences in pathological patterns between traumatic and non-traumatic origins of DOC. Traumatic brain injury (TBI) often leads to diffuse axonal injury and thalamic damage, followed by ischaemic brain damage and abnormalities in the brainstem (Adams et al., 1999). Diffuse axonal injury, which is caused by the shearing effect of the grey matter and white matter on the axons, produces severed axons that disconnect the thalamus from the cortex and isolate cortical areas from each other (Tong et al., 2004). Additional comorbid brain injuries that include cortical contusions, intracerebral haemorrhages, and raised intracranial pressure are commonly present in patients with severe TBI (Jennett et al., 2001; Kampfl et al., 1998). In general, TBI preferentially damages the white matter more than the gray matter, whereas the opposite pattern is shown in non-traumatic injuries (Kinney and Samuels, 1994). The most prevalent abnormality in patients with hypoxic-ischaemic brain injury was diffuse cortical and severe thalamic damage, with variable abnormalities in the basal ganglia and cerebellum, and minor disruptions in the brainstem (Adams et al., 2000).

Insights from neuroimaging

Positron emission tomography (PET). Although DOC shows variable clinical and neuropathological presentations, a global down-regulation and bilateral reductions in metabolism of the thalamus and frontoparietal network remain consistent findings. Seminal PET studies in VS patients have identified functional disconnections in long-range cortico-cortical (fronto-parietal network) and thalamo-cortical pathways (Laureys

et al., 2000b; Laureys et al., 1999). This could be due to either direct cortical damage or disconnections between the cortex and thalamus. The restoration of consciousness has been associated with the recovery of both fronto-parietal and thalamo-prefrontal networks. Brainstem metabolism appears to be relatively in tact in VS, allowing for arousal and autonomic functions (Laureys, 2009).

Functional magnetic resonance imaging (FMRI). Using resting-state fMRI, Vanhaudenhuyse et al. (2010) demonstrated that the default mode (DMN) network connectivity was decreased in comatose, VS, and MCS patients, in proportion to their degree of consciousness impairment, and primarily affected the precuneus. Reduced functional connectivity, as further research revealed, was not restricted to the DMN. The inter-hemispheric functional connectivity involving regions within the “extrinsic”, or task-positive network (pre- and postcentral gyrus, and intraparietal sulcus), were also shown to be reduced in DOC patients (Ovadia-Caro et al., 2012). Moreover, assessing all ten common resting-state networks originally derived from healthy volunteers in DOC patients, Demertzi et al. (2014), found not only fewer networks of neuronal origin compared to controls, but also reduced connectivity in the DMN, auditory, and the bilateral executive control networks. On the contrary, increased connectivity in deep structures of the limbic system (i.e. the ventral tegmental area, the insula, the orbitofrontal cortex, and the hypothalamus) has been witnessed in patients with DOC (Di Perri et al., 2014). The authors speculated that the hyperconnectivity within the limbic system may reflect the patients’ persistent engagement in self-reinforcing behavior leading to disruptions in connectivity. Moreover, Boly et al. (2009) demonstrated that the lack of functional connectivity between the cortex and thalamus

(i.e. between posterior cingulate/precuneal cortex and medial thalamus) may be sufficient to induce a vegetative state despite relative preservation of cortico-cortical connectivity within DMN. A loss of connectivity marks only one aspect of a multifaceted dysfunction in DOC

Diffusion tensor imaging (DTI). Reduced structural connectivity between the basal ganglia, thalamus, and frontal cortex has been shown in DOC patients (Weng et al., 2017). Similarly, Fernandez-Espejo et al. (2012) revealed that patients showed significant impairments in all of the pathways connecting cortical regions within the DMN, as well as pathway connecting the posterior cingulate cortex/precuneus with the thalamus, relative to healthy volunteers. Moreover, the structural integrity of this pathway as well as that of those connecting the posterior areas of the network, was correlated with the patients' behavioral signs of awareness, being higher in the MCS+, then MCS-, and lowest in VS patients. Evidence of late structural modification has been demonstrated in the white matter encompassing the medial parietal, occipital (MPO) areas in an MCS patient (Voss et al., 2006). Fractional anisotropy (FA) of the MPO was initially higher in this patient than in normal controls but dropped to normal ranges after an 18-month follow-up scan. This region additionally corresponded to increased metabolic activity, leading the authors to interpret these observations as an indication of late axonal regrowth in this region, although increases in FA could also reflect the presence of astrogliosis after injury (Croall et al., 2014).

Regional thalamic contributions

The thalamic intralaminar and midline nuclei, also referred to as the "nonspecific nuclei" of the thalamus due to their widespread projections to the cortex and elsewhere,

are proposed to underlie arousal and awareness systems and damages to these nuclei can result in DOC (Van der Werf et al., 2002). Because of their strong brainstem inputs, the intralaminar and midline nuclei are considered as part of the ascending reticular activating system (ARAS). The activation of these nuclei is associated with higher levels of arousal (Llinas and Pare, 1991) and consequently facilitates cortical activation that leads to greater vigilance and awareness of incoming information.

Studies have shown that specific subnuceli of the thalamus demonstrate greater neuronal loss as a result of global and multifocal cerebral injuries, in particular, the nuclei within the central thalamus (the anterior and posterior intralaminar nuclei and the paralaminar portions of related thalamic association nuclei—median dorsalis, ventral anterior, ventral lateral, and inferior pulvinar) are most typically involved and the degree of neuronal loss observed within these neuronal aggregates correlates with severity (Figure 1) (Maxwell et al., 2004). The nuclei within the central thalamus share specific anatomical and physiological specializations that regulate arousal level, sustained attention, working memory, and motor preparations (Schiff, 2008). Damage to these nuclei bilaterally can lead to global disorders of consciousness (e.g. coma, VS, MCS) (Schiff and Plum, 2000). As shown in Figure 1, in moderately disabled patients following severe TBI, neuronal damage is primarily found within the anterior intralaminar nuclei (central medial, central lateral, and paracentral nuclei). Patients with progressively severe disabilities demonstrate neuronal damage involving more ventral and lateral nuclei of the central thalamus (posterior intralaminar group). These observations are likely a result of the unique geometry of connections of the central thalamus. Neurons in these subnuclei have wide point-to-point connectivity across the cerebral cortex and are

thus likely to integrate neuronal cell death across these large territories (Van der Werf et al., 2002).

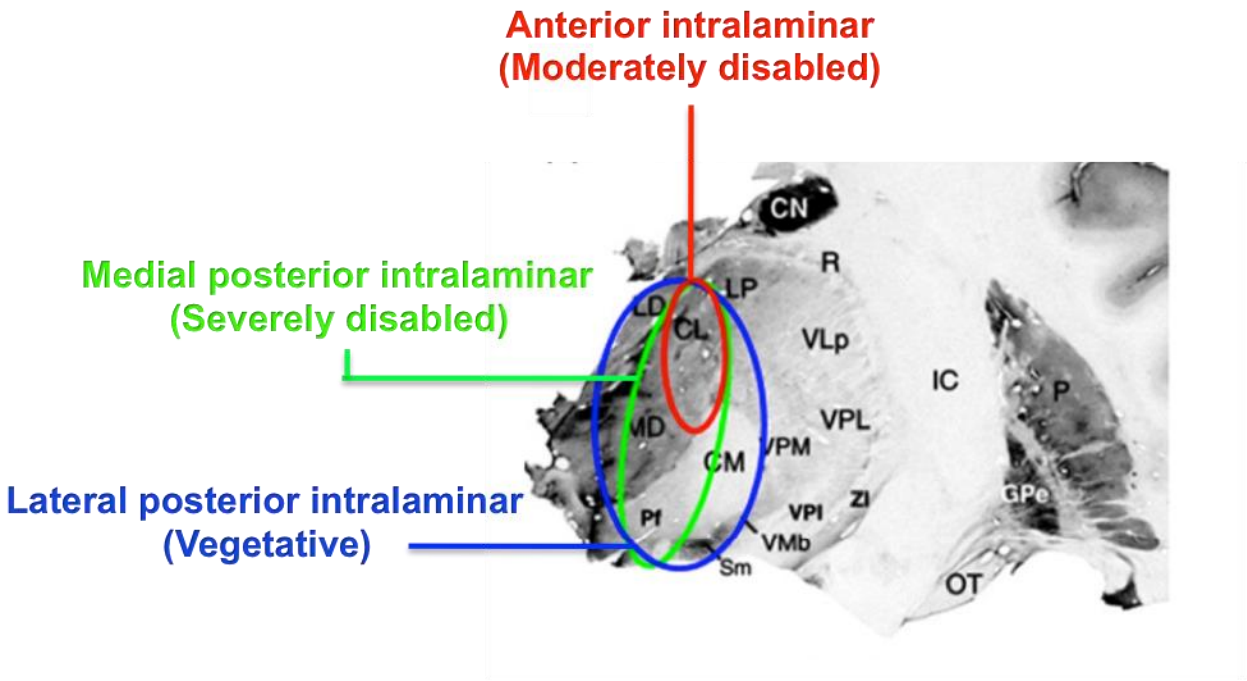

Figure 1. Post-mortem evidence of selective central thalamic damage and severity of outcome

Studies investigating regional volume changes of the thalamus have found the mediodorsal region to be preferentially damaged in DOC. Lower thalamic volume, mainly involving the mediodorsal nucleus and the internal medullar lamina, was significantly correlated with worse Disability Rating Scale scores (Fernandez-Espejo et al., 2010). Likewise, Lutkenhoff et al. (2013) found significant atrophy in the dorsomedial nucleus as well as the antero-dorsal limbic nuclei from examining secondary damages following TBI over the first six months post injury. The degree of atrophy in these nuclei was predictive of behavioral outcome. Secondary injuries triggered by the initial severe brain injury may still be occurring after the first week and may preferentially target these thalamic nuclei.

Neuropathological differences across subgroups of DOC

Histological evidence has revealed that VS is typically caused by extensive damage to the cortex, thalamus, or white matter tracts connecting the thalamus and the cortex, but that spare the brainstem and hypothalamus (Kinney and Samuels, 1994). MCS, on the other hand, presents less thalamic damage and less diffuse axonal injury (grade II or III diffuse axonal injury with multifocal cortical contusions) (Jennett et al., 2001). FMRI studies with passive auditory and noxious stimulations in VS patients have demonstrated disconnections between primary sensory and higher-order associative cortices, which are thought to be required for conscious perception (Laureys et al., 2000a; Laureys et al., 2002). On the other hand, patients with MCS have shown a partial preservation of the large-scale associative frontoparietal networks (Schiff et al., 2005). Poorer functional connectivity of the DMN using resting state fMRI has been observed in VS patients compared to MCS patients. However, increased connectivity in deep structures of the limbic system has been demonstrated to be more prominent in VS than MCS patients (Di Perri et al., 2014). Moreover, in VS patients, metabolic dysfunction in extrinsic and intrinsic networks as well as thalami were identified, but for MCS, metabolic disruptions are shown mainly for thalami and the internal (but not the external) awareness network, possibly accounting for their residual context-specific responsiveness of these patients to environmental demands (Thibaut et al., 2012). Differences in the cerebral metabolic rate of glucose (CMRglc) between VS and MCS were most pronounced in the frontoparietal cortex, at 42% and 60% of normal (Stender et al., 2014b). In brainstem and thalamus, metabolism declined equally in the two conditions. VS and MCS patients can be distinguished with 82% accuracy based on

cortical metabolism. There is also structural support for the differences between VS and MCS. Using shape analysis of the thalamus, Fernandez-Espejo et al. (2010) found that the DM atrophy was more pronounced in VS than in MCS patients. Using DTI methods, Fernandez-Espejo et al. (2011) have shown that VS and MCS patients can be differentiated based on the integrity of their global thalami and white matter using mean diffusivity (MD) histogram indices. In a later DTI study, Fernandez-Espejo et al. (2012) demonstrated that the diagnostic categories of DOC can be stratified based on fractional anisotropy (FA) measures of white matter tracts connecting specific components of the DMN. More specifically, decreased FA in the white matter tracts connecting the thalamus and the precuneus/posterior cingulate cortex was detected from MCS+ to MCS-. Moreover, functional differences between sub-categories of MCS have also been previously identified. In a PET study conducted by Bruno et al. (2012), reduced cerebral metabolism was found in the left cortical areas of the language network, premotor, and pre- and postcentral cortices for MCS- compared to MCS+ patients.

Differential diagnosis

Behavioral scales

Most diagnostic tools used to categorize different subgroups of DOC rely on repeated evaluations of patient's arousal and behavioral responses to various forms of stimulation. In particular, the integrity of the brainstem pathways (e.g. pupillary responses, ocular movements, oculovestibular reflexes, breathing patterns) and the presence of higher-level cortical functions (e.g. purposeful, intentional behavioral in response to internal or external stimuli) are the main areas of focus (Giacino et al.,

2009). Some commonly used behavioral scales include the Glasgow Coma Scale (GCS), which assesses eye opening, verbal, and motor responses, with a range of 1 to 15 on the level of consciousness (higher numbers indicate greater alertness) (Teasdale and Jennett, 1974), and the Coma Recovery Scale-Revised (CRS-R), which spans six subscales addressing auditory, visual, motor, oromotor, communication, and arousal functions with subscale items hierarchically arranged, corresponding to brainstem, subcortical, and cortically mediated functions (Giacino et al., 2004). The CRS-R now serves as the gold standard in differentiating between VS and MCS patients.

Misdiagnosis

DOC can result from focal brain injuries that produce widespread functional changes, or from more-global injuries. Because of such heterogeneous brain pathology associated with DOC, there currently exists no reliable neuroanatomical marker that aids in differentiating VS and MCS patients. Thus, diagnostic distinctions are based solely on behavioral criteria. However, a number of confounding factors, including sensorimotor impairments, arousal fluctuations, inconsistency in responses, difficulty in distinguishing intentional behavior from non-intentional movement, and medication side effects, challenge the accuracy and reliability of only using behavioral assessments to infer consciousness (Giacino et al., 2009). As a consequence of such limited diagnostic procedures, MCS patients have been frequently misdiagnosed as being in VS with rates of up to 40% (Andrews, 1996; Childs and Mercer, 1996; Schnakers et al., 2009). The accurate differential diagnosis of patients suffering from DOC, particularly at the boundary between unconsciousness and (minimal) consciousness, is clinically paramount, and can bear important care-taking and ethical consequences.

Neuroimaging approaches to diagnosis

In recent years, attempts at improving diagnostic accuracy have led to the development of various functional neuroimaging tools capable of assessing residual consciousness and have even allowed rudimentary communication in behaviorally unresponsive patients. However, in spite of these advances, neuroimaging protocols are not currently incorporated in the standard diagnostic routine. The protocols have included passive paradigms (presentation of speech or complex visual stimuli) or active paradigms (mental imagery tasks such motor imagery or spatial navigation) aimed at detecting covert consciousness (Coleman et al., 2009). Although neuroimaging and behavioral assessments are often in agreement, incongruities do sometimes exist. For example, in some patients diagnosed as VS, residual cognitive processing has been captured by functional magnetic resonance imaging (fMRI) in multiple domains, including language, auditory, motor, visuospatial, and visual processing (Bekinschtein et al., 2011; Boly et al., 2007; Coleman et al., 2007; Monti et al., 2013; Monti et al., 2010b). This evidence suggests that these patients were, in fact, at least minimally aware. In a recent clinical validation study, PET and active fMRI paradigms were evaluated for diagnostic accuracy and congruence with behavioral scores (Stender et al., 2014a). PET was found to be more accurate than active fMRI for differential diagnosis. Moreover, electroencephalography (EEG) based assessments have also demonstrated the potential in improving diagnostic accuracy. Due to its portability and inexpensiveness, EEG assessments of awareness may possess higher clinical viability than fMRI (Cruse et al., 2012).

Treatment interventions

Therapeutic interventions are developed to promote restoration of communication and self-care in individuals recovering from severe brain injury. Rehabilitative treatments using behavioral, pharmacological, or neuromodulatory strategies aim at enhancing attention and drive networks mediated by dopamine and other neurotransmitters (Giacino et al., 2013). The effects of these interventions help shed light on the neuropathological bases of DOC. However, due to the difficulty in conducting well-controlled treatment studies in large sample sizes in these patient populations, most of the published research on treatment effectiveness consists of uncontrolled case studies and thus, the effectiveness of these treatments remains inconclusive.

Sensorimotor regulation

Controlling the exposure of sensory input or reducing abnormal motor output are sensorimotor regulations aimed at facilitating recovery. Repeated multisensory stimulation with common, daily stimuli is frequently implemented to prevent sensory deprivation and improve sensory function (Abbate et al., 2014). The intensity and frequency of the sensory stimulation will be adjusted according to each patient's own thresholds to restore normal baseline levels. Motor based interventions such as range of motion exercises, splinting, and casting help prevent or recuperate neuromuscular problems from severe brain injury (Giacino et al., 2013).

Neuromodulation

Pharmacological treatments and brain stimulation methods are examples of neuromodulatory interventions (Figure 2) aiming at reestablishing normal neurophysiological functions following acquired brain injury. Multiple sites of action including the cortex, central thalamus, striatum, and globus pallidus may be targeted by these interventions.

Pharmacological interventions. Pharmacological drugs are utilized to enhance arousal, facilitate behavioral initiation, stimulate speech, and lower agitation in DOC patients. Dopamine agonists are the most commonly used, which may directly increase the level of dopamine within the central thalamus, and thereby increase its output and generate more cortical activity (Fridman et al., 2009; Schiff, 2012). Another site of action for dopamine agonists may be the striatum, which may counterbalance the observed deficits in the direct and indirect pathways (through D1 and D2, respectively), resulting in a net reduction of the inhibitory input to the central thalamus (Gerfen and Surmeier, 2011). Finally, the third site of action could involve direct stimulation of D1-postsynaptic receptors to i inhibit GABAergic pallidothalamic neurons (Mabrouk et al., 2011) Paradoxically, administration of GABA agonists, such as zolpidem, which directly target GABAergic-Aα-1 receptors abundantly located within the globus pallidus, may decrease pallidothalamic inhibition (Brown et al., 2010; Schiff, 2010) and consequently increase cortical activity (Brefel-Courbon et al., 2007).

Brain stimulation. Brain stimulation strategies are directed at activating cortical structures that have become downregulated as the result of mesodiencephalic dysfunction. Deep brain stimulation (DBS) applied to the central thalamus and midbrain reticular formation in VS patients has yielded improvements in eye opening, emotional

expressiveness, command following, communication, and limb movement (Kanno et al., 1987; Yamamoto et al., 2005) in association with EEG desynchronization and marked increases in regional cerebral blood flow and metabolic markers. These effects have been reported in both VS and MCS patients arising from both traumatic and nontraumatic etiologies (Kanno et al., 2009; Schiff et al., 2007). Repetitive transcranial magnetic stimulation (rTMS) has also demonstrated functional improvements in a VS (Louise-Bender Pape et al., 2009) and MCS case (Piccione et al., 2011). More recently, a study using transcranial direct current stimulation (tDCS) applied to the dorsolateral prefrontal cortex found increases in CRS-R scores in MCS patients after a short-duration of tDCS (Thibaut et al., 2014).

Mesocircuit hypothesis

A mesocircuit-level hypothesis, which incorporates basal ganglia structures (striatum and globus pallidus internus, GPi), thalamus, and cortex, has been proposed to account for the mechanisms associated with loss and recovery of consciousness in severe brain injury. The mesocircuit model (Figure 2) posits that the anterior forebrain is particularly vulnerable after multi-focal injuries that lead to widespread deafferentation or neuronal death (Schiff, 2010). Given that the central thalamus is preferentially damaged in DOC, reductions of excitatory outflow of corticostriatal, thalamocortical, and thalamostriatal circuits would follow. This causes a reduction of afferent inputs to the medium spiny neurons (MSNs) of the striatum. With reduced input, these MSNs cannot reach their firing threshold and would fail to inhibit the GPi, which then tonically inhibits the thalamus, resulting in reduced cortical activity.

Therapeutic interventions manipulating the mesocircuit have revealed functional improvements in patients. As mentioned in the previous section and shown in Figure 2, these include using dopamine agonists to target the fronto-striatal-thalamic regions, GABA agonists to target the globus pallidus, DBS to target the central thalamus, and TMS/tDCs to target the frontal cortex.

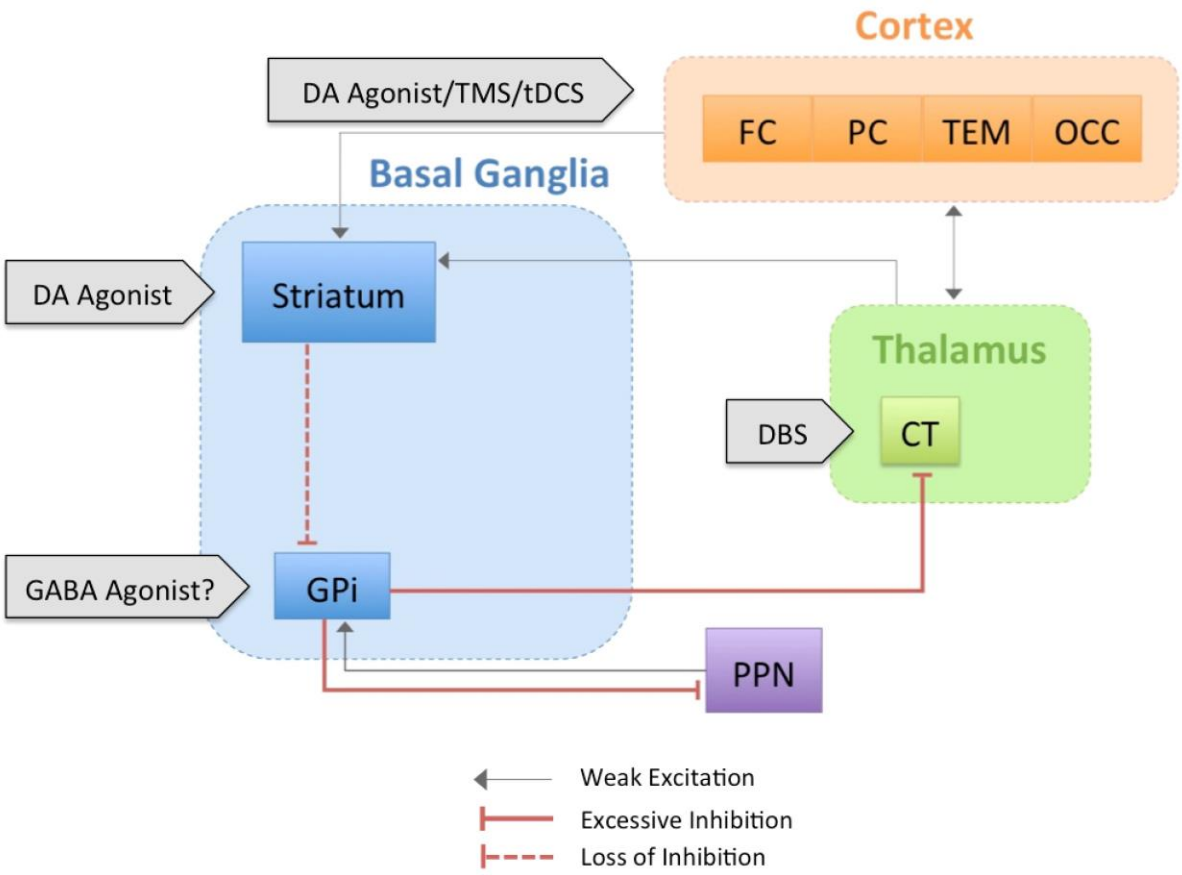

Figure 2. The mesocircuit model. Gray boxes indicate cases of successful treatment interventions targeting specific structures of the circuit. CT = Central Thalamus; PPN = Pedunculopontine Nucleus; FC = Frontal Cortex; PC = Parietal Cortex; TEM = Temporal Cortex; OCC = Occipital Cortex.

Moreover, several studies directly investigating the mesocircuit model have also demonstrated evidence in support of this hypothesis. Using PET, Fridman et al. (2014) found reduced metabolism in ventral and association portions of the striatum and

central thalamus yet increased globus pallidus (GPi and GPe were not differentiated) metabolism in DOC patients. A more recent study examining the integrity of white matter tracts between nodes of the mesocircuit and default mode network revealed impairments in subcortical-cortical and cortical-cortical tracts in DOC patients, but not in subcortical-subcortical tracts (Lant et al., 2016). Moreover, all tracts connecting with the precuneus appeared to be damaged.

External Globus Pallidus

The mesocircuit model depicts an oversimplified involvement of the basal ganglia (BG) structures, where only the striatum and GPi are illustrated. From the perspective of structural connectivity, a large amount of cortical outputs reach the striatum (striatum also receives inputs from the thalamus), in which the striatum then projects to either the GPi or GPe through the direct or indirect pathway, respectively (Purves, 2001). Activation of the direct pathway facilitates movement, whereas activation of the indirect pathway inhibits movement. GPe and GPi, though exerting opposing effects, together make up the globus pallidus, which is an immediate recipient of the inhibitory striatal medium spiny neuronal projections. While much attention has been given to the role of GPi in the framework of the mesocircuit mechanisms, there is no acknowledgement of the potential contribution of the GPe, which leaves some fundamental questions unanswered.

GPe is traditionally regarded as a homogenous relay structure of the motor-suppressing indirect pathway of the basal ganglia, where it connects with the striatum subthalamic nucleus (STN), and GPi. However, this structure is now recognized to contain distinct anatomical subdomains with different projection patterns and is involved

in both motor and nonmotor functions (Gittis et al., 2014). Much like the rest of the BG, a sensorimotor (posterior ventrolateral), associative (anterodorsal/middle), and limbic (anterior, ventral) zone have been verified within the GPe based on non-human primates (Grabli et al., 2004). Moreover, these behaviorally distinct territories of GPe are associated with different cortical areas. However, according to our knowledge, cortically defined subdivisions of the GPe have not been confirmed in humans.

Aside from its participation in sensorimotor, associative, and limbic functions as part of the cortico-basal-ganglia loops, GPe has also been found to contain direct frontal (Saunders et al., 2015; Vetrivelan et al., 2010) and thalamic (Gittis et al., 2014; Mastro et al., 2014) projections, bypassing other basal ganglia structures. Direct GABAergic GPe projections to the frontal cortex has been proposed to be involved in promoting sleep (Vetrivelan et al., 2010), whereas the role of direct GPe projections to the parafasicular nucleus (PF) of the thalamus has not been explicitly identified. The dense projections of the GPe neurons to the PF may suggest that they are an important component of the non-motor output pathways of the GPe, though they may also play a role in motor control based on findings that DBS of the PF has resulted in reduction of motor tremors in patients with movement disorders (Goff et al., 2009).

Diffusion Magnetic Resonance Imaging

Diffusion magnetic resonance imaging (MRI) is currently the only non-invasive tool for assessing tissue microstructure and structural connectivity. It has gained tremendous popularity over the last decade in the study of the healthy and diseased. Diffusion MRI measures the Brownian motion of water molecules restricted by the presence of molecular barriers (e.g. cell membranes, myelin, etc.) within biological

tissue (Basser et al., 1996). Following the path of least resistance, diffusion in the direction parallel to axonal fibers is faster than in the perpendicular direction, therefore giving rise to higher anisotropy in white matter.

Diffusion tensor imaging

Diffusion tensor imaging (DTI) is one of the most widely used and popular forms of diffusion MRI. It is frequently used in the clinical setting due to its feasibility and short scan duration. DTI requires the acquisition of a minimum of 6 directions, though more directions are recommended for quantitative assessment, and a b-value of around 1000 s/mm^{-2} (Jones et al., 2013). At this relatively low b-value, very little signal loss is witnessed. However, the tensor model is limited in its ability to accurately resolve intra-voxel inhomogeneity, such as crossing fibers.

High angular resolution diffusion imaging

To overcome the limitations of DTI, high angular resolution diffusion imaging (HARDI) has been introduced to allow for the discrimination of multiple fiber orientations within the same voxel (Berman et al., 2013). While HARDI offers a more accurate representation of the water diffusion, it requires more than 50 gradient directions at a high b-value (3000 $s\ mm^{-2}$) to be collected, which can be time consuming and susceptible to signal loss and decreased signal-to-noise ratio.

Tractography

Fiber tracking or tractography allows the reconstruction of white matter pathways between regions of interest and quantification of connection strength (e.g. streamline counts). Tracking can be performed either with deterministic (following the principal

eigenvector from voxel to voxel to delineate streamlines) (Yeh et al., 2013) or probabilistic (accounting for uncertainties associated with the principal eigenvector caused by a potential mix of multi-fiber orientation and noise) algorithms (Behrens et al., 2003). Probabilistic approaches offer an advantage over the deterministic method in that it allows tracking into regions with lower diffusion, such as in the gray matter. This is particularly useful for exploratory tractography in identifying non-major pathways. However, one of the main limitations of tractography is that it cannot differentiate between afferent and efferent pathways.

Overview of Studies

Study 1. We employed probabilistic tractography in a sample of 25 DOC patients to assess whether structural connectivity in various thalamo-cortical circuits could differentiate between VS, MCS-, and MCS+ patients. At the univariate level, we found that VS patients displayed reduced connectivity in most thalamo-cortical circuits of interest, including frontal, temporal, and sensorimotor connections, as compared to MCS+, but showed more pulvinar-occipital connections when compared to MCS-. Moreover, MCS- exhibited significantly less thalamo-premotor and thalamo-temporal connectivity than MCS+. At the multivariate level, we found that thalamic tracks reaching distributed cortical regions could discriminate, up to 100% accuracy, across each pairwise group comparison. Together, these findings highlight the role of thalamo-cortical connections in patients' behavioral profile and level of consciousness. Diffusion tensor imaging combined with machine learning algorithms could thus potentially facilitate diagnostic distinctions in DOC and shed light on the neural correlates of consciousness**.**

Study 2. Replicating and building upon Study 1, Study 2 implemented similar methodologies to address thalamofugal connectivity differences across a larger sample (n = 66) of DOC patients, including EMC patients. Greater connectivity between the thalamus and prefrontal cortex were observed in MCS- and EMCS when compared to VS, where EMCS additionally showed higher striatal and somatosensory connections with thalamus. However, when EMCS was compared to MCS- and MCS+, reduced connectivity was detected in the thalamo-occipital circuit. While greater thalamic connectivity, particularly with respect to increasing prefrontal activity, either directly (thalamo-prefrontal) or indirectly (thalamo-striatal), is proposed to underlie important aspects of consciousness, reduced thalamo-occipital connectivity as seen paradoxically in patients on the higher consciousness spectrum compared to the lower end may reflect the brain's compensatory mechanism in patients with more extensive damage to higher-order cortices, such as fronto-parietal-temporal regions, comparatively.

Study 3 and 4. These studies were dedicated to increasing our understanding of an underappreciated, yet multifaceted structure that could contribute to the mechanisms of loss and recovery of consciousness—GPe. We used 50 healthy volunteers' HARDI data available through the Human Connectome Project to characterize GPe's connectivity patterns and subregional makeup. Prior research on GPe was largely conducted in animals, leaving much to be confirmed in humans. Through probabilistic tractography, we first revealed that GPe can be subdivided into an anteroventral, anterodorsal, and posterior territory corresponding to limbic, associative, and sensorimotor functions, respectively, albeit with some overlap presumed to be areas of integration. We then attempted to verify the existence of "direct" GPe connections with

cortex and thalamus using GPi as a control. Our results not only confirmed the existence of these GPe connections in humans, but also unveiled dissociating patterns of prefrontal and thalamic connectivity between GPe and GPi. While GPe showed connections with the entire prefrontal cortex and medial aspects of the thalamus known to contain nuclei that are preferentially damaged in DOC, GPi selectively connected with more motor-related frontal and thalamic structures. These findings of the GPe help to better address a downregulated anterior forebrain activity following severe brain injury and a paradoxical increase in arousal after administration of zolpidem. An update to the existing mesocircuit model with the incorporation of the GPe and its influential connections is therefore proposed.

References

Adams, J.H., Graham, D.I., Jennett, B. (2000) The neuropathology of the vegetative state after an acute brain insult. Brain : a journal of neurology, 123 (Pt 7):1327-38.

Adams, J.H., Jennett, B., McLellan, D.R., Murray, L.S., Graham, D.I. (1999) The neuropathology of the vegetative state after head injury. Journal of clinical pathology, 52:804-6.

Alexander, G.E., DeLong, M.R., Strick, P.L. (1986) Parallel organization of functionally segregated circuits linking basal ganglia and cortex. Annual review of neuroscience, 9:357-81.

Andrews, K. (1996) International Working Party on the Management of the Vegetative State: summary report. Brain injury : [BI], 10:797-806.

Avants, B.B., Tustison, N.J., Song, G., Cook, P.A., Klein, A., Gee, J.C. (2011) A reproducible evaluation of ANTs similarity metric performance in brain image registration. NeuroImage, 54:2033-44.

Basser, R.L., Rasko, J.E., Clarke, K., Cebon, J., Green, M.D., Hussein, S., Alt, C., Menchaca, D., Tomita, D., Marty, J., Fox, R.M., Begley, C.G. (1996) Thrombopoietic effects of pegylated recombinant human megakaryocyte growth and development factor (PEG-rHuMGDF) in patients with advanced cancer. Lancet, 348:1279-81.

Behrens, T.E., Johansen-Berg, H., Woolrich, M.W., Smith, S.M., Wheeler-Kingshott, C.A., Boulby, P.A., Barker, G.J., Sillery, E.L., Sheehan, K., Ciccarelli, O., Thompson, A.J., Brady, J.M., Matthews, P.M. (2003) Non-invasive mapping of

connections between human thalamus and cortex using diffusion imaging. Nature neuroscience, 6:750-7.

Bekinschtein, T.A., Manes, F.F., Villarreal, M., Owen, A.M., Della-Maggiore, V. (2011) Functional imaging reveals movement preparatory activity in the vegetative state. Frontiers in human neuroscience, 5:5.

Berman, J.I., Lanza, M.R., Blaskey, L., Edgar, J.C., Roberts, T.P. (2013) High angular resolution diffusion imaging probabilistic tractography of the auditory radiation. AJNR. American journal of neuroradiology, 34:1573-8.

Bernat, J.L. (2006) Chronic disorders of consciousness. Lancet, 367:1181-92.

Boly, M., Coleman, M.R., Davis, M.H., Hampshire, A., Bor, D., Moonen, G., Maquet, P.A., Pickard, J.D., Laureys, S., Owen, A.M. (2007) When thoughts become action: an fMRI paradigm to study volitional brain activity in non-communicative brain injured patients. NeuroImage, 36:979-92.

Boly, M., Tshibanda, L., Vanhaudenhuyse, A., Noirhomme, Q., Schnakers, C., Ledoux, D., Boveroux, P., Garweg, C., Lambermont, B., Phillips, C., Luxen, A., Moonen, G., Bassetti, C., Maquet, P., Laureys, S. (2009) Functional connectivity in the default network during resting state is preserved in a vegetative but not in a brain dead patient. Human brain mapping, 30:2393-400.

Bonelli, R.M., Cummings, J.L. (2007) Frontal-subcortical circuitry and behavior. Dialogues in clinical neuroscience, 9:141-51.

Brefel-Courbon, C., Payoux, P., Ory, F., Sommet, A., Slaoui, T., Raboyeau, G., Lemesle, B., Puel, M., Montastruc, J.L., Demonet, J.F., Cardebat, D. (2007)

Clinical and imaging evidence of zolpidem effect in hypoxic encephalopathy. Annals of neurology, 62:102-5.

Brown, E.N., Lydic, R., Schiff, N.D. (2010) General anesthesia, sleep, and coma. The New England journal of medicine, 363:2638-50.

Bruno, M.A., Majerus, S., Boly, M., Vanhaudenhuyse, A., Schnakers, C., Gosseries, O., Boveroux, P., Kirsch, M., Demertzi, A., Bernard, C., Hustinx, R., Moonen, G., Laureys, S. (2012) Functional neuroanatomy underlying the clinical subcategorization of minimally conscious state patients. Journal of neurology, 259:1087-98.

Bruno, M.A., Vanhaudenhuyse, A., Thibaut, A., Moonen, G., Laureys, S. (2011) From unresponsive wakefulness to minimally conscious PLUS and functional locked-in syndromes: recent advances in our understanding of disorders of consciousness. Journal of neurology, 258:1373-84.

Childs, N.L., Mercer, W.N. (1996) Misdiagnosing the persistent vegetative state. Misdiagnosis certainly occurs. BMJ, 313:944.

Coleman, M.R., Bekinschtein, T., Monti, M.M., Owen, A.M., Pickard, J.D. (2009) A multimodal approach to the assessment of patients with disorders of consciousness. Progress in brain research, 177:231-48.

Coleman, M.R., Rodd, J.M., Davis, M.H., Johnsrude, I.S., Menon, D.K., Pickard, J.D., Owen, A.M. (2007) Do vegetative patients retain aspects of language comprehension? Evidence from fMRI. Brain : a journal of neurology, 130:2494-507.

Cruse, D., Chennu, S., Fernandez-Espejo, D., Payne, W.L., Young, G.B., Owen, A.M. (2012) Detecting awareness in the vegetative state: electroencephalographic evidence for attempted movements to command. PloS one, 7:e49933.

Dehaene, S., Changeux, J.P. (2011) Experimental and theoretical approaches to conscious processing. Neuron, 70:200-27.

Demertzi, A., Gomez, F., Crone, J.S., Vanhaudenhuyse, A., Tshibanda, L., Noirhomme, Q., Thonnard, M., Charland-Verville, V., Kirsch, M., Laureys, S., Soddu, A. (2014) Multiple fMRI system-level baseline connectivity is disrupted in patients with consciousness alterations. Cortex; a journal devoted to the study of the nervous system and behavior, 52:35-46.

Di Perri, C., Stender, J., Laureys, S., Gosseries, O. (2014) Functional neuroanatomy of disorders of consciousness. Epilepsy & behavior : E&B, 30:28-32.

Draganski, B., Kherif, F., Kloppel, S., Cook, P.A., Alexander, D.C., Parker, G.J., Deichmann, R., Ashburner, J., Frackowiak, R.S. (2008) Evidence for segregated and integrative connectivity patterns in the human Basal Ganglia. The Journal of neuroscience : the official journal of the Society for Neuroscience, 28:7143-52.

Feldman, H.M., Yeatman, J.D., Lee, E.S., Barde, L.H., Gaman-Bean, S. (2010) Diffusion tensor imaging: a review for pediatric researchers and clinicians. Journal of developmental and behavioral pediatrics : JDBP, 31:346-56.

Fernandez-Espejo, D., Bekinschtein, T., Monti, M.M., Pickard, J.D., Junque, C., Coleman, M.R., Owen, A.M. (2011) Diffusion weighted imaging distinguishes the vegetative state from the minimally conscious state. NeuroImage, 54:103-12.

Fernandez-Espejo, D., Junque, C., Bernabeu, M., Roig-Rovira, T., Vendrell, P., Mercader, J.M. (2010) Reductions of thalamic volume and regional shape changes in the vegetative and the minimally conscious states. Journal of neurotrauma, 27:1187-93.

Fernandez-Espejo, D., Soddu, A., Cruse, D., Palacios, E.M., Junque, C., Vanhaudenhuyse, A., Rivas, E., Newcombe, V., Menon, D.K., Pickard, J.D., Laureys, S., Owen, A.M. (2012) A role for the default mode network in the bases of disorders of consciousness. Annals of neurology, 72:335-43.

Fridman, E.A., Beattie, B.J., Broft, A., Laureys, S., Schiff, N.D. (2014) Regional cerebral metabolic patterns demonstrate the role of anterior forebrain mesocircuit dysfunction in the severely injured brain. Proceedings of the National Academy of Sciences of the United States of America.

Fridman, E.A., Calvar, J., Bonetto, M., Gamzu, E., Krimchansky, B.Z., Meli, F., Leiguarda, R.C., Zafonte, R. (2009) Fast awakening from minimally conscious state with apomorphine. Brain injury : [BI], 23:172-7.

Gerfen, C.R., Surmeier, D.J. (2011) Modulation of striatal projection systems by dopamine. Annual review of neuroscience, 34:441-66.

Giacino, J.T., Ashwal, S., Childs, N., Cranford, R., Jennett, B., Katz, D.I., Kelly, J.P., Rosenberg, J.H., Whyte, J., Zafonte, R.D., Zasler, N.D. (2002) The minimally conscious state: definition and diagnostic criteria. Neurology, 58:349-53.

Giacino, J.T., Kalmar, K., Whyte, J. (2004) The JFK Coma Recovery Scale-Revised: measurement characteristics and diagnostic utility. Arch Phys Med Rehabil, 85:2020-9.

Giacino, J.T., Katz, D.I., Whyte, J. (2013) Neurorehabilitation in disorders of consciousness. Seminars in neurology, 33:142-56.

Giacino, J.T., Schnakers, C., Rodriguez-Moreno, D., Kalmar, K., Schiff, N., Hirsch, J. (2009) Behavioral assessment in patients with disorders of consciousness: gold standard or fool's gold? Progress in brain research, 177:33-48.

Gittis, A.H., Berke, J.D., Bevan, M.D., Chan, C.S., Mallet, N., Morrow, M.M., Schmidt, R. (2014) New roles for the external globus pallidus in basal ganglia circuits and behavior. The Journal of neuroscience : the official journal of the Society for Neuroscience, 34:15178-83.

Goff, L.K., Jouve, L., Melon, C., Salin, P. (2009) Rationale for targeting the thalamic centre-median parafascicular complex in the surgical treatment of Parkinson's disease. Parkinsonism & related disorders, 15 Suppl 3:S167-70.

Grabli, D., McCairn, K., Hirsch, E.C., Agid, Y., Feger, J., Francois, C., Tremblay, L. (2004) Behavioural disorders induced by external globus pallidus dysfunction in primates: I. Behavioural study. Brain : a journal of neurology, 127:2039-54.

Hagmann, P., Jonasson, L., Maeder, P., Thiran, J.P., Wedeen, V.J., Meuli, R. (2006) Understanding diffusion MR imaging techniques: from scalar diffusion-weighted imaging to diffusion tensor imaging and beyond. Radiographics : a review publication of the Radiological Society of North America, Inc, 26 Suppl 1:S205-23.

Iglesias, J.E., Liu, C.Y., Thompson, P.M., Tu, Z. (2011) Robust brain extraction across datasets and comparison with publicly available methods. IEEE transactions on medical imaging, 30:1617-34.

Jenkinson, M., Bannister, P., Brady, M., Smith, S. (2002) Improved optimization for the robust and accurate linear registration and motion correction of brain images. NeuroImage, 17:825-41.

Jennett, B., Adams, J.H., Murray, L.S., Graham, D.I. (2001) Neuropathology in vegetative and severely disabled patients after head injury. Neurology, 56:486-90.

Jennett, B., Plum, F. (1972) Persistent vegetative state after brain damage. Rn, 35:ICU1-4.

Johansen-Berg, H., Behrens, T.E., Sillery, E., Ciccarelli, O., Thompson, A.J., Smith, S.M., Matthews, P.M. (2005) Functional-anatomical validation and individual variation of diffusion tractography-based segmentation of the human thalamus. Cerebral cortex, 15:31-9.

Jones, D.K., Knosche, T.R., Turner, R. (2013) White matter integrity, fiber count, and other fallacies: the do's and don'ts of diffusion MRI. NeuroImage, 73:239-54.

Kampfl, A., Schmutzhard, E., Franz, G., Pfausler, B., Haring, H.P., Ulmer, H., Felber, S., Golaszewski, S., Aichner, F. (1998) Prediction of recovery from post-traumatic vegetative state with cerebral magnetic-resonance imaging. Lancet, 351:1763-7.

Kanno, T., Kamei, Y., Yokoyama, T., Jain, V.K. (1987) Neurostimulation for patients in vegetative status. Pacing and clinical electrophysiology : PACE, 10:207-8.

Kanno, T., Morita, I., Yamaguchi, S., Yokoyama, T., Kamei, Y., Anil, S.M., Karagiozov, K.L. (2009) Dorsal column stimulation in persistent vegetative state. Neuromodulation : journal of the International Neuromodulation Society, 12:33-8.

Kinney, H.C., Samuels, M.A. (1994) Neuropathology of the persistent vegetative state. A review. Journal of neuropathology and experimental neurology, 53:548-58.

Kriegeskorte, N., Goebel, R., Bandettini, P. (2006) Information-based functional brain mapping. Proceedings of the National Academy of Sciences of the United States of America, 103:3863-8.

Lant, N.D., Gonzalez-Lara, L.E., Owen, A.M., Fernandez-Espejo, D. (2016) Relationship between the anterior forebrain mesocircuit and the default mode network in the structural bases of disorders of consciousness. NeuroImage. Clinical, 10:27-35.

Laureys, S. (2005) The neural correlate of (un)awareness: lessons from the vegetative state. Trends in cognitive sciences, 9:556-9.

Laureys S, B.M., Moonen G, and Maquet P. (2009) Coma. Encyclopedia of Neuroscience, 2:1133-1142.

Laureys, S., Faymonville, M.E., Degueldre, C., Fiore, G.D., Damas, P., Lambermont, B., Janssens, N., Aerts, J., Franck, G., Luxen, A., Moonen, G., Lamy, M., Maquet, P. (2000a) Auditory processing in the vegetative state. Brain : a journal of neurology, 123 (Pt 8):1589-601.

Laureys, S., Faymonville, M.E., Luxen, A., Lamy, M., Franck, G., Maquet, P. (2000b) Restoration of thalamocortical connectivity after recovery from persistent vegetative state. Lancet, 355:1790-1.

Laureys, S., Faymonville, M.E., Peigneux, P., Damas, P., Lambermont, B., Del Fiore, G., Degueldre, C., Aerts, J., Luxen, A., Franck, G., Lamy, M., Moonen, G., Maquet, P. (2002) Cortical processing of noxious somatosensory stimuli in the persistent vegetative state. NeuroImage, 17:732-41.

Laureys, S., Goldman, S., Phillips, C., Van Bogaert, P., Aerts, J., Luxen, A., Franck, G., Maquet, P. (1999) Impaired effective cortical connectivity in vegetative state: preliminary investigation using PET. NeuroImage, 9:377-82.

Llinas, R.R., Pare, D. (1991) Of dreaming and wakefulness. Neuroscience, 44:521-35.

Louise-Bender Pape, T., Rosenow, J., Lewis, G., Ahmed, G., Walker, M., Guernon, A., Roth, H., Patil, V. (2009) Repetitive transcranial magnetic stimulation-associated neurobehavioral gains during coma recovery. Brain stimulation, 2:22-35.

Lutkenhoff, E.S., Chiang, J., Tshibanda, L., Kamau, E., Kirsch, M., Pickard, J.D., Laureys, S., Owen, A.M., Monti, M.M. (2015) Thalamic and extrathalamic mechanisms of consciousness after severe brain injury. Annals of neurology.

Lutkenhoff, E.S., McArthur, D.L., Hua, X., Thompson, P.M., Vespa, P.M., Monti, M.M. (2013) Thalamic atrophy in antero-medial and dorsal nuclei correlates with six-month outcome after severe brain injury. NeuroImage. Clinical, 3:396-404.

Mabrouk, O.S., Li, Q., Song, P., Kennedy, R.T. (2011) Microdialysis and mass spectrometric monitoring of dopamine and enkephalins in the globus pallidus reveal reciprocal interactions that regulate movement. Journal of neurochemistry, 118:24-33.

Mastro, K.J., Bouchard, R.S., Holt, H.A., Gittis, A.H. (2014) Transgenic mouse lines subdivide external segment of the globus pallidus (GPe) neurons and reveal distinct GPe output pathways. The Journal of neuroscience : the official journal of the Society for Neuroscience, 34:2087-99.

Maxwell, W.L., MacKinnon, M.A., Smith, D.H., McIntosh, T.K., Graham, D.I. (2006) Thalamic nuclei after human blunt head injury. Journal of neuropathology and experimental neurology, 65:478-88.

Maxwell, W.L., Pennington, K., MacKinnon, M.A., Smith, D.H., McIntosh, T.K., Wilson, J.T., Graham, D.I. (2004) Differential responses in three thalamic nuclei in moderately disabled, severely disabled and vegetative patients after blunt head injury. Brain : a journal of neurology, 127:2470-8.

Monti, M.M., Laureys, S., Owen, A.M. (2010a) The vegetative state. BMJ, 341:c3765.

Monti, M.M., Pickard, J.D., Owen, A.M. (2013) Visual cognition in disorders of consciousness: from V1 to top-down attention. Human brain mapping, 34:1245-53.

Monti, M.M., Vanhaudenhuyse, A., Coleman, M.R., Boly, M., Pickard, J.D., Tshibanda, L., Owen, A.M., Laureys, S. (2010b) Willful modulation of brain activity in disorders of consciousness. The New England journal of medicine, 362:579-89.

Newcombe, V.F., Williams, G.B., Scoffings, D., Cross, J., Carpenter, T.A., Pickard, J.D., Menon, D.K. (2010) Aetiological differences in neuroanatomy of the vegetative state: insights from diffusion tensor imaging and functional implications. Journal of neurology, neurosurgery, and psychiatry, 81:552-61.

Ovadia-Caro, S., Nir, Y., Soddu, A., Ramot, M., Hesselmann, G., Vanhaudenhuyse, A., Dinstein, I., Tshibanda, J.F., Boly, M., Harel, M., Laureys, S., Malach, R. (2012) Reduction in inter-hemispheric connectivity in disorders of consciousness. PloS one, 7:e37238.

Pereira, F., Mitchell, T., Botvinick, M. (2009) Machine learning classifiers and fMRI: a tutorial overview. NeuroImage, 45:S199-209.

Piccione, F., Cavinato, M., Manganotti, P., Formaggio, E., Storti, S.F., Battistin, L., Cagnin, A., Tonin, P., Dam, M. (2011) Behavioral and neurophysiological effects of repetitive transcranial magnetic stimulation on the minimally conscious state: a case study. Neurorehabilitation and neural repair, 25:98-102.

Purves, D., Augustine, G.J., Fitzpatrick D., et al. (2001) Circuits within the Basal Ganglia System. Sunderland, MA. Sinauer Associates.

Saunders, A., Oldenburg, I.A., Berezovskii, V.K., Johnson, C.A., Kingery, N.D., Elliott, H.L., Xie, T., Gerfen, C.R., Sabatini, B.L. (2015) A direct GABAergic output from the basal ganglia to frontal cortex. Nature, 521:85-9.

Schiff, N.D. (2008) Central thalamic contributions to arousal regulation and neurological disorders of consciousness. Annals of the New York Academy of Sciences, 1129:105-18.

Schiff, N.D. (2010) Recovery of consciousness after brain injury: a mesocircuit hypothesis. Trends in neurosciences, 33:1-9.

Schiff, N.D. (2012) Moving toward a generalizable application of central thalamic deep brain stimulation for support of forebrain arousal regulation in the severely injured brain. Annals of the New York Academy of Sciences, 1265:56-68.

Schiff, N.D., Giacino, J.T., Kalmar, K., Victor, J.D., Baker, K., Gerber, M., Fritz, B., Eisenberg, B., Biondi, T., O'Connor, J., Kobylarz, E.J., Farris, S., Machado, A., McCagg, C., Plum, F., Fins, J.J., Rezai, A.R. (2007) Behavioural improvements with thalamic stimulation after severe traumatic brain injury. Nature, 448:600-3.

Schiff, N.D., Plum, F. (2000) The role of arousal and "gating" systems in the neurology of impaired consciousness. Journal of clinical neurophysiology : official publication of the American Electroencephalographic Society, 17:438-52.

Schiff, N.D., Rodriguez-Moreno, D., Kamal, A., Kim, K.H., Giacino, J.T., Plum, F., Hirsch, J. (2005) fMRI reveals large-scale network activation in minimally conscious patients. Neurology, 64:514-23.

Schnakers, C., Vanhaudenhuyse, A., Giacino, J., Ventura, M., Boly, M., Majerus, S., Moonen, G., Laureys, S. (2009) Diagnostic accuracy of the vegetative and minimally conscious state: clinical consensus versus standardized neurobehavioral assessment. BMC neurology, 9:35.

Smith, S.M. (2002) Fast robust automated brain extraction. Human brain mapping, 17:143-55.

Smith, S.M., Jenkinson, M., Woolrich, M.W., Beckmann, C.F., Behrens, T.E., Johansen-Berg, H., Bannister, P.R., De Luca, M., Drobnjak, I., Flitney, D.E., Niazy, R.K., Saunders, J., Vickers, J., Zhang, Y., De Stefano, N., Brady, J.M., Matthews, P.M. (2004) Advances in functional and structural MR image analysis and implementation as FSL. NeuroImage, 23 Suppl 1:S208-19.

Smith, S.M., Nichols, T.E. (2009) Threshold-free cluster enhancement: addressing problems of smoothing, threshold dependence and localisation in cluster inference. NeuroImage, 44:83-98.

Stender, J., Gosseries, O., Bruno, M.A., Charland-Verville, V., Vanhaudenhuyse, A., Demertzi, A., Chatelle, C., Thonnard, M., Thibaut, A., Heine, L., Soddu, A., Boly, M., Schnakers, C., Gjedde, A., Laureys, S. (2014a) Diagnostic precision of PET

imaging and functional MRI in disorders of consciousness: a clinical validation study. Lancet.

Stender, J., Kupers, R., Rodell, A., Thibaut, A., Chatelle, C., Bruno, M.A., Gejl, M., Bernard, C., Hustinx, R., Laureys, S., Gjedde, A. (2014b) Quantitative rates of brain glucose metabolism distinguish minimally conscious from vegetative state patients. Journal of cerebral blood flow and metabolism : official journal of the International Society of Cerebral Blood Flow and Metabolism.

Teasdale, G., Jennett, B. (1974) Assessment of coma and impaired consciousness. A practical scale. Lancet, 2:81-4.

Thibaut, A., Bruno, M.A., Chatelle, C., Gosseries, O., Vanhaudenhuyse, A., Demertzi, A., Schnakers, C., Thonnard, M., Charland-Verville, V., Bernard, C., Bahri, M., Phillips, C., Boly, M., Hustinx, R., Laureys, S. (2012) Metabolic activity in external and internal awareness networks in severely brain-damaged patients. Journal of rehabilitation medicine : official journal of the UEMS European Board of Physical and Rehabilitation Medicine, 44:487-94.

Thibaut, A., Bruno, M.A., Ledoux, D., Demertzi, A., Laureys, S. (2014) tDCS in patients with disorders of consciousness: Sham-controlled randomized double-blind study. Neurology, 82:1112-8.

Tong, K.A., Ashwal, S., Holshouser, B.A., Nickerson, J.P., Wall, C.J., Shutter, L.A., Osterdock, R.J., Haacke, E.M., Kido, D. (2004) Diffuse axonal injury in children: clinical correlation with hemorrhagic lesions. Annals of neurology, 56:36-50.

Tononi, G. (2012) Integrated information theory of consciousness: an updated account. Archives italiennes de biologie, 150:293-329.

Tremblay, L., Worbe, Y., Thobois, S., Sgambato-Faure, V., Feger, J. (2015) Selective dysfunction of basal ganglia subterritories: From movement to behavioral disorders. Movement disorders : official journal of the Movement Disorder Society, 30:1155-70.

Tsubokawa, T., Yamamoto, T., Katayama, Y., Hirayama, T., Maejima, S., Moriya, T. (1990) Deep-brain stimulation in a persistent vegetative state: follow-up results and criteria for selection of candidates. Brain injury : [BI], 4:315-27.

Van der Werf, Y.D., Witter, M.P., Groenewegen, H.J. (2002) The intralaminar and midline nuclei of the thalamus. Anatomical and functional evidence for participation in processes of arousal and awareness. Brain research. Brain research reviews, 39:107-40.

Vanhaudenhuyse, A., Noirhomme, Q., Tshibanda, L.J., Bruno, M.A., Boveroux, P., Schnakers, C., Soddu, A., Perlbarg, V., Ledoux, D., Brichant, J.F., Moonen, G., Maquet, P., Greicius, M.D., Laureys, S., Boly, M. (2010) Default network connectivity reflects the level of consciousness in non-communicative brain-damaged patients. Brain : a journal of neurology, 133:161-71.

Vetrivelan, R., Qiu, M.H., Chang, C., Lu, J. (2010) Role of Basal Ganglia in sleep-wake regulation: neural circuitry and clinical significance. Frontiers in neuroanatomy, 4:145.

Voss, H.U., Uluc, A.M., Dyke, J.P., Watts, R., Kobylarz, E.J., McCandliss, B.D., Heier, L.A., Beattie, B.J., Hamacher, K.A., Vallabhajosula, S., Goldsmith, S.J., Ballon, D., Giacino, J.T., Schiff, N.D. (2006) Possible axonal regrowth in late recovery

from the minimally conscious state. The Journal of clinical investigation, 116:2005-11.

Yamamoto, T., Katayama, Y. (2005) Deep brain stimulation therapy for the vegetative state. Neuropsychological rehabilitation, 15:406-13.

Yamamoto, T., Kobayashi, K., Kasai, M., Oshima, H., Fukaya, C., Katayama, Y. (2005) DBS therapy for the vegetative state and minimally conscious state. Acta neurochirurgica. Supplement, 93:101-4.

Yeh, F.C., Verstynen, T.D., Wang, Y., Fernandez-Miranda, J.C., Tseng, W.Y. (2013) Deterministic diffusion fiber tracking improved by quantitative anisotropy. PloS one, 8:e80713.

Study 1: Disentangling Disorders of Consciousness: Insights from Diffusion Tensor Imaging and Machine Learning

Introduction

Consciousness in clinical neurology is defined by two main components: wakefulness and awareness (of the self or environment) (Laureys, 2005). Individuals surviving severe brain injury, traumatic (T) or non-traumatic (NT), sometimes fail to fully recover consciousness after the initial state of acute coma, and remain, permanently or transiently, in a condition of disorder of consciousness (DOC) (Monti et al., 2010). Patients in a vegetative state (VS) are characterized by wakefulness in the absence of discernable signs of awareness (Jennett and Plum, 1972). Patients in a minimally conscious state (MCS), on the other hand, demonstrate wakefulness along with some reproducible, yet intermittent, evidence of awareness (Giacino et al., 2002). Due to the wide spectrum of behaviors observed in minimally conscious patients, MCS can be further subdivided into MCS+ (patients exhibiting high-level behavioral responses such as command following, intelligible verbalizations, or yes/no responses) and MCS- (patients exhibiting low-level, non-reflexive responses such as visual pursuit, localization of noxious stimuli, or appropriate contingent behavior to emotional stimuli) (Bruno et al., 2011).

Because of the heterogeneous brain pathology associated with DOC, there currently exists no reliable neuroanatomical marker that aids in differentiating VS and MCS patients. Thus, diagnostic distinctions are based solely on behavioral criteria, which can be prone to misdiagnosis, with rates of up to 40% (Andrews et al., 1996; Childs and Mercer, 1996; Schnakers et al., 2009). The accurate differential diagnosis of

patients suffering from DOC, particularly at the boundary between unconsciousness and (minimal) consciousness, is clinically paramount, and can bear important care-taking and ethical ramifications.

In order to improve differential diagnosis, a better understanding of the underlying pathology is imperative. DOC has been described as a “disconnection syndrome” that can be triggered by several pathological mechanisms. VS is typically caused by extensive damage to the cortex, thalamus, or white matter tracts connecting the thalamus and cortex (Kinney and Samuels, 1994). MCS, on the other hand, presents a similar but less severe extent of damage (Jennett et al., 2001). While a number of brain regions may contribute to the maintenance of consciousness, recent models of loss and recovery of consciousness after severe brain injury stress the “necessary” role of the thalamo-cortical complex (Laureys, 2005; Laureys and Tononi, 2008; Schiff, 2010). Indeed, the degree of thalamic atrophy has been shown to correlate with patients’ behavioral profile (Lutkenhoff et al., 2015) and, in the acute setting, to predict the chances of behavioral recovery (Lutkenhoff et al., 2013). Furthermore, intact thalamo-cortical functional connectivity has been shown to characterize DOC patients able to demonstrate voluntary deployment of top-down auditory attention (Monti et al., 2015), and has also been shown, in a single case report, to be associated with functional recovery from VS (Laureys et al., 2000). Conversely, also in a single case report, it has been shown that, where thalamo-cortical connectivity is impaired, a patient can be in a VS despite preserved cortico-cortical connectivity (Boly et al., 2009). Nonetheless, the relationship between preservation of individual thalamo-cortical circuits and patients’ behavioral presentation and diagnosis remains unclear.

In line with the thalamo-cortical hypothesis of DOC, Fernandez-Espejo et al. (2011) have shown that VS and MCS patients can be distinguished based on the integrity of their global thalami and white matter using mean diffusivity histogram indices from diffusion tensor imaging (DTI). DTI measures the local movement of water molecules throughout the brain in an attempt to elucidate the tissue microstructure and provides a valuable tool for assessing anatomical connectivity in-vivo (Pierpaoli et al., 1996). Although the findings from Fernandez-Espejo et al. (2011) offer indirect support for a differential degree of global thalamo-cortical disconnection between VS and MCS, recent theories focus on the role of specific subdivisions of the thalamus and their corticopetal connections in DOC (Schiff, 2010). It is therefore crucial to identify and distinguish specific contributions of the thalamo-cortical circuits that underlie the different levels of consciousness impairment.

In the present study, we use probabilistic diffusion tractography to evaluate structural connectivity between the thalamus and cortex in VS, MCS-, and MCS+ patients, and to identify connectivity differences that could be used as reliable biomarkers for the stratification of patients with DOC. To achieve this aim, we first employ a univariate analysis approach to determine which thalamic subregion(s), as defined by their pattern of cortical connectivity, differ most significantly between patient groups. Subsequently, we employ a multivariate approach to uncover which regions along the thalamic tracks are maximally informative in distinguishing among patient groups.

Methods

Patient population

The original databank consisted of a convenience sample of 56 severely brain-injured patients who fulfilled the diagnostic criteria for VS (n=22; 13T/9NT), MCS- (n=15; 12T/3NT), and MCS+ (n=19; 13T/6NT) based on the Coma Recovery Scale-Revised (CRS-R) (Giacino et al., 2004). However, 31 patients were excluded either due to excessive motion or extensive structural atrophy that obscured the identification of our regions of interest. This resulted in a sample size of 25 patients (6 females/19 males; mean age 39.5±14.2 years), with 10 VS (4T/6NT), 7 MCS- (6T/1NT), and 8 MCS+ (7T/1NT). Demographic and clinical information for the final dataset are shown in Table 1. This study was approved by the Cambridge Local Ethics Committee, and informed consent was signed by patients' legal surrogate. Data were collected between 2006 and 2011, when A.M.O. and M.M.M. were affiliated with the MRC Cognition and Brain Sciences Unit and the Wolfson Brain Imaging Centre. A portion of this patient cohort has been described in previous neuroimaging studies that employed different analysis techniques (Fernandez-Espejo et al., 2011; Newcombe et al., 2010).

MRI acquisition

All imaging data were collected on a 3T Siemens Magnetom Tim Trio scanner at the Wolfson Brain Imaging Centre (Addenbrooke's Hospital Cambridge, UK). Diffusion-weighted data were acquired using echo planar imaging (63 axial slices, 2 mm thickness; field of view = 192 mm x 192 mm; matrix size = 96 × 96; voxel size = 2 mm isotropic; flip angle = 90°; TR = 8300 ms; TE = 98 ms;). 12 non-collinear gradient directions were collected 5 times using 5 b-values ranging from 340 to 1590 s/mm2, resulting in 60 diffusion-weighted volumes. 5 non-diffusion weighted volumes were also acquired, so a total of 65 volumes were available per patient. The use of multiple b-

values has been shown to improve the accuracy and repeatability of DTI results (Correia et al., 2009). In addition, a 3D T1-weighted structural scan, magnetization prepared rapid gradient echo (MPRAGE) (160 sagittal slices, 1mm thickness; matrix size = 256 × 231; voxel size = 1 mm isotropic; flip angle = 9°; TR = 2250 ms; TE = 2.98 ms) was obtained.

Image analysis

***Preprocessing*.** Data analysis was primarily carried out using FSL 5.0.4 (FMRIB's Software Library) (Smith et al., 2004). After manually removing any diffusion-weighted volumes with substantial distortion, the remaining volumes were corrected for eddy current distortions and head motion by affine registration to a b = 0 image. Between 1-6, out of 60 diffusion-weighted volumes, were removed from 14 patients. There were no significant differences in the average number of volumes removed across groups (VS = 2, MCS- = 3, and MCS+ = 2 volumes removed). Next, skull stripping was applied to the b = 0 image using the Brain Extraction Tool (BET) (Smith, 2002) and to the T1-weighted structural image using the Robust Brain Extraction (ROBEX) tool (Iglesias et al., 2011).

Regions of interests (ROIs). For each hemisphere, a seed mask (thalamus) and seven cortical target masks (prefrontal [PFC], premotor/supplementary motor area [PMC/SMA], primary motor [M1], primary somatosensory [S1], posterior parietal [PPC], temporal, and occipital cortices) were transformed from standard space (MNI-152 2mm) into each patient's T1-weighted structural space using Advanced Nonlinear Transformations (ANTs) tool (Avants et al., 2011). The anatomical landmarks of these ROIs have been previously described in Behrens et al. (2003). Transformations

between the patients' structural and diffusion space were created with FLIRT (Jenkinson et al., 2002). All masks were visually inspected to ensure accuracy and manually edited as needed prior to any data analysis. To improve the delineation of the thalamic masks, as many masks overlapped with parts of the cerebral spinal fluid (CSF), we removed any voxels from the thalamus mask that intersected with the CSF. Figure 1A illustrates both a lateral and medial view of the ROIs.

Probabilistic tractography. Using tools within FSL's diffusion toolbox (FDT), we estimated a probability distribution function on the principal fiber direction at each voxel. Then, 5000 samples were drawn from the connectivity distribution from each voxel in the thalamic seed mask. Two subsequent approaches followed: (i) The probability of connection from the thalamus to each cortical target was calculated, where each voxel within the thalamus was quantified by the total number of samples reaching any target. This resulted in seven cortical connectivity clusters of the thalamus, one for each cortical target, which will later be submitted to the univariate analysis. (ii) A path distribution map from the left or right thalamus (i.e. reconstructed thalamic tracks) was created to identify all pathways originating from the thalamus and projecting throughout the whole brain, including the cortical targets. Each voxel within the path distribution map represented the number of samples that successfully passed through that voxel from the thalamus. This output will be used in the multivariate analysis. All tractography outputs were thresholded to exclude voxels with connectivity values less than 10 and divided by the total number of samples sent (5000 samples x the number of seed voxels). This normalization step controlled for the variability of the patients' thalamus

size. A small threshold was chosen based on the overall low connectivity profile of these severely brain-injured patients.

Statistical analysis

Univariate analysis. Each of the seven thalamo-cortical connectivity clusters was then compared between VS and MCS+, VS and MCS-, and MCS- and MCS+. Voxelwise statistics were performed using randomise (5000 permutations) and threshold-free cluster enhancement was applied to correct for multiple comparisons ($p < 0.05$, corrected) (Smith and Nichols, 2009). Only cluster sizes with at least 10 contiguous voxels are reported. Between-group tests were carried out with and without covariates (i.e., gender, age, and months post-ictus [MPI]), since these factors are sometimes considered to be important for patient prognosis (Monti et al., 2010). Nonetheless, as we report below, no factor correlated with our dependent measure.

Multivariate classification. Since the aim of this study was to increase the accuracy of differential diagnoses, we employed multivariate classification techniques to assess the reliability of neuronal markers (i.e. patterns of thalamic projections). Considering the widespread connectivity of the thalamus and the variable, multifocal pathologies of DOC patients, we implemented a searchlight mapping technique (Kriegeskorte et al., 2006) to identify which regions along the thalamic tracks reaching the cortex varied most reliably across groups. We centered a 5-voxel sphere at each voxel in the brain and used the thalamic connectivity values from voxels within each sphere as features in each of three binary support vector machine (SVM) classifications (MCS+ vs VS, MCS- vs VS, and MCS+ vs MCS-). Classification accuracy was assessed in a leave-2-subjects-out cross-validation fashion in order to avoid any

circularity or “double-dipping” in the procedure (Kriegeskorte et al., 2009). The achieved accuracy was assigned to the voxel that the sphere was centered around, resulting in a whole-brain accuracy for each classification. Significance was determined by the binomial inverse of the cumulative distribution function to identify the smallest number of correct classifications out of the total number of classifications (number of subjects raised to the number of groups in the classification [n^k]), where the distribution was centered around the chance value obtained by randomly shuffling the labels before classification (Pereira et al., 2009). The p-value cutoff was 0.05, bonferronni corrected for the number of searchlight masks. To ensure that our results highlight the most significant regions, only clusters with at least 50 contiguous voxels are reported. The effects of potential covariates were regressed out prior to the SVM classifications.

Results

Identifying thalamic subregions based on cortical connectivity

Connectivity-based thalamic segmentation revealed different regions within the thalamus that were preferentially connected to each ipsilateral cortical target. The group mean of each thalamo-cortical cluster is depicted for VS, MCS-, and MCS+ in Figure 1B. Although some overlap were observed between putative thalamic subregions, areas containing high probabilities of connection to distinct cortical targets were relatively consistent with previous reports of connectivity-based, and histologically verified, thalamic subregions (Behrens et al., 2003; Johansen-Berg et al., 2005). Collapsing across groups and reporting primary connections, PFC connections were largely found in the mediodorsal nucleus (MD), intralaminar nuclei (ILN), ventral anterior (VA), and ventral lateral (VL) complex; PPC, occipital, and temporal regions were predominantly

connected to the pulvinar (PUL); S1 connections were mainly localized within the ventral posterior lateral nucleus (VPL); PMC/SMA was strongly associated with VL. M1 also revealed some connections in VL and VPL regions.

Univariate tests of thalamo-cortical subregions

The proportion of cortical connections in the thalamic subdivisions was compared between each group to uncover univariate differences (Figure 1C, Table 2). As compared to VS, MCS+ patients exhibited greater thalamo-cortical connections across the majority of cortical targets, except for PPC and occipital regions. While no univariate differences were observed for MCS- > VS, the reverse contrast uncovered greater left pulvinar-occipital connectivity in VS patients. Finally, comparison of the two MCS subgroups demonstrated that MCS+ patients showed greater connectivity between the thalamus and bilateral premotor cortices, as well as left temporal cortex.

We note that when additional variables were included as covariates (gender, age, and MPI), which were uncorrelated with our dependent variables, most of the findings failed to remain significant, except for the left pulvinar-temporal connectivity difference for MCS+ > MCS-.

Multivariate classification of thalamic tracks

Using the left or right whole-brain thalamic tracks (Figure 2) as features for 2-way SVM searchlight classifications between patient groups, we identified extensive areas in the cortical gray matter and associated white matter regions that significantly distinguished between VS versus MCS+, VS versus MCS-, and MCS- versus MCS+ (Figure 3, Table 3). The percent accuracy cutoff for VS vs. MCS+ was 81%, whereas the accuracy cutoff for VS vs. MCS- and MCS- vs. MCS+ was 84%. The multivariate

results, which were significant despite the inclusion of potential confounding variables such as gender, age, and MPI, supported a large portion of the univariate findings. Important features in the successful discrimination across all groups were found in thalamic tracks that traversed parts of frontal, parietal, and sensorimotor zones. However, the percent accuracy, cluster size, and precise locations within these main regions varied across each 2-way classification.

The VS versus MCS+ classification relied mainly upon widespread thalamo-cortical networks, with roughly equal contributions from both left and right thalamic tracks. In particular, thalamic tracks reaching frontal, parietal, and sensorimotor areas were the most prominent, where the largest clusters were found within prefrontal, but 100% accuracies were detected in more posterior regions, including posterior cingulate and inferior parietal (bordering S1). The VS versus MCS- classification relied upon similar widespread thalamo-cortical networks, but depended on projections primarily from the left thalamus. 100% accuracies were identified in paracentral, inferior parietal, and lateral occipital cortices. Finally, similar thalamo-cortical regions appeared for the MCS- versus MCS+ classification, but the right thalamic projections were more informative than the left in successful distinction of the two groups. 100% accuracies were discovered in sensorimotor regions, including paracentral and S1.

Discussion

In this paper we assessed differences in thalamo-cortical connectivity across varying levels of consciousness impairment (VS, MCS-, and MCS+) using probabilistic diffusion tractography. Although diverse patterns of local differences in thalamo-cortical connectivity were evident in each pairwise group comparison, the key features shared by univariate and multivariate comparisons involved thalamic connections with prefrontal and sensorimotor regions. To date, this study is one of the very few to have reported reliable differences between the subcategories of MCS and VS, and the very first to have found systematic differences between VS and MCS-.

VS versus MCS+

As expected, the univariate and multivariate comparison of groups at the extreme points of the DOC spectrum (i.e. VS vs. MCS+) revealed the greatest degree of thalamo-cortical connectivity differences across multiple networks. MCS+ patients generally exhibited more thalamo-cortical connections, compared to VS. These findings suggest that having a better preserved thalamo-cortical system may explain the more complex behavioral repertoire observed in these minimally conscious patients and are consistent with previous studies implicating thalamo-cortical circuits in wakefulness and ongoing conscious processing (Alkire et al., 2000; Tononi, 2012) and therefore in DOC (Schiff, 2010).

Moreover, the thalamic nuclei (ILN, MD, VA, VL, and PUL) that contributed to the increased thalamic connectivity with association cortices in MCS+, compared to VS, may be considered part of the central thalamus. The nuclei within the central thalamus, which include the intralaminar complex and paralaminar portions of related thalamic

association nuclei—MD, VA, VL, and PUL (Schiff, 2008) have been found to be preferentially damaged following severe brain injury and the degree of damage grades with behavioral outcome (Lutkenhoff et al., 2015; Lutkenhoff et al., 2013; Maxwell et al., 2006). In addition, deep brain stimulation of the central thalamus in DOC patients has yielded functional improvements (Kanno et al., 1987; Schiff et al., 2007; Tsubokawa et al., 1990; Yamamoto and Katayama, 2005).

Classifying VS and MCS+ patients based on their thalamic projections yielded significant multivariate differences across extensive cortical networks. Tracks originating from both left and right thalami that reached frontal, parietal, and sensorimotor areas were significantly different between groups. Distributed regions within the prefrontal and parietal areas have been regarded as the neurobiological underpinnings of conscious processing (Dehaene and Changeux, 2011). Moreover, seminal PET studies in VS patients have revealed functional disconnections in similar networks, where both fronto-parietal and thalamo-frontal networks have been associated with the recovery of consciousness (Laureys et al., 2000; Laureys et al., 1999); dysfunctioning in fronto-parietal networks may be due to either direct cortical damage or cortico-cortical or thalamo-cortical disconnections (Laureys, 2005). The thalamo-sensorimotor differences observed in our study may reflect the severity of sensorimotor deficits in VS patients that may prevent them from responding to behavioral stimulation and thus from demonstrating signs of discernible awareness.

VS versus MCS-

Distinguishing patients in VS from MCS- based on overt behavior is particularly challenging due to the latter patient group's limited behavioral repertoire, which may be

an important contribution to the high misdiagnosis rates in this patient group. The ability to reliably discriminate these two groups on the basis of brain connectivity alone is therefore a particularly important aspect of this report. While greater pulvinar-occipital connectivity in VS, compared to MCS-, was the only univariate difference detected in this between-group comparison, the more sensitive and robust multivariate analysis uncovered multiple thalamo-cortical networks that could systematically classify between the two groups. These networks were similar to the ones that distinguished VS from MCS+, but also included thalamo-occipital differences and were more lateralized to the tracks originating from the left thalamus. We interpret this laterality observation as an indication of the differences in the degree of thalamo-cortical injuries, with extensive, bilateral damages to the thalamus and/or cortex as characteristic of VS (Kinney and Samuels, 1994), and a lesser degree of thalamo-cortical damage commonly witnessed in minimally conscious patients (Jennett et al., 2001). On the other hand, the greater pulvinar-occipital connectivity in VS compared to MCS- patients may reflect the possibility of VS patients undergoing compensatory changes in disease progression or recovery. Evidence of late axonal regrowth as implied by increased fractional anisotropy (FA) has been previously reported in a single MCS patient (Voss et al., 2006). However, although increased FA is often interpreted as marking greater structural integrity, the occurrence of astrogliosis after injury can also contribute to a higher FA (Croall et al., 2014). Likewise, post-injury mechanisms may also bias diffusion vector estimations that could potentially lead to an increased connectivity between regions. Considering that visual pursuit is often the first sign of patients transitioning from VS to MCS (Giacino and Whyte, 2005), the pulvinar, whose main functions are visual (Cortes and van

Vreeswijk, 2012), would certainly be a sensible locus for compensatory mechanisms. Nonetheless, given the relatively small group-wise sample size under investigation, the lack of multiple time points to investigate interval changes in the present data, and the low prior evidence for such mechanisms in DOC, interpretation of this finding will only be possible through assessment of the issue in future studies.

MCS- versus MCS+

Functional and structural differences between sub-categories of MCS have been previously reported. Reduced metabolism by means of PET was found in left cortical areas of the language network and sensorimotor cortices in MCS- compared to MCS+ patients (Bruno et al., 2012). Our univariate results complement these functional findings by offering structural support for reduced connectivity of bilateral premotor and left temporal cortices (possibly including language related regions) with the thalamus. Moreover, in a DTI study, decreased fractional anisotropy (FA) in the white matter tracts connecting the thalamus and precuneus/posterior cingulate was detected in MCS- compared to MCS+ (Fernandez-Espejo et al., 2012). Likewise, our classification algorithm was able to successfully differentiate MCS- from MCS+ based on connections of thalamus with precuneus as well as a number of other recipient regions. Other thalamo-cortical differences were comparable to the previous group comparisons, but lateralized to the projections from the right thalamus, suggesting that perhaps, the two MCS subgroups may be less equally impaired in the right thalamus. Again, this laterality finding may concur with the notion that the severity of thalamic damage correlates with clinical manifestation (Maxwell et al., 2006).

Limitations

Finally, interpretation of the findings should be mindful of a number of limitations. Our sample size was limited by a number of factors. First, DOC patients are a relatively rare population, which poses many medical and logistic challenges. Second, despite collecting data for a sample of 56 patients, quality control procedures reduced the analysis sample to 25. This was mainly due to the artifacts introduced by high rates of spontaneous in-scanner motion (see Monti et al., 2015, for a similar report) as well as the severe pathology often present in DOC patients, which makes it difficult to delineate with precision and confidence regions of interest, process the data with existing software (Lutkenhoff et al., 2014) and achieve proper co-registration with so-called standard space templates, impairing group analysis. While appropriate, these procedures have the unwanted consequence of decreasing our sample size, degrading power, and potentially penalizing to a greater extent for patients at the high-pathology end of the spectrum, both of which affect the generalizability of our findings. Thus, while patient exclusion was approximately balanced across conditions (i.e., 10 VS, 7 MCS-, 8MCS+), it will be important to revisit these findings in an independent sample. We do emphasize, however, that there is good congruence between our findings and current models of DOC, which mitigates the issue. Alongside the challenges of acquiring data in this patient cohort, we were unable to obtain diffusion data with the optimal number of directions. While 12 directions may be sub-optimal for the robust estimation of diffusion parameters, the use of multiple b-values and multiple repetitions may mitigate this issue (Correia et al., 2009; Goodlett et al., 2007). Likewise, potential effects from removing a few distorted volumes during the preprocessing step may also be mitigated by the availability of 60 diffusion-weighted volumes from the repeated sampling. And, since

there were no systematic differences in the number of volumes removed as a function of group, the likelihood of a bias toward any specific group is reduced. Moreover, there existed an imbalanced distribution of the patients' etiology, where majority of MCS patients were of traumatic origin; this prevented us from carefully evaluating the impact of this factor on our results, and from being able to compare the two groups. In addition, most of our univariate findings failed to remain significant when gender, age, and MPI were included as covariates. Although this result is likely due to the low sample size, and consequential low power, further degraded by the inclusion of the additional regressors uncorrelated with the dependent variables, our univariate results should be taken with some caution. Nonetheless, our findings fit well with the existing literature and with the results reported in the more sensitive multivariate analysis. Finally, it should also be remarked that diffusion tractography does not take into consideration potential differences across efferent and afferent thalamic fibers, which might play different roles in the context of loss and recovery of consciousness after severe brain injury.

Conclusion

In the effort to disentangle DOC with the use of DTI and machine learning algorithms, we have shown that structural connectivity of individual thalamo-cortical networks and the preservation of this system in general can account for the gradations of consciousness observed in these severely brain-injured patients. While univariate differences between VS and MCS+ included majority of thalamo-cortical connections of interest, other comparisons between groups closer in the DOC spectrum uncovered limited differences. The addition of the multivariate analysis helped corroborate and

extend some of the univariate findings by accounting for any potential effects of covariates and highlighting the importance of thalamic connections with fronto-parietal cortices and sensorimotor areas. The combination of probabilistic tractography with searchlight classification presents a novel approach to identifying biomarkers that could complement existing behavioral assessments and aid in differential diagnoses.

Tables

Table 1. Patients' demographic and clinical information

						CRS-R Scores						
Patient	Diagnosis	Gender	MPI	Age	Etiology	Auditory	Visual	Motor	Oromotor	Communication	Arousal	Total
P01	VS	F	18	48	NT	1	1	2	1	0	2	7
P02	VS	F	8	52	NT	1	1	2	1	0	2	7
P03	VS	M	10	35	NT	1	1	2	1	0	1	6
P04	VS	M	14	67	T	0	1	2	1	0	1	5
P05	VS	M	8	42	NT	1	1	2	1	0	2	7
P06	VS	M	13	62	NT	1	0	2	2	0	2	7
P07	VS	F	8	38	T	NA	NA	NA	NA	NA	NA	8
P08	VS	M	9	35	NT	1	1	2	1	0	2	7
P09	VS	M	13	34	T	1	0	2	1	0	2	6
P10	VS	M	19	31	T	NA	NA	NA	NA	NA	NA	NA
P11	MCS-	M	11	26	T	2	3	3	1	0	2	11
P12	MCS-	M	19	23	T	1	3	2	1	0	2	9
P13	MCS-	F	3	38	T	1	3	2	1	0	2	9
P14	MCS-	M	8	18	T	1	3	4	1	0	2	11
P15	MCS-	M	30	36	T	2	3	2	2	0	2	11
P16	MCS-	M	15	54	NT	2	3	1	1	0	3	10
P17	MCS-	F	13	38	T	2	3	2	2	0	2	11
P18	MCS+	M	7	17	T	3	3	2	2	0	2	12
P19	MCS+	M	11	29	T	3	3	2	1	0	2	11
P20	MCS+	M	6	56	NT	3	3	2	2	1	2	13
P21	MCS+	M	8	25	T	2	4	2	1	0	2	11
P22	MCS+	M	11	23	T	3	3	2	1	1	2	12
P23	MCS+	M	8	45	T	3	3	2	1	0	2	11
P24	MCS+	M	14	56	T	4	3	3	2	0	2	14
P25	MCS+	F	12	59	T	3	5	2	2	0	2	14

Abbreviations: MPI, months post-ictus; NT, non-traumatic; T, traumatic

Table 2. Univariate differences of thalamo-cortical connections

Statistical Tests	Cortical ROIs	Thalamic Regions	Cluster Size (Voxels)
MCS+ > VS	L. PFC	MD, ILN, VA, VL,	148
	R. PFC	MD, ILN, VA, VL	97
	L. PMC	MD, ILN, VL, VPL	58
	R. PMC	ILN, VL, VPL, VPM	72
	R. M1	VL, VPL	30
	R. S1	VL, VPL	16
	L. Temporal	PUL	20
	R. Temporal	PUL	55
VS > MCS+	−	−	−
MCS+ > MCS-	L. PMC	VL, ILN, VPL	53
	R. PMC	VPL, VPM	14
	L. Temporal	PUL*	51 (84*)
MCS- > MCS+	−	−	−
MCS- > VS	−	−	−
VS > MCS-	L. Occipital	PUL	16

Only significant clusters ($p < 0.05$, corrected) with at least 10 voxels are reported. Voxel Size: 2 x 2 x 2 mm.
* denotes significance after controlling for gender, age, and months post-ictus.
Abbreviations: MD, mediodorsal nucleus; ILN, intralaminar nuclei; VA, ventral anterior nucleus; VL,ventral lateral nucleus; VPL, ventral posterior lateral Nucleus; VPM, ventral posterior medial nucleus; PUL, pulvinar.

Table 3. Multivariate differences of thalamic tracks

A. Peak classification accuracies and cluster sizes

Track Region	VS versus MCS+				VS versus MCS-				MCS- versus MCS+			
	L. Thal Tracks		R. Thal Tracks		L. Thal Tracks		R. Thal Tracks		L. Thal Tracks		R. Thal Tracks	
Prefrontal	ipsi.	contra.	ipsi.	contra.	ipsi.	contra.	ipsi.	contra.	ipsi.	contra.	ipsi.	contra.
Sup. Frontal	88 (409)	–	88 (323)		–	86 (59)	–	–	–	–	93 (60)	93 (52)
Mid.Frontal	–	94 (309)	88 (173)	88 (312)	–	93 (99)	–	–	–	–	93 (163)	–
Inf. Frontal	–	–	81 (61)	81 (100)	–	–	–	–	–	–	86 (75)	–
Ant. Cingulate	81 (78)		–		–		–		–		93 (191)	
Sensorimotor												
PMC/SMA	–	88 (92)	–	–	–	–	–	–	–	–	–	–
Paracentral	–		–		100 (478)		–		86 (69)		100 (72)	
M1	88 (102)	–	–	–	93 (72)	–	–	–	–	–	–	93 (78)
S1	91 (124)	–	–	93 (67)	91 (82)	–	–	–	–	–	100 (50)*	97 (229)
Posterior Parietal												
Post. Cingulate	100 (67)		–		–		–		–		–	
Precuneus	95 (154)		–		–		–		86 (120)		–	
Inf. Parietal	100 (184)*	88 (60)	–	94 (147)	100 (60)	93 (59)	86 (55)	–	–	–	93 (62)	93 (89)
Sup. Parietal	–	–	88 (84)	–	–	–	–	–	–	–	–	–
Occipital												
Cuneus	–	–	–	–	93 (100)		–	–	–	–	–	87 (118)
Lat. Occipital	–	–	–	–	93 (60)	100 (178)	–	–	–	–	–	–
Subcortical WM												
ACR	–	–	88 (119)	–	–	–	–	–	–	–	93 (290)	93 (114)
SCR	–	–	–	–	–	–	–	–	–	–	93 (271)	–

Peak classification accuracy % (cluster size in voxels). Only significant clusters ($p < 0.05$, corrected) with at least 50 voxels are reported. Voxel Size: 2 x 2 x 2 mm. Cortical clusters may contain both gray matter and corresponding white matter regions. * Cluster spans S1 and Inf. Parietal border

B. Peak MNI coordinates

Track Region	VS versus MCS+				VS versus MCS-				MCS- versus MCS+			
	L. Thal Tracks		R. Thal Tracks		L. Thal Tracks		R. Thal Tracks		L. Thal Tracks		R. Thal Tracks	
Prefrontal	ipsi.	contra.	ipsi.	contra.	ipsi.	contra.	ipsi.	contra.	ipsi.	contra.	ipsi.	contra.
Sup. Frontal	-28,40,-8	–	-12,40,18		–	18,32,42	–	–	–	–	20,30,24	-24,22,26
Mid.Frontal	–	36,58,2	36,58,22	-36,32,18	–	32,48,30	–	–	–	–	30,48,28	–
Inf. Frontal	–	–	48,34,12	-38,10,16	–	–	–	–	–	–	50,32,0	–
Ant. Cingulate	20,24,24		–		–		–		–		-34,12,16	
Sensorimotor												
PMC/SMA	–	6,-34,68	–	–	–	–	–	–	–	–	–	–
Paracentral	–		–		-16,-34,48		–		-2,-34,50		2,-20,60	
M1	-28,-24,38	–	–	–	-32,-24,42	–	–	–	–	–	–	-58,-6,20
S1	-48,8,56	–	–	-42,-30,40	-58,-14,24	–	–	–	–	–	66,-8,26	-58,-12,40
Posterior Parietal												
Post. Cingulate	4,-22,38		–		–		–		–		–	
Precuneus	14,-70,66		–		–		–		-12,-66,50		–	
Inf. Parietal	-52,-32,52	54,-38,18	–	-54,-28,40	-28,-86,30	34,-38,44	40,-24,22	–	–	–	44,-72,14	-26,-92,32
Sup. Parietal	–	–	30,-80,28	–	–	–	–	–	–	–	–	–
Occipital												
Cuneus	–	–	–	–	-4,-90,10		–	–	–	–	–	-6,-86,16
Lat. Occipital	–	–	–	–	-20,-100,14	24,-86,14	–	–	–	–	–	–
Subcortical WM												
ACR	–	–	32,14,18	–	–	–	–	–	–	–	28,24,16	-20,20,26
SCR	–	–	–	–	–	–	–	–	–	–	26,-16,20	–

x,y,z in mm coordinates
Abbreviations: WM, white matter; Sup., superior; Mid., middle; Inf., inferior; Ant., anterior; PMC/SMA, premotor/supplementary motor area; M1, primary motor; S1, primary somatosensory; Post., posterior; Lat., lateral; ACR, anterior corona radiata; SCR, superior corona radiata; ipsi, ipsilateral; contra., contralateral.

Figures

Figure 1. Structural connectivity between thalamus and cortex

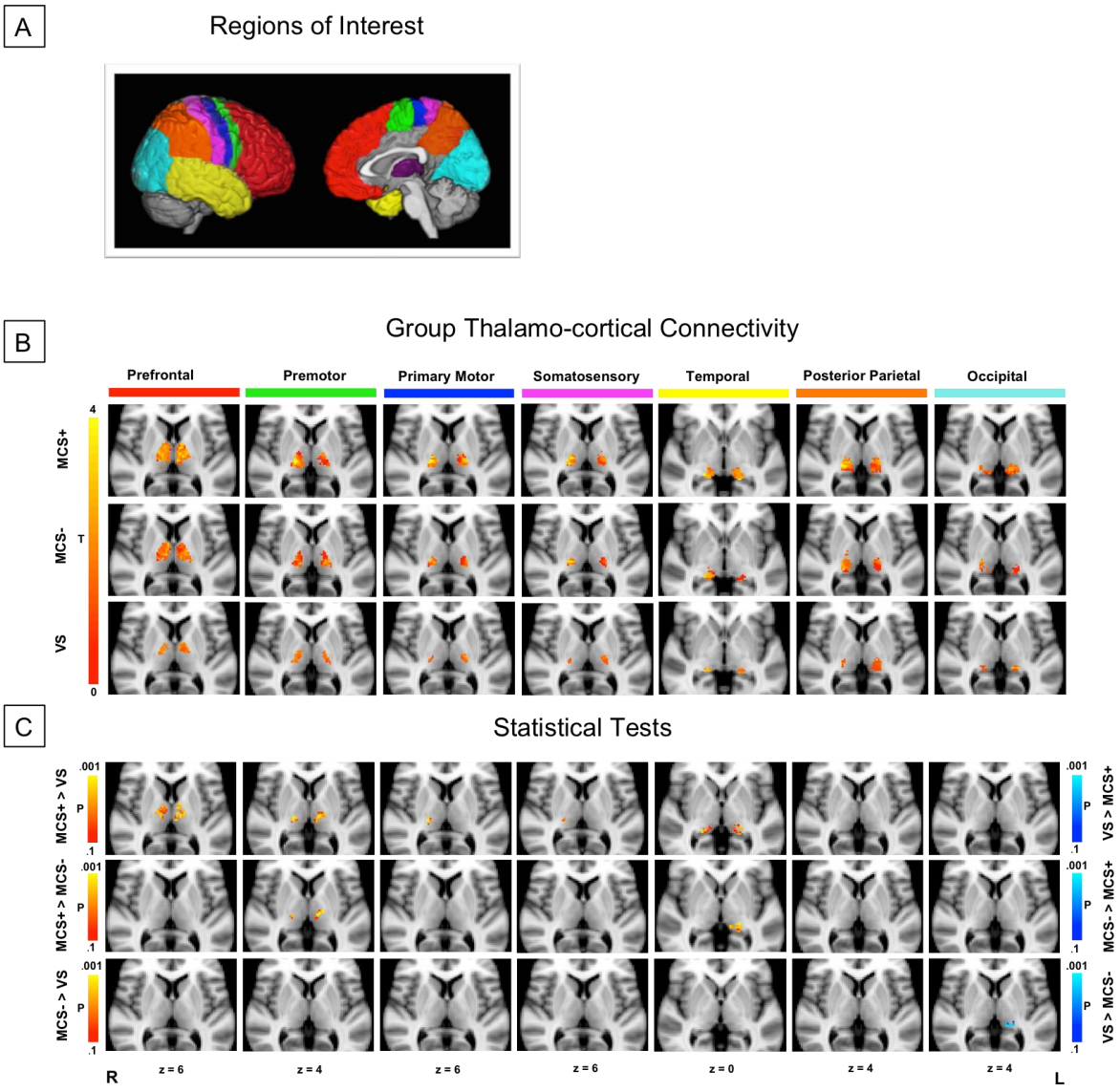

(A) ROIs used for probabilistic tractography: seven cortical target masks and one thalamic seed mask, per hemisphere. (B) Connectivity-based thalamic segmentation revealed seven subregions of the thalamus with target-specific connections. Group mean thalamo-cortical connectivity maps are displayed to reveal thalamic clusters shared by at least 25% of the patients in each group. (C) Statistical pairwise comparisons showed differential patterns of thalamo-cortical connectivity between VS, MCS-, and MCS+.

Figure 2. **Reconstructed whole-brain thalamic tracks**

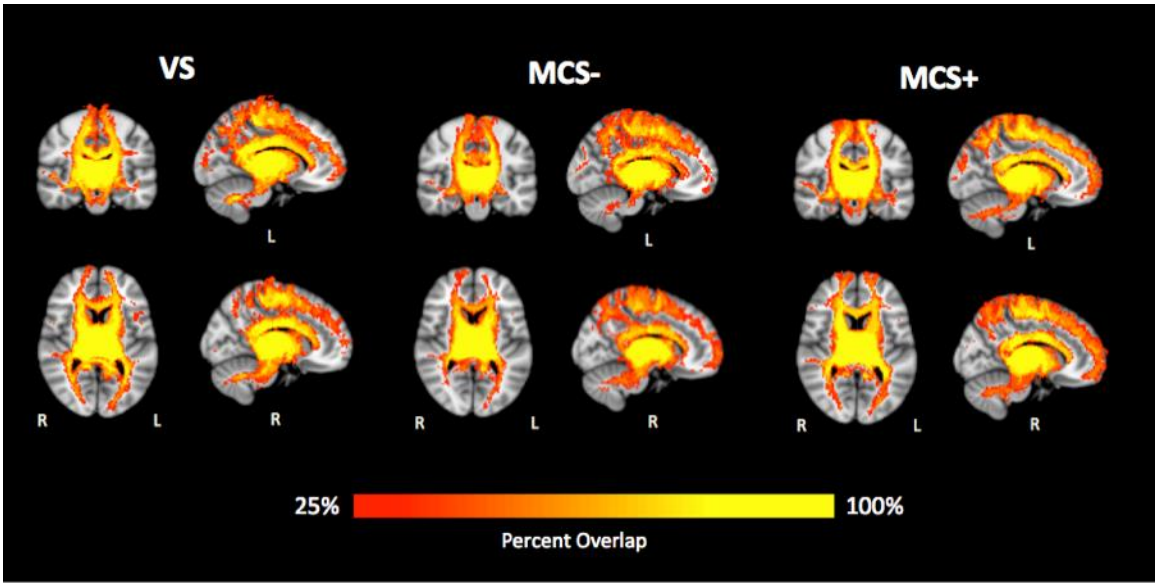

Only tracks shared by at least 25% of the patients for each group are shown. Left and right thalamic tracks are combined for visualization purposes.

Figure 3. **Searchlight classification results**

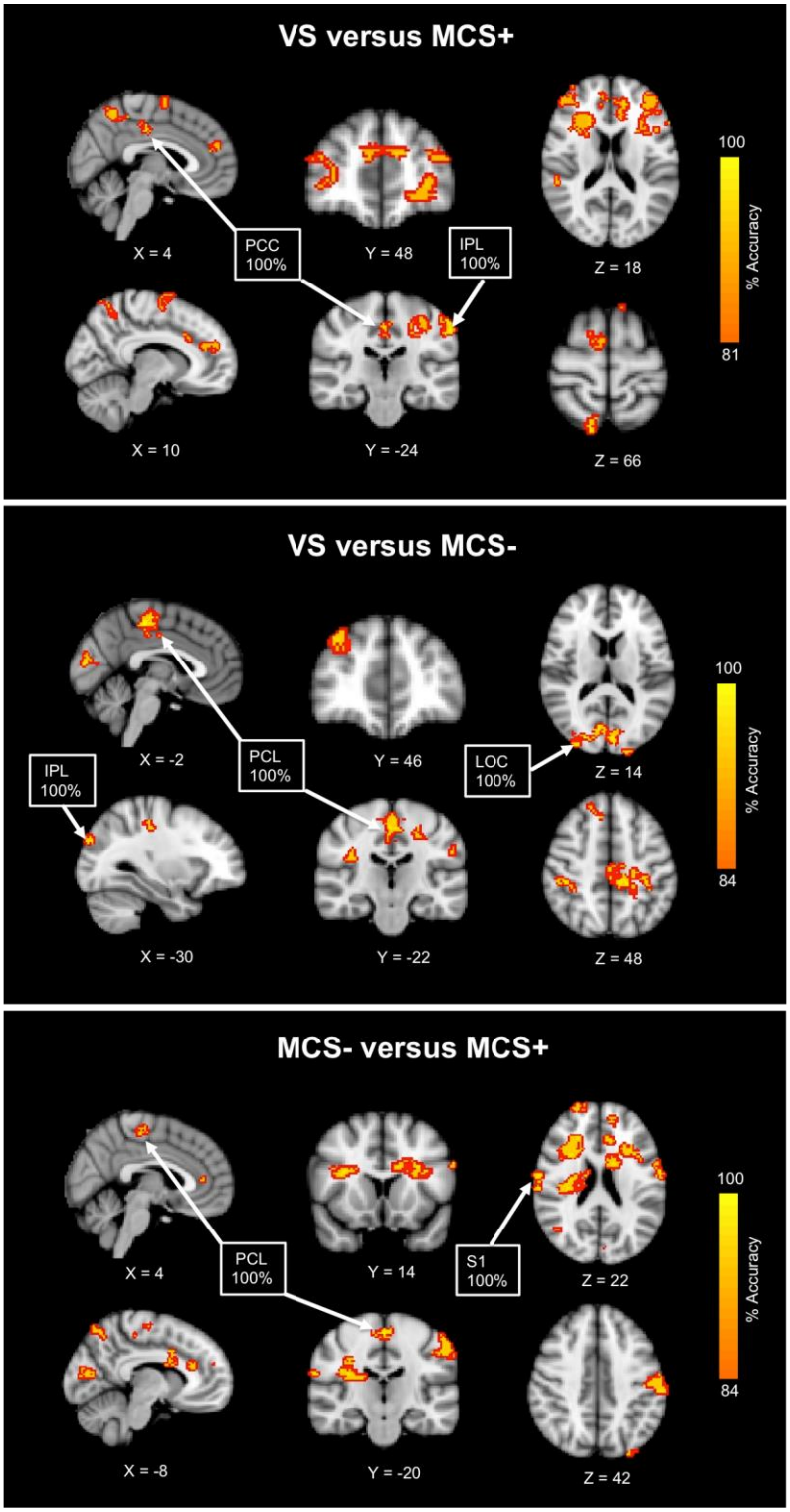

Tracks originating from the thalamus and projecting to the cortex that successfully distinguished between VS versus MCS+, VS versus MCS-, and MCS- versus MCS+ are shown. Results from the left and right

thalamic tracks are combined for visualization purposes. For enhanced display of the clusters, accuracy maps are thickened with a red border.

Abbreviations: PCC, posterior cingulate cortex; IPL, inferior parietal lobule; PCL, paracentral lobule; LOC, lateral occipital complex; S1, primary somatosensory.

References

Alkire, M.T., Haier, R.J., Fallon, J.H. (2000) Toward a unified theory of narcosis: brain imaging evidence for a thalamocortical switch as the neurophysiologic basis of anesthetic-induced unconsciousness. Consciousness and cognition, 9:370-86.

Andrews, K., Murphy, L., Munday, R., Littlewood, C. (1996) Misdiagnosis of the vegetative state: retrospective study in a rehabilitation unit. BMJ, 313:13-6.

Avants, B.B., Tustison, N.J., Song, G., Cook, P.A., Klein, A., Gee, J.C. (2011) A reproducible evaluation of ANTs similarity metric performance in brain image registration. NeuroImage, 54:2033-44.

Behrens, T.E., Johansen-Berg, H., Woolrich, M.W., Smith, S.M., Wheeler-Kingshott, C.A., Boulby, P.A., Barker, G.J., Sillery, E.L., Sheehan, K., Ciccarelli, O., Thompson, A.J., Brady, J.M., Matthews, P.M. (2003) Non-invasive mapping of connections between human thalamus and cortex using diffusion imaging. Nature neuroscience, 6:750-7.

Boly, M., Tshibanda, L., Vanhaudenhuyse, A., Noirhomme, Q., Schnakers, C., Ledoux, D., Boveroux, P., Garweg, C., Lambermont, B., Phillips, C., Luxen, A., Moonen, G., Bassetti, C., Maquet, P., Laureys, S. (2009) Functional connectivity in the default network during resting state is preserved in a vegetative but not in a brain dead patient. Human brain mapping, 30:2393-400.

Bruno, M.A., Majerus, S., Boly, M., Vanhaudenhuyse, A., Schnakers, C., Gosseries, O., Boveroux, P., Kirsch, M., Demertzi, A., Bernard, C., Hustinx, R., Moonen, G., Laureys, S. (2012) Functional neuroanatomy underlying the clinical

subcategorization of minimally conscious state patients. Journal of neurology, 259:1087-98.

Bruno, M.A., Vanhaudenhuyse, A., Thibaut, A., Moonen, G., Laureys, S. (2011) From unresponsive wakefulness to minimally conscious PLUS and functional locked-in syndromes: recent advances in our understanding of disorders of consciousness. Journal of neurology, 258:1373-84.

Childs, N.L., Mercer, W.N. (1996) Misdiagnosing the persistent vegetative state. Misdiagnosis certainly occurs. BMJ, 313:944.

Correia, M.M., Carpenter, T.A., Williams, G.B. (2009) Looking for the optimal DTI acquisition scheme given a maximum scan time: are more b-values a waste of time? Magnetic resonance imaging, 27:163-75.

Cortes, N., van Vreeswijk, C. (2012) The role of pulvinar in the transmission of information in the visual hierarchy. Frontiers in computational neuroscience, 6:29.

Croall, I.D., Cowie, C.J., He, J., Peel, A., Wood, J., Aribisala, B.S., Mitchell, P., Mendelow, A.D., Smith, F.E., Millar, D., Kelly, T., Blamire, A.M. (2014) White matter correlates of cognitive dysfunction after mild traumatic brain injury. Neurology, 83:494-501.

Dehaene, S., Changeux, J.P. (2011) Experimental and theoretical approaches to conscious processing. Neuron, 70:200-27.

Fernandez-Espejo, D., Bekinschtein, T., Monti, M.M., Pickard, J.D., Junque, C., Coleman, M.R., Owen, A.M. (2011) Diffusion weighted imaging distinguishes the vegetative state from the minimally conscious state. NeuroImage, 54:103-12.

Fernandez-Espejo, D., Soddu, A., Cruse, D., Palacios, E.M., Junque, C., Vanhaudenhuyse, A., Rivas, E., Newcombe, V., Menon, D.K., Pickard, J.D., Laureys, S., Owen, A.M. (2012) A role for the default mode network in the bases of disorders of consciousness. Annals of neurology, 72:335-43.

Giacino, J., Whyte, J. (2005) The vegetative and minimally conscious states: current knowledge and remaining questions. The Journal of head trauma rehabilitation, 20:30-50.

Giacino, J.T., Ashwal, S., Childs, N., Cranford, R., Jennett, B., Katz, D.I., Kelly, J.P., Rosenberg, J.H., Whyte, J., Zafonte, R.D., Zasler, N.D. (2002) The minimally conscious state: definition and diagnostic criteria. Neurology, 58:349-53.

Giacino, J.T., Kalmar, K., Whyte, J. (2004) The JFK Coma Recovery Scale-Revised: measurement characteristics and diagnostic utility. Archives of physical medicine and rehabilitation, 85:2020-9.

Goodlett, C., Fletcher, P.T., Lin, W., Gerig, G. (2007) Quantification of measurement error in DTI: theoretical predictions and validation. Medical image computing and computer-assisted intervention : MICCAI ... International Conference on Medical Image Computing and Computer-Assisted Intervention, 10:10-7.

Iglesias, J.E., Liu, C.Y., Thompson, P.M., Tu, Z. (2011) Robust brain extraction across datasets and comparison with publicly available methods. IEEE transactions on medical imaging, 30:1617-34.

Jenkinson, M., Bannister, P., Brady, M., Smith, S. (2002) Improved optimization for the robust and accurate linear registration and motion correction of brain images. NeuroImage, 17:825-41.

Jennett, B., Adams, J.H., Murray, L.S., Graham, D.I. (2001) Neuropathology in vegetative and severely disabled patients after head injury. Neurology, 56:486-90.

Jennett, B., Plum, F. (1972) Persistent vegetative state after brain damage. Rn, 35:ICU1-4.

Johansen-Berg, H., Behrens, T.E., Sillery, E., Ciccarelli, O., Thompson, A.J., Smith, S.M., Matthews, P.M. (2005) Functional-anatomical validation and individual variation of diffusion tractography-based segmentation of the human thalamus. Cerebral cortex, 15:31-9.

Kanno, T., Kamei, Y., Yokoyama, T., Jain, V.K. (1987) Neurostimulation for patients in vegetative status. Pacing and clinical electrophysiology : PACE, 10:207-8.

Kinney, H.C., Samuels, M.A. (1994) Neuropathology of the persistent vegetative state. A review. Journal of neuropathology and experimental neurology, 53:548-58.

Kriegeskorte, N., Goebel, R., Bandettini, P. (2006) Information-based functional brain mapping. Proceedings of the National Academy of Sciences of the United States of America, 103:3863-8.

Kriegeskorte, N., Simmons, W.K., Bellgowan, P.S., Baker, C.I. (2009) Circular analysis in systems neuroscience: the dangers of double dipping. Nature neuroscience, 12:535-40.

Laureys, S. (2005) The neural correlate of (un)awareness: lessons from the vegetative state. Trends in cognitive sciences, 9:556-9.

Laureys, S., Faymonville, M.E., Luxen, A., Lamy, M., Franck, G., Maquet, P. (2000) Restoration of thalamocortical connectivity after recovery from persistent vegetative state. Lancet, 355:1790-1.

Laureys, S., Goldman, S., Phillips, C., Van Bogaert, P., Aerts, J., Luxen, A., Franck, G., Maquet, P. (1999) Impaired effective cortical connectivity in vegetative state: preliminary investigation using PET. NeuroImage, 9:377-82.

Laureys, S., Tononi, G. (2008) The Neurology of Consciousness. London. Academic Press-Elsevier.

Lutkenhoff, E.S., Chiang, J., Tshibanda, L., Kamau, E., Kirsch, M., Pickard, J.D., Laureys, S., Owen, A.M., Monti, M.M. (2015) Thalamic and extrathalamic mechanisms of consciousness after severe brain injury. Annals of neurology.

Lutkenhoff, E.S., McArthur, D.L., Hua, X., Thompson, P.M., Vespa, P.M., Monti, M.M. (2013) Thalamic atrophy in antero-medial and dorsal nuclei correlates with six-month outcome after severe brain injury. NeuroImage. Clinical, 3:396-404.

Lutkenhoff, E.S., Rosenberg, M., Chiang, J., Zhang, K., Pickard, J.D., Owen, A.M., Monti, M.M. (2014) Optimized brain extraction for pathological brains (optiBET). PloS one, 9:e115551.

Maxwell, W.L., MacKinnon, M.A., Smith, D.H., McIntosh, T.K., Graham, D.I. (2006) Thalamic nuclei after human blunt head injury. Journal of neuropathology and experimental neurology, 65:478-88.

Monti, M.M., Laureys, S., Owen, A.M. (2010) The vegetative state. BMJ, 341:c3765.

Monti, M.M., Rosenberg, M., Finoia, P., Kamau, E., Pickard, J.D., Owen, A.M. (2015) Thalamo-frontal connectivity mediates top-down cognitive functions in disorders of consciousness. Neurology, 84:167-73.

Newcombe, V.F., Williams, G.B., Scoffings, D., Cross, J., Carpenter, T.A., Pickard, J.D., Menon, D.K. (2010) Aetiological differences in neuroanatomy of the vegetative state: insights from diffusion tensor imaging and functional implications. Journal of neurology, neurosurgery, and psychiatry, 81:552-61.

Pereira, F., Mitchell, T., Botvinick, M. (2009) Machine learning classifiers and fMRI: a tutorial overview. NeuroImage, 45:S199-209.

Pierpaoli, C., Jezzard, P., Basser, P.J., Barnett, A., Di Chiro, G. (1996) Diffusion tensor MR imaging of the human brain. Radiology, 201:637-48.

Schiff, N.D. (2008) Central thalamic contributions to arousal regulation and neurological disorders of consciousness. Annals of the New York Academy of Sciences, 1129:105-18.

Schiff, N.D. (2010) Recovery of consciousness after brain injury: a mesocircuit hypothesis. Trends in neurosciences, 33:1-9.

Schiff, N.D., Giacino, J.T., Kalmar, K., Victor, J.D., Baker, K., Gerber, M., Fritz, B., Eisenberg, B., Biondi, T., O'Connor, J., Kobylarz, E.J., Farris, S., Machado, A., McCagg, C., Plum, F., Fins, J.J., Rezai, A.R. (2007) Behavioural improvements with thalamic stimulation after severe traumatic brain injury. Nature, 448:600-3.

Schnakers, C., Vanhaudenhuyse, A., Giacino, J., Ventura, M., Boly, M., Majerus, S., Moonen, G., Laureys, S. (2009) Diagnostic accuracy of the vegetative and

minimally conscious state: clinical consensus versus standardized neurobehavioral assessment. BMC neurology, 9:35.

Smith, S.M. (2002) Fast robust automated brain extraction. Human brain mapping, 17:143-55.

Smith, S.M., Jenkinson, M., Woolrich, M.W., Beckmann, C.F., Behrens, T.E., Johansen-Berg, H., Bannister, P.R., De Luca, M., Drobnjak, I., Flitney, D.E., Niazy, R.K., Saunders, J., Vickers, J., Zhang, Y., De Stefano, N., Brady, J.M., Matthews, P.M. (2004) Advances in functional and structural MR image analysis and implementation as FSL. NeuroImage, 23 Suppl 1:S208-19.

Smith, S.M., Nichols, T.E. (2009) Threshold-free cluster enhancement: addressing problems of smoothing, threshold dependence and localisation in cluster inference. NeuroImage, 44:83-98.

Tononi, G. (2012) Integrated information theory of consciousness: an updated account. Archives italiennes de biologie, 150:293-329.

Tsubokawa, T., Yamamoto, T., Katayama, Y., Hirayama, T., Maejima, S., Moriya, T. (1990) Deep-brain stimulation in a persistent vegetative state: follow-up results and criteria for selection of candidates. Brain injury : [BI], 4:315-27.

Voss, H.U., Uluc, A.M., Dyke, J.P., Watts, R., Kobylarz, E.J., McCandliss, B.D., Heier, L.A., Beattie, B.J., Hamacher, K.A., Vallabhajosula, S., Goldsmith, S.J., Ballon, D., Giacino, J.T., Schiff, N.D. (2006) Possible axonal regrowth in late recovery from the minimally conscious state. The Journal of clinical investigation, 116:2005-11.

Yamamoto, T., Katayama, Y. (2005) Deep brain stimulation therapy for the vegetative state. Neuropsychological rehabilitation, 15:406-13.

Study 2: Generalizing Findings Using Diffusion Tensor Based Methods to Disentangle Disorders of Consciousness

Introduction

Disorders of consciousness (DOC) can result from traumatic or non-traumatic brain injuries severe enough to induce a state of coma. While some survivors may wake up and fully recover consciousness, others transition into a vegetative state (VS) or minimally conscious state (MCS) (Monti et al., 2010). Patients in VS are able to maintain wakefulness but show no signs of awareness (Jennett and Plum, 1972). The presence of varying levels of awareness along with wakefulness warrants an MCS diagnosis (Giacino et al., 2002), which is further broken down into MCS- (low-level behavior) and MCS+ (higher-level behavior; regaining language and communication). Patients exhibiting functional recovery are said to be emerging from MCS (EMCS).

The stratification of DOC currently relies on clinicians' subjective judgment of residual consciousness based on patients' limited behavioral responses that may be inconsistent and subjected to a number of other confounding factors (Giacino et al., 2009). Consequently, high rates of misdiagnosis remain common (Schnakers et al., 2009), especially between patients on the lower end of the consciousness spectrum (i.e. VS and MCS-). However, variable patterns of brain pathology in DOC challenge the development of reliable neuroanatomical markers to assist in differential diagnosis. Despite such, growing research has suggested that dysfunction of the thalamo-cortical system is a major contributor to disorders of consciousness (Fernández-Espejo et al., 2010; Lant et al., 2016; Lutkenhoff et al., 2013, 2015; Maxwell et al., 2006; Schiff, 2008; Zheng et al., 2017). In our previous study, we have revealed that DOC patients with

varying levels of consciousness differed in structural connectivity between distinct thalamo-cortical circuits and could be classified with high accuracy on the basis of whole-brain thalamic track patterns (Zheng et al., 2017).

To increase the validity, reliability, and generalizability of potential neuroanatomical markers to help disentangle patients with DOC, we carried out a replication study following similar methods established by Zheng et al. (2017) in a larger cohort of patients from a different center with higher resolution diffusion tensor imaging (DTI) data. In addition to assessing structural connectivity between the thalamus and cortex, we analyzed connectivity between the thalamus and basal ganglia (BG), as some structures within BG have been implicated in DOC (Schiff, 2010). Two sets of analyses were carried out. A univariate approach compared differences between patient groups in the thalamic subregions, characterized by the connectivity with cortical and basal ganglia targets. By means of a searchlight method, the multivariate analysis evaluated differences along the reconstructed whole-brain thalamic tracks that could help to classify patients.

Methods

Patient population

MRI data from 86 DOC patients diagnosed by the Coma Recovery Scale-Revised (CRS-R) (Giacino et al., 2004) were obtained from the University of Liège. Twenty patients were subsequently excluded due to poor image quality, failed registration, or extensive brain abnormalities that prevented the delineation of our regions-of-interest (ROIs). The remaining dataset included 31 VS, 7 MCS-, 15 MCS+,

and 13 EMCS, totaling 66 patients (39M/27F; mean age 44.5 ± 14.8 years). Demographic and clinical details are listed in Table 1. Written informed consent was gathered from each patient's legal guardian. This study was approved by the Ethics Committee of the University Hospital of Liège.

Data acquisition

MRI data were captured on a 3T Siemens Tim Trio scanner. Only T1-weighted and diffusion weighted data were used in this study. Anatomical T1-weighted images were collected in 120 slices (TR = 2,300 ms, TE= 2.47 ms, voxel size = 1 x 1 x 1.2 mm^3, flip angle = 9°, matrix size = 256 x 240). Diffusion-weighted images (DWI) were acquired using 64 non-collinear gradient directions with b-value of 1,000 s/mm^2 and repeated twice (45 axial slices, TR = 5,700 ms, TE = 87 ms, voxel size = 1.8 x 1.8 x 3.3 mm^3, flip angle = 90°, matrix size = 128 x 128). A non-diffusion weighted volume (b = 0) was collected at the beginning of the scan.

Image analysis

In replicating our previous study, the procedures for the data analyses were similar to Zheng et al. (2017) and will be reiterated below.

Preprocessing. DWI data first underwent automatic quality control to identify and remove volumes with substantial artifacts as well as to correct for eddy currents and head motion by affine registration to the b = 0 reference volume using DTIPrep (Oguz et al., 2014). Next, brain extraction was performed on the b = 0 image with the Brain Extraction Tool (BET) (Smith Stephen M., 2002), and on the T1-weighted

structural image with Optimized Brain Extraction for Pathological Brains (optiBET) (Lutkenhoff et al., 2014).

Regions of interests (ROIs). A whole thalamus seed mask and seven cortical target masks (prefrontal [PFC], premotor/supplementary motor area [PMC/SMA], posterior parietal [PPC], temporal [TEM], occipital [OCC], primary motor [M1], and primary somatosensory [S1] cortices) were retrieved from FSL atlases per hemisphere. The anatomical demarcations of the cortical targets have been described in detail in (Behrens et al., 2003) and used in our previous study (Zheng et al., 2017). In addition, five basal ganglia masks (striatum [STR], external globus pallidus [GPe], internal globus pallidus [GPi], substantia nigra [SN], and subthalamic nucleus [STN]) from BG atlas developed by (Keuken and Forstmann, 2015). All masks (Figure 1A) were originally in standard MNI space and transformed into each patient's T1 structural space using Advanced Nonlinear Transformations (ANTs) (Avants et al., 2011). Then, the masks in structural space were transformed into each patient's diffusion space with FLIRT (Jenkinson et al., 2002). Due to the presence of many subcortical masks spilling into the CSF, a CSF mask was generated and used to intersect with these masks to remove unwanted voxels. All masks were submitted to a final visual inspection and modified as needed before any data analysis.

Probabilistic tractography. Probabilistic tractography was accomplished using FSL's diffusion toolbox (FDT). First, the probability distribution function on the principal fiber orientation at each voxel (modeling 3 fibers per voxel) was calculated. Then, tractography was run in native diffusion space for each hemisphere separately from the thalamus to the seven cortical and five subcortical targets with 5,000 samples drawn per

seed voxel. For each patient and each hemisphere, the outputs included: (a) 12 thalamic clusters, where each voxel within the cluster indicated the number of samples that successfully reached a target, and (b) whole brain reconstructed thalamic tracks revealing pathways starting from the thalamus and traversing the targets and continuing throughout the brain. Each voxel within the thalamic pathways corresponded to the number of samples that passed through that voxel from the thalamus. To remove unlikely connections, a threshold of 500 (10% of 5,000 samples sent per voxel) was applied to the thalamo-cortical and thalamo-BG clusters. However, smaller thresholds were needed for the smaller BG targets. A threshold of 50 was initially implemented, but proved to be too stringent for GPi, SN, and STh, so the criterion was lowered to 25 for these targets, with the exception of GPe (remaining at 50). Moreover, a threshold of 0.1% of total numbers of samples sent (5,000 samples × number of seed voxels) (Rilling et al., 2011) was used on the whole-brain thalamic tracks. All outputs were then normalized by dividing by the total numbers of samples sent. The thalamic clusters will undergo univariate analysis, whereas the whole-brain thalamic tracks will be submitted to multivariate analysis.

Statistical analysis

Univariate analysis. Between-group comparisons were performed in a pairwise fashion (VS v. MCS-, VS v. MCS+, VS v. EMCS, MCS- v. MCS+, MCS- v. EMCS, MCS+ v. EMCS). Voxelwise tests were carried out for each of the seven thalamo-cortical and five thalamo-BG connectivity clusters using BROCCOLI's randomise (5000 permutations) function (Eklund et al., 2014). The covariates included gender, age, etiology, and days post-ictus (DPI). For multiple comparisons correction, the results

were thresholded at p <0.05, family-wise error rate corrected, using a cluster-defining primary threshold of 2.5 ($p < 0.01$). Only clusters with at least 10 contiguous voxels are reported.

Multivariate classification. To assess the practicality of relying upon thalamofugal projections to automatically "diagnose" a patient's DOC status, we implemented a four-way-classification (VS v. MCS+ v. MCS- v. EMCS) using a linear nu-support vector classifier (nu-SVC, c=1; specifically, we used a leave-4-patients-out cross-validation approach that balanced training class labels by randomly removing over-represented exemplars to match the class with the least (i.e. MCS- group with 7 patients). Each cross-validation was repeated 20 times to ensure the balancing process sampled from the distribution in an unbiased fashion. Average classification accuracy across iterations is reported.

To reveal which brain regions contained thalamic projections informative enough for a successful classification, we used a searchlight-mapping approach, where we iteratively centered a 5-voxel-radius sphere around each voxel in the brain, using the connectivity values from each voxel contained within that sphere as features in the classification and subsequently assigned resultant accuracies to the voxel upon which the sphere was centered.

To assess significance, we created a null-distribution using the binomial inverse of the cumulative distribution function, where the center of the distribution was the 4-way expected accuracy of 25% and the number of datapoints was the total number of classifications conducted $(n \times k \times i = 7 \times 4 \times 20 = 560)$. We set a significance cutoff to be the top 5% of the distribution ($p < 0.05$), Bonferroni corrected for the total number of

searchlight masks (i.e. 193 successful classifications or 34.5% accuracy). Finally, we report regions where 50 contiguous voxels were assigned significant accuracy values.

Results

Patterns of cortical and BG connectivity within thalamus

The differential cortical connectivity patterns within thalamus (Fig. 1B) mapped closely onto the probabilistic thalamic atlas by Behrens et al. (2003) and results from our previous study. In summary, PFC was preferentially connected with mediodorsal (MD), intralaminar (IL), ventral anterior (VA), and ventral lateral (VL) nuclei, whereas PPC, TEM, and OCC were predominantly connected with PUL. Sensorimotor connections occupied VL and VPL. For BG connectivity within thalamus, we found STR and GPe connections to reside in similar thalamic subregions as PFC connections, while GPi, SN, and STN were concentrated in sensorimotor thalamic zones (VL and VPL).

Univariate tests of thalamo-cortical and thalamo-BG connectivity

Voxelwise comparisons of thalamo-cortical and thalamo-BG connectivity clusters revealed significant differences for VS v. EMCS, VS v. MCS-, MCS- v. EMCS, and MCS+ v. EMCS after controlling for age, gender, etiology, and DPI (Table 2, Fig. 1). While EMCS showed higher left THAL-S1, bilateral THAL-PFC and THAL-STR connectivity when compared to VS, it exhibited lower THAL-OCC connectivity when compared against MCS+ (right) and MCS- (bilateral). MCS- also demonstrated greater left THAL-PFC connectivity than VS. No significant differences were observed for VS v. MCS+ and MCS- v. MCS+.

Multivariate classification of whole-brain thalamic tracks

Using whole-brain thalamic tractograms (Fig. 2) as features for a 4-way classification of patient groups resulted in discriminative features found throughout the brain, encompassing every major cortical division (Table 3, Fig. 3). Highlighting the main results, frontal pole, sensorimotor regions, precuneus, lateral occipital cortex (LOC), and cerebellum appeared to be the largest significant clusters.

Discussion

We identified two main patterns of univariate thalamofugal connectivity differences between a subset of DOC groups that were relatively consistent with results from Zheng et al. (2017)–differences in thalamo-PFC and thalamo-OCC connectivity, although the specific group comparisons yielding the significant results differed between the two studies. In the previous study, no EMCS group was available, and MCS+, contrasting with VS, demonstrated significantly greater prefrontal connectivity with components of the central thalamus. In this study, comparing VS to MCS subcategories, greater connections between the thalamus and prefrontal cortex were uncovered in MCS- and EMCS, with EMCS additionally exhibiting higher thalamo-S1 and thalamo-striatal connectivity. The integrity of the thalamo-prefrontal system has been proposed to subserve willful behavior and repeatedly shown to be involved in the context of DOC (Laureys et al., 2000; Monti et al., 2015; Schiff, 2010; Zheng et al., 2017). Moreover, the topographical pattern of striatal connectivity within the thalamus resembled greatly of prefrontal connectivity within thalamus, both occupying regions known to be part of the central thalamus, a collection of thalamic nuclei crucial for regulating arousal and awareness (Schiff, 2008), whereby selective damage has been correlated with severity

of consciousness impairment (Lutkenhoff et al., 2013, 2015; Maxwell et al., 2006) and targeted deep brain stimulation (DBS) of this area has been associated with behavioral improvement (Schiff et al., 2007). Given that the striatum is intimately connected with PFC, the presence of similar subregions of preferred thalamic connectivity suggests that the thalamus, striatum, and prefrontal cortex may encompass a shared circuitry. This is in alignment with the mesocircuit hypothesis positing that the connections between the central thalamus, striatum, and prefrontal cortex may be particularly vulnerable following severe brain injury. Nonetheless, a recent DTI study found that DOC patients exhibited abnormal connectivity between the striatum, thalamus, and frontal cortex when compared to controls (Weng et al., 2017).

On the other hand, when EMCS was compared against MCS+ and MCS-, lower thalamo-occipital connectivity was detected. This paradoxical pattern of reduced connectivity in patients on the higher end of the consciousness spectrum compared to the lower end has been previously shown in Zheng et al. (2017), but for the VS > MCS- contrast. We speculate that following severe brain injury leading to impaired consciousness, higher-order cortices such as frontoparietal and temporal regions, whose activity have been consistently revealed to be reduced in a meta-analysis of DOC studies (Hannawi et al., 2015), may be more damaged compared to the occipital cortex. Thus, with the occipital cortex relatively spared, the brain may rely more heavily on this region to undergo changes as part of the compensatory or recovery process.

Employing a 4-way classification scheme to detect systematic differences along the thalamic tracks successfully distinguished VS, MCS-, MCS+, and EMCS patients, with thalamic tracks reaching the motor region displaying the highest classification

accuracy, up to 53%, where 25% is chance. Differences in thalamo-motor connectivity across these patient groups may underlie the severity of their motor impairment, which may hinder their ability to respond to behavioral stimulation and demonstrate residual awareness (Fernández-Espejo et al., 2015; Zheng et al., 2017). Considering that DOC exhibit highly variable patterns of pathology, coupled with secondary injuries and compensatory changes, we found additional discriminative regions that spanned every major cortical zone. This widespread pattern of classifiable differences was also observed in Zheng et al. (2017). Some of these regions have been widely reported in DOC literature, including frontoparietal networks (Di Perri et al., 2014; Laureys et al., 1999, 2004; Laureys, 2005). Other less extensively reported regions that were identified in the multivariate classification involved thalamic tracks into the lateral occipital cortex (LOC) and cerebellum. Thalamic projections to the LOC have been consistently informative in our classifications, where 100% accuracy had been detected in classifying between VS and MCS- in our previous study. These findings additionally corroborate the univariate results. Regarding the cerebellum, variable abnormalities in this region have been noted in DOC patients with hypoxic-ischaemic brain injury (Adams et al., 2000), and cerebellar white matter changes over time in an MCS patient have correlated with motor improvements (Voss et al., 2006). Discriminative features in the cerebellum may additionally highlight the variability in motor functions across these patients.

Limitations

A few limitations should be addressed. First, due to the rarity of DOC patients and the need to exclude a sizable portion of the patients after quality control, on top of

further subdividing MCS into three subgroups, the sample size for each group was greatly reduced, especially for the MCS categories, which were highly imbalanced with the VS group. This may have introduced greater difficulty in finding significant differences between VS and MCS, particularly for VS and MCS+. The fact that thalamo-prefrontal differences resurfaced in this study underscores the system's critical role in consciousness, consistent with existing literature. Secondly, while our data were greatly enhanced with 64 directions compared to only 12 directions from our previous study, the difficulty in resolving crossing fibers still persists as a major limitation of DTI. Our estimation of the diffusion parameters with modeling multiple fibers per voxel for probabilistic tractography could partially mitigate the concern. Lastly, the polarity of the connections could not be distinguished in diffusion tractography, so whether the thalamic connectivity differences were due to efferent or afferent pathways remain indiscernible.

Conclusion

We conducted a replication study in a separate cohort of DOC patients to evaluate differences in thalamofugal connectivity across VS, MCS-, MCS+, and EMCS patients. Setting aside specific group comparisons, a general pattern of increased thalamo-prefrontal and decreased thalamo-occipital connections for patients on the higher end of the DOC spectrum compared to the lower end was replicated across the previous and current study. We additionally implemented a 4-way classification approach using whole-brain thalamic tractograms to automatically disentangle patients with varying levels of consciousness impairment and localized regions in distributed thalamo-cortical networks that were highly informative. DTI coupled with searchlight

classification could provide reliable biomarkers to assist in the clinical assessment of disorders of consciousness.

Tables

Table 1. Demographic and clinical information

						CRS-R Scores						
Patient	Diagnosis	Gender	Age	DPI	Etiology	Motor	Visual	Arousal	Auditory	Comm.	Oromotor	Total
P01	VS	M	66	21	NT	2	0	2	1	0	2	7
P02	VS	F	52	284	O	2	1	2	0	0	2	7
P03	VS	M	73	93	NT	2	1	2	1	0	2	8
P04	VS	M	68	19	T	2	1	2	1	0	2	8
P05	VS	F	30	569	T	NA	NA	NA	NA	NA	NA	NA
P06	VS	F	44	8	NT	2	2	1	2	0	2	9
P07	VS	M	21	170	O	1	0	1	0	0	1	3
P08	VS	M	21	196	T	2	0	2	1	0	2	7
P09	VS	F	53	20	O	2	0	1	1	0	1	5
P10	VS	F	38	1684	NT	1	0	2	1	0	1	5
P11	VS	F	62	32	NT	1	1	1	1	0	1	5
P12	VS	M	47	8	NT	1	0	2	2	0	2	7
P13	VS	M	55	26	NT	2	0	2	0	0	1	5
P14	VS	M	41	320	NT	2	0	2	1	0	1	6
P15	VS	M	55	66	NT	2	0	1	1	0	1	5
P16	VS	F	25	235	T	2	0	1	1	0	2	6
P17	VS	F	34	34	NT	2	0	1	0	0	1	4
P18	VS	F	54	561	NT	2	1	1	1	0	1	6
P19	VS	M	51	296	NT	2	0	1	1	0	1	5
P20	VS	F	27	117	O	1	1	2	1	0	1	6
P21	VS	M	53	51	NT	2	1	2	1	0	1	7
P22	VS	F	45	34	NT	2	1	2	1	0	1	7
P23	VS	F	44	109	NT	2	0	2	1	0	2	7
P24	VS	F	64	24	NT	NA	NA	NA	NA	NA	NA	NA
P25	VS	M	41	414	T	1	1	2	0	0	1	5

P26	VS	M	49	2884	NT	1	1	2	1	0	2	7
P27	VS	M	57	258	NT	2	0	2	1	0	1	6
P28	VS	M	60	9	NT	0	0	2	1	0	0	7
P29	VS	F	40	732	NT	1	0	2	2	0	1	6
P30	VS	F	31	843	T	2	0	2	1	0	1	6
P31	VS	M	31	1451	T	2	1	2	1	0	1	7
P32	MCS-	M	24	319	NT	3	1	2	2	0	2	10
P33	MCS-	F	58	25	NT	2	3	2	2	0	1	10
P34	MCS-	M	55	495	NT	5	4	2	2	0	2	15
P35	MCS-	M	62	18	NT	NA	NA	NA	NA	NA	NA	NA
P36	MCS-	M	39	1597	T	2	3	2	2	0	2	11
P37	MCS-	F	50	233	T	5	0	2	0	0	1	8
P38	MCS-	F	48	471	NT	1	2	2	2	0	2	9
P39	MCS+	M	26	1462	O	2	3	2	3	0	2	12
P40	MCS+	M	30	589	T	3	1	2	3	0	2	11
P41	MCS+	F	74	19	NT	1	0	1	1	1	1	5
P42	MCS+	M	50	258	T	2	4	2	3	0	2	13
P43	MCS+	M	51	20	NT	2	5	2	3	1	3	16
P44	MCS+	M	54	35	T	3	4	2	3	0	1	13
P45	MCS+	F	38	37	NT	0	3	2	3	0	2	10
P46	MCS+	M	24	2690	O	5	3	2	3	0	1	14
P47	MCS+	M	30	400	T	5	4	2	3	2	2	18
P48	MCS+	F	30	45	T	2	3	2	3	0	2	12
P49	MCS+	M	25	2129	T	2	0	2	3	0	2	9
P50	MCS+	F	47	209	NT	2	0	2	3	0	1	8
P51	MCS+	F	63	115	NT	2	3	2	3	2	3	15
P52	MCS+	M	72	3067	NT	2	3	2	3	0	2	12
P53	MCS+	M	25	533	T	2	4	2	3	0	2	13
P54	EMCS	M	37	1346	NT	5	5	3	4	2	3	22
P55	EMCS	F	34	388	T	6	5	3	4	2	3	23
P56	EMCS	M	18	429	T	5	4	2	3	2	3	19

P57	EMCS	M	52	151	T	6	5	3	4	2	3	23
P58	EMCS	M	66	52	T	5	4	3	3	2	3	20
P59	EMCS	M	37	263	NT	6	5	3	4	2	3	23
P60	EMCS	F	45	38	NT	6	5	1	4	2	3	21
P61	EMCS	M	24	425	T	6	5	3	4	2	3	23
P62	EMCS	F	54	2122	T	2	5	3	4	2	1	17
P63	EMCS	M	24	35	T	6	5	2	4	2	1	20
P64	EMCS	M	44	298	T	6	5	2	4	2	2	21
P65	EMCS	F	36	2113	T	6	5	3	4	2	3	23
P66	EMCS	M	61	413	NT	6	5	3	4	2	3	23

Abbreviations: Comm. = Communication; T = Traumatic; NT = Nontraumatic; O = Other

Table 2. Univariate results: thalamo-cortical and thalamo-striatal connectivity differences

Statistical Tests	Target ROI	Thalamic Subregions	Total Cluster Size (Voxels)
EMCS > VS	L. PFC	MD, ILN, VA, VL	169
		ILN, VA, VL, MD	
	R. PFC	VPM, AN, VPL	223
	L. S1	VPL, LP, PUL, VL	47
	L. STR	VL, VA, MD, ILN	235
	R. STR	VA, ILN, VL	93
		ILN, VL, MD, VPM,	
MCS- > VS	L. PFC	VPL	170
MCS+ > EMCS	R. OCC	PUL	38
MCS- > EMCS	L. OCC	PUL	44
	R. OCC	PUL	27

Voxel Size = 2 x 2 x 2 mm

Abbreivations: MD = Mediodorsal; ILN = Intralaminar Nucleus; VA = Ventral Anterior Nucleus; VL = Ventral Lateral Nucleus; VPM = Ventral Posterior Medial; VPL = Ventral Posterior Lateral; LP = Lateral Posterior; PUL = Pulvinar

Table 3. 4-way searchlight classification results

Track Region	4-Way Classification			
	L. Thal Tracks		R. Thal Tracks	
Prefrontal	ipsi.	contra.	ipsi.	contra.
Frontal Pole	–	46 (178)	46 (453)	46 (642)
Sup. Frontal	–	–	–	40 (106)
Mid. Frontal	41 (53)	–	–	45 (58)
Orbitofrontal	–	–	42 (111)	48 (69)
Ant. Cing.	39 (50)		46 (72)	
Sensorimotor				
M1/PMC/SMA	53 (253)	44 (286)	47 (236)	45 (480)
S1	–	45 (126)	48 (273)	41 (88)
Posterior Parietal				
Precuneus	39 (105)		46 (92)	
Inf. Parietal	–	–	40 (69)	–
Sup. Parietal	–	45 (56)	43 (113)	44 (79)
Temporal				
Temporal Pole				51 (125)
Occipital				
Lat. Occipital	40 (133)	42 (184)	49 (175)	43 (322)
Subcortical				
Cerebellum	37 (71)	–	–	40 (324)

Abbreviations: Ant. Cing. = Anterior Cingulate; Inf. = Inferior; Sup. = Superior; Lat = Lateral; M1 = Primary Motor Cortex; S1 = Primary Somatosensory Cortex; PMC = Premotor Cortex; SMA = Supplemental Motor Area

Figures

Figures 1. Thalamo-cortical and thalamo-basal ganglia connectivity

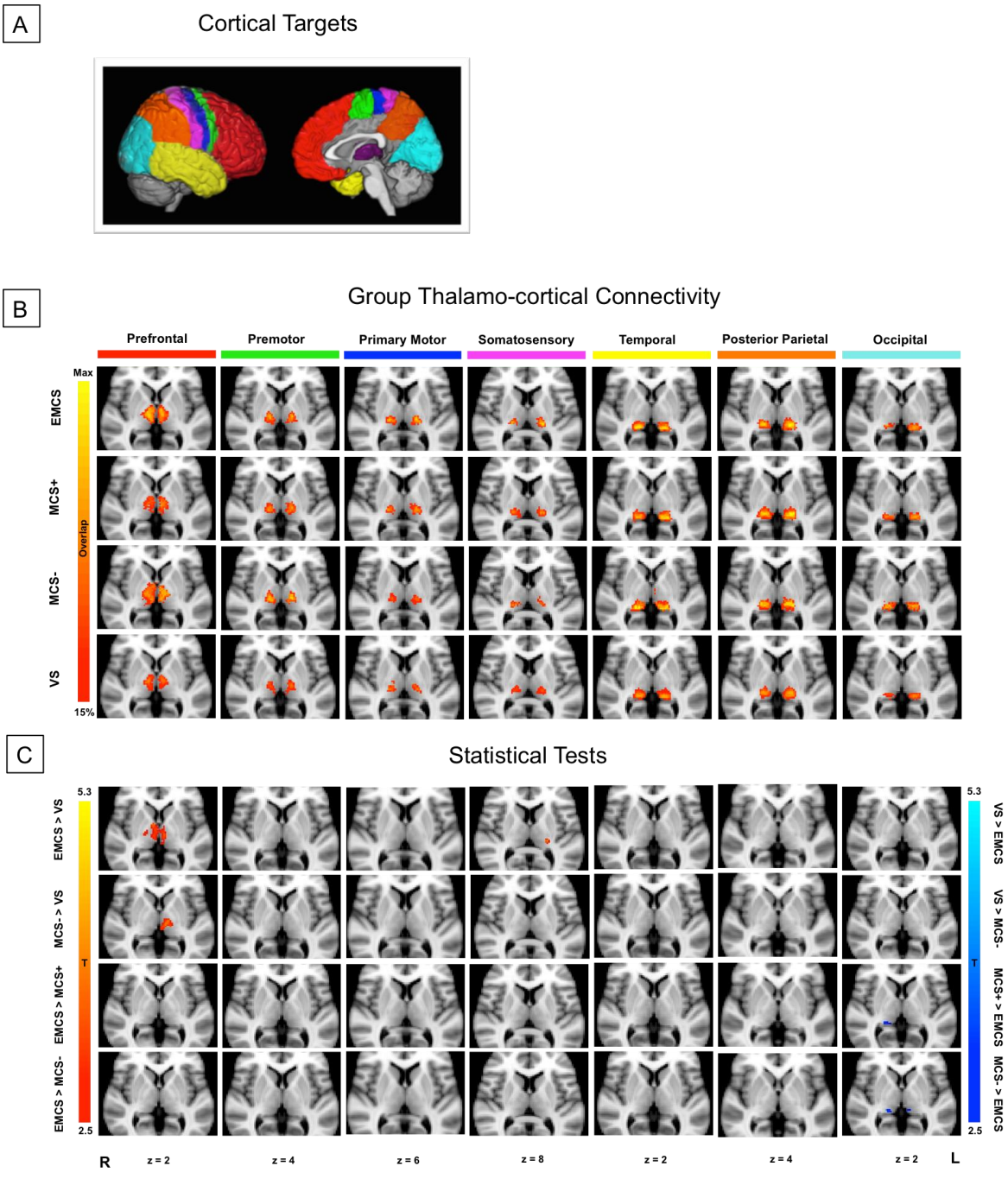

D

Subcortical Targets

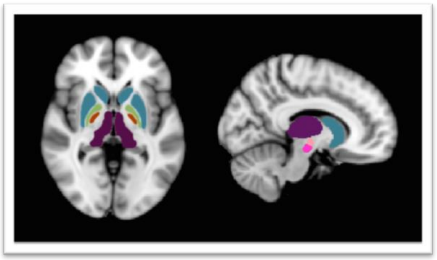

E

Group Thalamo-Basal Ganglia Connectivity

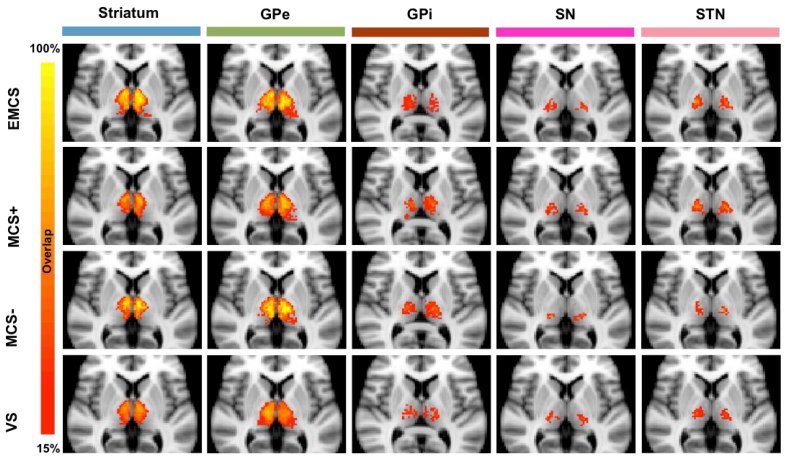

F

Statistical Tests

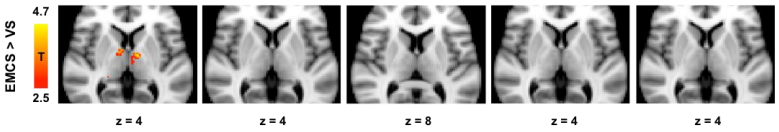

Thalamo-cortical results are shown in A-C. Thalamo-basal ganglia results are displayed from D-F.

Figures 2. Whole-brain thalamic pathways

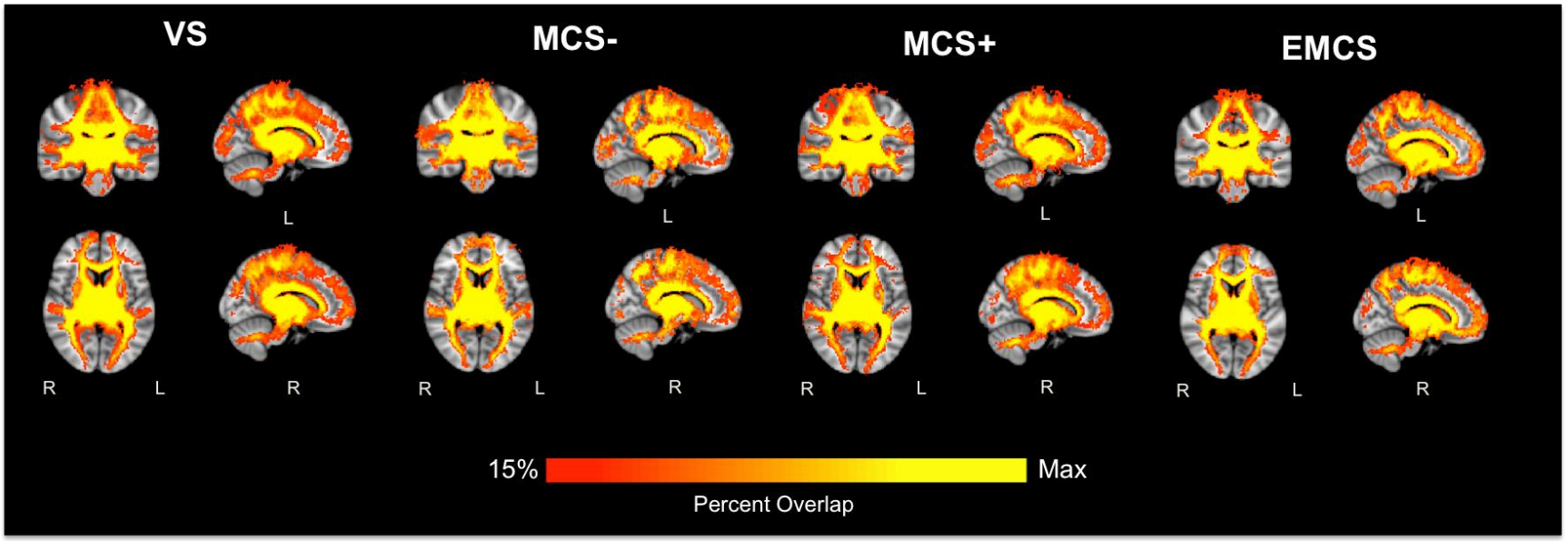

Left and right thalamic pathways are combined for ease of visualization.

Figure 3. 4-way classification results

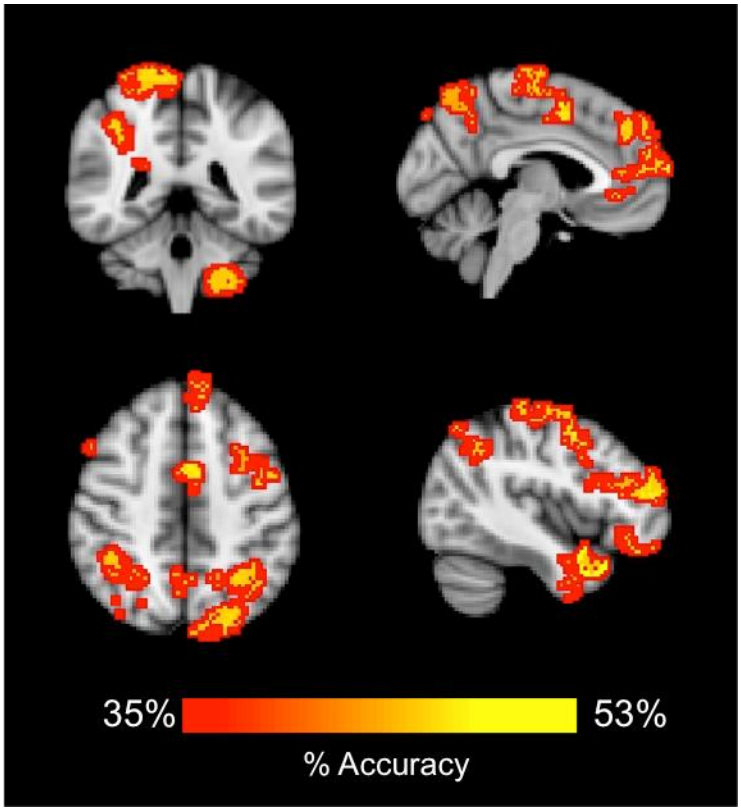

Results from the left and right thalamic tracks are combined for visualization purposes. For enhanced display of the clusters, accuracy maps are thickened with a red border.

References

Adams, J. H., Graham, D. I., and Jennett, B. (2000). The neuropathology of the vegetative state after an acute brain insult. *Brain J. Neurol.* 123 (Pt 7), 1327–1338.

Avants, B. B., Tustison, N. J., Song, G., Cook, P. A., Klein, A., and Gee, J. C. (2011). A Reproducible Evaluation of ANTs Similarity Metric Performance in Brain Image Registration. *NeuroImage* 54, 2033–2044. doi:10.1016/j.neuroimage.2010.09.025.

Behrens, T. E. J., Johansen-Berg, H., Woolrich, M. W., Smith, S. M., Wheeler-Kingshott, C. a. M., Boulby, P. A., et al. (2003). Non-invasive mapping of connections between human thalamus and cortex using diffusion imaging. *Nat. Neurosci.* 6, 750–757. doi:10.1038/nn1075.

Di Perri, C., Stender, J., Laureys, S., and Gosseries, O. (2014). Functional neuroanatomy of disorders of consciousness. *Epilepsy Behav. EB* 30, 28–32. doi:10.1016/j.yebeh.2013.09.014.

Eklund, A., Dufort, P., Villani, M., and LaConte, S. (2014). BROCCOLI: Software for fast fMRI analysis on many-core CPUs and GPUs. *Front. Neuroinformatics* 8. doi:10.3389/fninf.2014.00024.

Fernández-Espejo, D., Junque, C., Bernabeu, M., Roig-Rovira, T., Vendrell, P., and Mercader, J. M. (2010). Reductions of thalamic volume and regional shape changes in the vegetative and the minimally conscious states. *J. Neurotrauma* 27, 1187–1193. doi:10.1089/neu.2010.1297.

Fernández-Espejo, D., Rossit, S., and Owen, A. M. (2015). A Thalamocortical Mechanism for the Absence of Overt Motor Behavior in Covertly Aware Patients. *JAMA Neurol.* 72, 1442–1450. doi:10.1001/jamaneurol.2015.2614.

Giacino, J. T., Ashwal, S., Childs, N., Cranford, R., Jennett, B., Katz, D. I., et al. (2002). The minimally conscious state: definition and diagnostic criteria. *Neurology* 58, 349–353.

Giacino, J. T., Schnakers, C., Rodriguez-Moreno, D., Kalmar, K., Schiff, N., and Hirsch, J. (2009). Behavioral assessment in patients with disorders of consciousness: gold standard or fool's gold? *Prog. Brain Res.* 177, 33–48. doi:10.1016/S0079-6123(09)17704-X.

Hannawi, Y., Lindquist, M. A., Caffo, B. S., Sair, H. I., and Stevens, R. D. (2015). Resting brain activity in disorders of consciousness. *Neurology* 84, 1272–1280. doi:10.1212/WNL.0000000000001404.

Jenkinson, M., Bannister, P., Brady, M., and Smith, S. (2002). Improved optimization for the robust and accurate linear registration and motion correction of brain images. *NeuroImage* 17, 825–841.

Jennett, B., and Plum, F. (1972). Persistent vegetative state after brain damage. A syndrome in search of a name. *Lancet Lond. Engl.* 1, 734–737.

Keuken, M. C., and Forstmann, B. U. (2015). A probabilistic atlas of the basal ganglia using 7 T MRI. *Data Brief* 4, 577–582. doi:10.1016/j.dib.2015.07.028.

Lant, N. D., Gonzalez-Lara, L. E., Owen, A. M., and Fernández-Espejo, D. (2016). Relationship between the anterior forebrain mesocircuit and the default mode network in the structural bases of disorders of consciousness. *NeuroImage Clin.* 10, 27–35. doi:10.1016/j.nicl.2015.11.004.

Laureys, S. (2005). The neural correlate of (un)awareness: lessons from the vegetative state. *Trends Cogn. Sci.* 9, 556–559. doi:10.1016/j.tics.2005.10.010.

Laureys, S., Faymonville, M., Luxen, A., Lamy, M., Franck, G., and Maquet, P. (2000). Restoration of thalamocortical connectivity after recovery from persistent vegetative state. *The Lancet* 355, 1790–1791. doi:10.1016/S0140-6736(00)02271-6.

Laureys, S., Goldman, S., Phillips, C., Van Bogaert, P., Aerts, J., Luxen, A., et al. (1999). Impaired effective cortical connectivity in vegetative state: preliminary investigation using PET. *NeuroImage* 9, 377–382. doi:10.1006/nimg.1998.0414.

Laureys, S., Owen, A. M., and Schiff, N. D. (2004). Brain function in coma, vegetative state, and related disorders. *Lancet Neurol.* 3, 537–546. doi:10.1016/S1474-4422(04)00852-X.

Lutkenhoff, E. S., Chiang, J., Tshibanda, L., Kamau, E., Kirsch, M., Pickard, J. D., et al. (2015). Thalamic and extrathalamic mechanisms of consciousness after severe brain injury. *Ann. Neurol.* 78, 68–76. doi:10.1002/ana.24423.

Lutkenhoff, E. S., McArthur, D. L., Hua, X., Thompson, P. M., Vespa, P. M., and Monti, M. M. (2013). Thalamic atrophy in antero-medial and dorsal nuclei correlates with six-month outcome after severe brain injury. *NeuroImage Clin.* 3, 396–404. doi:10.1016/j.nicl.2013.09.010.

Maxwell, W. L., MacKinnon, M. A., Smith, D. H., McIntosh, T. K., and Graham, D. I. (2006). Thalamic nuclei after human blunt head injury. *J. Neuropathol. Exp. Neurol.* 65, 478–488. doi:10.1097/01.jnen.0000229241.28619.75.

Monti, M. M., Rosenberg, M., Finoia, P., Kamau, E., Pickard, J. D., and Owen, A. M. (2015). Thalamo-frontal connectivity mediates top-down cognitive functions in disorders of consciousness. *Neurology* 84, 167–173. doi:10.1212/WNL.0000000000001123.

Monti, M. M., Vanhaudenhuyse, A., Coleman, M. R., Boly, M., Pickard, J. D., Tshibanda, L., et al. (2010). Willful modulation of brain activity in disorders of consciousness. *N. Engl. J. Med.* 362, 579–589. doi:10.1056/NEJMoa0905370.

Oguz, I., Farzinfar, M., Matsui, J., Budin, F., Liu, Z., Gerig, G., et al. (2014). DTIPrep: quality control of diffusion-weighted images. *Front. Neuroinformatics* 8. doi:10.3389/fninf.2014.00004.

Rilling, J. K., Glasser, M. F., Jbabdi, S., Andersson, J., and Preuss, T. M. (2011). Continuity, divergence, and the evolution of brain language pathways. *Front. Evol. Neurosci.* 3, 11. doi:10.3389/fnevo.2011.00011.

Schiff, N. D. (2008). Central thalamic contributions to arousal regulation and neurological disorders of consciousness. *Ann. N. Y. Acad. Sci.* 1129, 105–118. doi:10.1196/annals.1417.029.

Schiff, N. D. (2010). Recovery of consciousness after brain injury: a mesocircuit hypothesis. *Trends Neurosci.* 33, 1–9. doi:10.1016/j.tins.2009.11.002.

Schiff, N. D., Giacino, J. T., Kalmar, K., Victor, J. D., Baker, K., Gerber, M., et al. (2007). Behavioural improvements with thalamic stimulation after severe traumatic brain injury. *Nature* 448, 600–603. doi:10.1038/nature06041.

Schnakers, C., Vanhaudenhuyse, A., Giacino, J., Ventura, M., Boly, M., Majerus, S., et al. (2009). Diagnostic accuracy of the vegetative and minimally conscious state: Clinical consensus versus standardized neurobehavioral assessment. *BMC Neurol.* 9, 35. doi:10.1186/1471-2377-9-35.

Smith Stephen M. (2002). Fast robust automated brain extraction. *Hum. Brain Mapp.* 17, 143–155. doi:10.1002/hbm.10062.

Voss, H. U., Uluç, A. M., Dyke, J. P., Watts, R., Kobylarz, E. J., McCandliss, B. D., et al. (2006). Possible axonal regrowth in late recovery from the minimally conscious state. *J. Clin. Invest.* 116, 2005–2011. doi:10.1172/JCI27021.

Weng, L., Xie, Q., Zhao, L., Zhang, R., Ma, Q., Wang, J., et al. (2017). Abnormal structural connectivity between the basal ganglia, thalamus, and frontal cortex in patients with disorders of consciousness. *Cortex* 90, 71–87. doi:10.1016/j.cortex.2017.02.011.

Zheng, Z. S., Reggente, N., Lutkenhoff, E., Owen, A. M., and Monti, M. M. (2017). Disentangling disorders of consciousness: Insights from diffusion tensor imaging and machine learning. *Hum. Brain Mapp.* 38, 431–443. doi:10.1002/hbm.23370.

Study 3: Connectivity-Based Segmentation of the Human External Globus Pallidus with High Angular Resolution Diffusion Imaging

Introduction

The external segment of the globus pallidus (GPe) is the second largest structure within the basal ganglia (BG), after the striatum. Though possessing the most extensive efferent connections within BG (Qiu et al., 2016), this structure has largely been underappreciated. Until recently, the GPe was perceived as a homogenous relay structure as a part of the motor-suppressing indirect pathway of BG. Recent insights from animal studies, however, reveal a diverse makeup of cell types with different projection patterns occupying the GPe (Gittis et al., 2014; Mastro et al., 2014) and at least three functional subdivisions representing a limbic, associative, and sensorimotor territory that correspond to anteroventral, middle (anterodorsal), and posterior ventrolateral GPe, respectively (François et al., 2004; Grabli et al., 2004). These functional territories are believed to be conserved throughout the extent of the BG circuit and are closely related to different frontal cortical regions (Alexander et al., 1986; Haber, 2003; Parent and Hazrati, 1995). The limbic circuit is implicated in motivation or goal selection, the associative circuit in selection of action, and the sensorimotor circuit in selection and execution of movement (Tremblay et al., 2015). Dysfunctions in these circuits have been associated with various behavioral and movement disorders, including obsessive-compulsive disorder (OCD), attention deficit/hyperactivity disorder (AD/HD), Tourette's syndrome, Parkinson's disease, etc. (Tremblay et al., 2015).

While behaviorally distinct subregions of GPe have been identified through a few animal studies (François et al., 2004; Grabli et al., 2004), such functional and

anatomical organization has not been well characterized in humans. A non-invasive technique such as diffusion-weighted imaging, which allows the analysis of water diffusion to infer tissue microstructure, offers an indispensable tool to study structural connectivity in-vivo (Pierpaoli and Basser, 1996). Connectivity-based segmentation using probabilistic tractography (Behrens et al., 2003), has been successfully demonstrated in a number of brain regions using the diffusion tensor imaging (DTI) model. However, the DTI model is limited in its ability to represent the complexity of crossing fibers. Thus, high angular resolution diffusion imaging (HARDI) is needed to help resolve this limitation and provide a more accurate representation of water diffusion within a voxel (Berman et al., 2013). In this study, we thus aim to delineate the three functional-anatomical subdomains of GPe in humans and explore their connectivity patterns with cortical and subcortical targets using HARDI data from the human connectome project (HCP).

Methods

HCP data. 50 healthy subjects' data from the HCP Q3 release (http://www.humanconnectome.org) were initially included in this study (Van Essen et al., 2012). However, three subjects were excluded due to poor clustering results that precluded a clear identification of an anterior, middle, and posterior GPe cluster. 47 subjects (23 males; 24 females; ages 22-35 years) remained in the final analysis. A Siemens Skyra 3T scanner was used to acquire all the imaging data. For the purpose of this study, only T1-weighted (TR = 2400 ms; TE = 2.14 ms; flip angle = 8°; FOV = 224x224 mm; voxel size = 0.7mm isotropic) and diffusion-weighted HARDI (TR = 5520 ms; TE = 89.5 ms; flip angle = 78°; FOV = 210x180 mm; voxel size = 1.25 mm isotropic;

3 shells of b = 1000, 2000, and 3000 s/mm^2 with 90 diffusion directions per shell) were used. Preprocessing was already performed by the HCP, which included B0 image intensity normalization, EPI distortions correction, eddy current correction, motion correction, and gradient-nonlinearities correction (Glasser et al., 2013).

GPe segmentation. The goal of this step was to parcellate GPe into three subregions based on connectivity with the rest of the brain. Preprocessed diffusion data were analyzed using FSL's diffusion toolbox. After estimating the probability distribution of fiber orientations using 3 fibers per voxel with 1000 burn-in iterations and multi-shell modeling (Jbabdi et al., 2012), probabilistic tractography was carried out with 5000 samples drawn per voxel from the GPe seed mask, which was obtained from the Keuken and Forstmann probabilistic basal ganglia atlas (Keuken and Forstmann, 2015) and transformed into individual subject space. Moreover, a down-sampled lower resolution whole brain mask (5 x 5 x 5 mm^3) was used as the target. Connectivity values between each seed voxel and each whole-brain target voxel were recorded and a cross-correlation matrix was generated. Automated segmentation of GPe was achieved through k-means clustering (Hartigan and Wong, 1979) with three clusters specified. Three clusters were chosen based on a priori knowledge from existing literature suggesting a limbic, associative, and sensorimotor zone existing within structures of BG (Alexander et al., 1986) in particular, the monkey GPe (Grabli et al., 2004).

Post-hoc connectivity patterns of GPe clusters. After parcellating GPe into 3 distinct clusters, each cluster was subsequently used as a seed for assessing connectivity with individual cortical and subcortical target regions using Freesurfer (FS) labels available through the HCP database and additional BG masks (internal globus

pallidus [GPi], subthalamic nucleus [STN], and substantia nigra [SN] from the Keuken and Forstmann atlas otherwise not found in FS). After running probabilistic tractography, a threshold of 50 (1% of 5000 samples) (Zhang et al., 2014) was applied to remove spurious connections. Next, the total number of streamlines from each GPe cluster that successfully reached each target was computed. These connectivity values were then normalized and rescaled to account for the differences in seed and target sizes, following steps introduced by Eickhoff et al. (2010). To account for differences in seed size, individual connectivity values were divided by the waytotal (5000 x seed mask size) and then rescaled by multiplying by the average of all waytotals across all seeds and targets. To adjust for the target sizes, the resulting connectivity values were then divided by the size of the targets on an individual basis and then again multiplied by the average size of all targets.

Statistical analysis. To determine whether connectivity strengths to individual targets were significantly different across the three GPe subregions, we first employed repeated measures ANOVA and then post-hoc pairwise comparisons upon finding significance of the ANOVA test. To correct for multiple comparisons, the Benjamini and Hochberg (1995) was implemented, with a false discovery rate set at 5%.

Identification of analogous subregions in BG-thalamic circuitry. As initially proposed by Alexander et al. (1986), different functional territories are maintained throughout the basal ganglia-thalamic circuitry. Therefore, to find the analogous parts in other BG structures and thalamus that are associated with the different GPe clusters, we ran additional tractography analyses with striatum (STR), GPi, SN, STN and thalamus (THAL) set as seeds and the 3 GPe subregions as targets. Again, a threshold

of 50 was used to remove unlikely connections. Then, averaged group connectivity maps were calculated for each seed and target combination before submitting to a winner-takes-all segmentation approach

Results

GPe segmentation. For each hemisphere, kmeans clustering revealed 3 distinct clusters within GPe that reliably corresponded to an anterior (anteroventral), middle (anterodorsal), and posterior subregion (Fig. 1a) in all but 3 subjects. These 3 subjects were excluded in subsequent analyses. Group tractograms from each GPe subregion are shown in Fig. 1b. The group results were achieved by binarizing each subject's individual results in MNI space after thresholding and then summing across all 47 subjects.

Connectivity patterns of GPe subregions. Connectivity strengths (i.e. normalized and rescaled total streamline counts) between each target region and GPe seed are plotted in Fig. 2a and 2b. Despite some similarity in the connectivity patterns across the three clusters, the anterior and middle clusters were more preferentially connected with prefrontal target regions, with anterior GPe favoring frontal pole (FP) and orbitofrontal cortices (OFC), while middle GPe preferred superior frontal gyrus (SFG) and the pars triangularis (PTr) of the inferior frontal gyrus. On the other hand, the posterior cluster was predominantly connected with sensorimotor and selected posterior parietal regions. Low connection probabilities were noted in temporal and occipital cortices. For connection with subcortical structures, all three GPe clusters revealed high connectivity with GPi, with anterior and middle GPe additionally recruiting SN and STN

for their top connections. The results from in-depth investigation of regional BG andTHAL connectivity with GPe clusters are described later.

Statistical comparisons. In the effort to statistically compare connectivity strengths across the GPe clusters, repeated measures ANOVA revealed significant main effects of “seed” ($F = 12$; $p < .001$) and “target” ($F = 342$; $p < 0.0001$), as well as significant “seed × target” interaction ($F = 20$; $p < 0.001$), which reflects differences in individual target connectivity among the GPe seeds. To determine which GPe cluster was most significantly connected with each target, follow-up t-tests were carried out in a pairwise fashion, separately for each hemisphere. Multiple comparisons correction by means of the Benjamini-Hochberg method was applied to p-values generated from all the pairwise comparisons. The p-value cutoff was determined at $p \leq .03$.

Here, we only describe significant connectivity differences between GPe subregions if one subregion is more connected with a target than both the other two subregions. Anterior GPe, when compared against middle and posterior subregions, was significantly more connected with FP, rostral middle frontal gyrus (rMFG), lateral OFC, and SN, bilaterally; and pars orbitalis (POr), accumbens (ACB), and caudate (CAU), right ipsilaterally, and STN, left ipsilaterally. Moreover, we expected anterior GPe to be significantly more connected with medial OFC (involved in limbic processing); however, while the right anterior cluster was more connected with medial OFC than the middle cluster, it did not quite reach statistical significance ($p = .039$) in comparison to posterior GPe with regards to medial OFC connectivity. Comparing cortical connectivity strengths with significantly greater middle GPe than with anterior and posterior GPe, we found targets associated with bilateral SFG and pars triangularis (PTr), and left

ipsilateral pars opercularis (POp). Bilateral sensorimotor regions such as paracentral (PCL), precentral (M1), and postcentral (S1) gyri were significantly more connected with the posterior portion of GPe. While we expected to also see caudal middle frontal gyrus (cMFG), putative premotor/supplemental motor area, to be more significantly connected with posterior GPe, connectivity with middle GPe was equally as high. The majority of posterior parietal, temporal, and occipital regions were also more preferentially connected with the posterior subregion, albeit with generally low connectivity. Moreover, right rostral ACC (rACC) was more connected with posterior GPe than anterior and middle subregions, although rACC connections were much lower in general. (See Fig. 2b for a detailed depiction of all significant pairwise comparisons.)

Identification of analogous subregions in BG-thalamic circuitry. In further characterizing the pattern of connectivity between GPe clusters and the remaining BG structures and thalamus, we found that the anterior-posterior gradient of GPe organization was relatively conserved within these subcortical structures. For example, anterior GPe connections were more concentrated in the anterior ventral portions of striatum, anterior GPi, ventral and medial parts of thalamus including the medial aspect of mediodorsal nucleus (MDm) and ventral anterior nucleus (VA) along with partial ventral lateral nucleus (VL). Moreover, anterior GPe connections also occupied the medial portions of STN and SN. Posterior GPe connected with the body and tail of caudate, posterior putamen, posterior GPi, lateral-most SN, posterolateral STN, and dorsolateral and ventrolateral thalamic nuclear group as well as anterior thalamus. Middle GPe connections occupied dorsal anterior caudate and putamen, and middle segments of GPi, SN, and STN, embedded between anterior and posterior segments.

For thalamic connections with middle GPe, the lateral mediodorsal (MDl) and VA nuclei were identified.

Discussion

Previous animal studies have revealed three functional-anatomical subdomains within GPe that contribute separately to a limbic (anterior, ventral GPe), associative (middle GPe), and sensorimotor (posterior ventrolateral GPe) network. These three subdomains were found to preferentially connect with prefrontal and motor cortices (Grabli et al., 2004). Our results corroborate and extend the existing animal literature by confirming a similarly topographically organized GPe in humans along with evidence for overlap of the functional subdivisions.

Anterior GPe. Research in non-human primates has led to the designation of the anterior ventral GPe as a limbic territory based on stereotypies observed after disruption of this subregion and tracer labeling found in associated limbic areas such as ventromedial striatum, rostromedial prefrontal, and orbitofrontal cortices (François et al., 2004; Gittis et al., 2014; Grabli et al., 2004). Likewise, the anterior ventral portion of GPe in our human subjects displayed connectivity with structures consistent with a limbic profile, namely, lateral OFC, POr, FP (Draganski et al., 2008), medial aspect of MD (Vertes et al., 2015), ACB (Goto and Grace, 2008), medial SN (Haber et al., 1995), and other anterior BG nuclei (Haber et al., 1995; Hamani et al., 2004; Karachi et al., 2005). Moreover, the anterior GPe also revealed robust connectivity with rMFG, which contains the associative dorsolateral prefrontal cortex (DLPFC). This implies that the anterior GPe may not be purely limbic but also exhibit associative/cognitive tendencies. While the three functional circuits within BG are perceived to be largely segregated, the

existence of overlapping connections alludes to more of a functional gradient rather than clear-cut anatomical subdivisions (Karachi et al., 2005; Lambert et al., 2012; Parent and Hazrati, 1995) and promotes the notion of signal integration through converging pathways in cortico-BG circuits.

Posterior GPe. Cortical connections of the posterior GPe were found to reside primarily in the sensorimotor cortices and superior parietal lobule (SPL). The former aligns well with primate studies linking the posterior portion of GPe with motor functions. For example, injection of bicuculline into posterior GPe has been shown to produce abnormal movements (dyskensia, hemiballism) (François et al., 2004; Grabli et al., 2004), and injection of rabies virus into M1 and premotor cortex (PMC) have resulted in neuronal labeling in the posterior GPe, with PMC additionally recruiting the anterodorsal associative GPe (Kelly and Strick, 2004). This may explain why our cMFG (corresponding to PMC/SMA) connectivity was not significantly different between middle and posterior GPe. Moreover, additional sensorimotor-related structures such as the lateral-most extent of SN (presumably SN pars reticulata) (Kha et al., 2001; Zhang et al., 2017), posterior portions of remaining BG nuclei, and ventrolateral thalamic nuclear group (Yelnik et al., 2007) were significantly more connected with posterior GPe. Regarding the robust connectivity with the SPL, a region with diverse cognitive operations (Koenigs et al., 2009), the posterior pallidum (not differentiated) has been reported by Draganski et al. (2008) to project to parietal cortical areas. Other non-sensorimotor related connections of posterior GPe included supposedly limbic regions, such as insula, amygdala, hippocampus, and anterior thalamus. This arrangement shares similarity with the recent discovery of a fourth subdivision of the striatum, located

toward the posterior end (though normally considered sensorimotor), that receives inputs from limbic regions (Hunnicutt et al., 2016). Furthermore, the lack of differentiation between anterior and posterior GPe connectivity with medial OFC could be additional evidence for the posterior subregion partaking in some limbic role. Here, we propose that the posterior GPe may be involved in not only sensorimotor but also associative and limbic functions.

Middle GPe. Situated between the anterior and posterior GPe, the middle GPe exhibited the most variability across subjects. With cortical connectivity mostly concentrated in prefrontal regions, the middle GPe was more significantly connected with SFG, PTr, POp than the former two subregions. These prefrontal targets are known to be involved in higher cognitive functions such as working memory and language processing (Gabrieli et al., 1998). Furthermore, middle GPe connections were found in the lateral aspect of MD, which has been shown to connect with diffuse areas of dorsal and lateral PFC as well as the frontal eye fields (Giguere and Goldman-Rakic, 1988; Xiao et al., 2009) and in the middle or dorsal anterior sections of remaining BG structures, most of which have been regarded as associative territories (Haber et al., 2000; Haber and Calzavara, 2009; Hoover and Strick, 1993; Lambert et al., 2012). Evidence from primate studies also supports middle GPe as an associative territory with relations to PFC, where bicuculline injections into the associative GPe resulted in hyperactive behaviors (Grabli et al., 2004) and viral tracer labeling identified cortical neurons in rostral PMC and caudal PFC (Gittis et al., 2014). It is possible that the rostral PMC may be preferentially connected with middle GPe (Saga et al., 2017) and that the caudal PMC with posterior GPe. Given that DLPFC is made up of mostly SFG and MFG

(Kikinis et al., 2010), to our surprise, the anterior, but not middle GPe, appeared to be most significantly connected with rMFG, though middle GPe still contained a large number of streamlines that reached the rMFG target. Further subdividing the rMFG mask into a rostral and caudal portion for investigating connectivity with the GPe clusters could help shed light on the potential differential contributions from the subregions. Altogether, these findings point to the possibility that the middle GPe, though primarily associative, may also bear higher-order motor characteristics.

Limitations

A number of limitations of MR-based diffusion techniques must be held in mind when interpreting the present results, including the inability to differentiate afferent and efferent connections, susceptibility to false positives and negatives, decreased long-range connections due to superficial white matter tracts, and accurately resolving crossing fibers (Jones et al., 2013; Reveley et al., 2015; Thomas et al., 2014). With respect to our study, the inability to recognize afferent from efferent GPe connections may prevent us from understanding the functional role of this node within the broader cortico-subcortical network. Nonetheless, existing animal tracer studies may help shed some light on the directionality of GPe connections. Diffusion tractography can be particularly prone to false positives or negatives depending on the level of thresholding. While determining what threshold to use is rather subjective, we chose a threshold that was previously used in Zhang et al. (2014) in which similar clustering method was used to segment the region of interest. Moreover, the negative impact of superficial white matter in long-range tractography may be more severe for tracking from the cortex if not nearby a major white matter tract than from a subcortical region, such as GPe, in our

case. We tested this hypothesis by running tractography in both directions for GPe and prefrontal cortex (PFC) and found streamlines from PFC to GPe to be much lower than from GPe to PFC. The last issue with resolving crossing fibers can be mitigated by the use of high angular resolution data (HARDI).

Conclusions

Connectivity based parcellation using probabilistic tracotgraphy revealed a tripartite, topographical organization of the human GPe that coincided with previously described non-human primate anatomy. Through statistical comparisons of selective cortical and subcortical connectivity, the anteroventral, middle, and posterior GPe were confirmed in humans to contain limbic, associative, and sensorimotor properties, respectively, though not uniquely. The existence of partial overlaps is not a novel finding, as growing evidence suggests cross-communication between the circuits. Here, we additionally propose that the anteroventral GPe is limbic-associative, middle GPe is associative-motor (higher-order), and posterior GPe, containing the most diffuse connections, is sensorimotor-limbic with possible associative tendencies as well. The ability to differentiate these anatomical subdomains based on their connectivity patterns could help enhance neurosurgical targeting, particularly in the human GPe, as this region is now recommended as an alternative therapeutic target for treating both motor and nonmotor symptoms of Parkinson's disease.

Figures

Figure 1. Group GPe results

A. Group GPe segmentation results

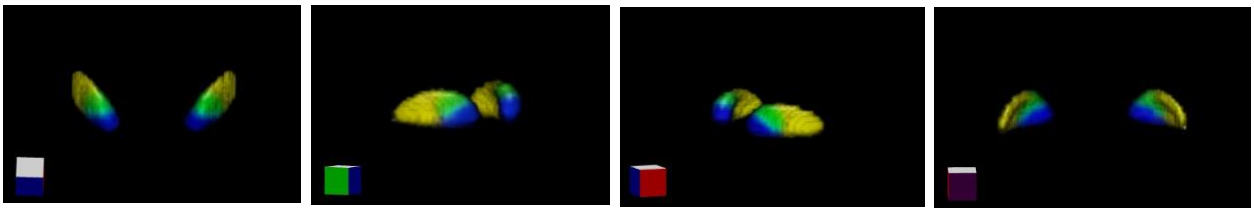

B. Group probabilistic tracts for 3 GPe subregions

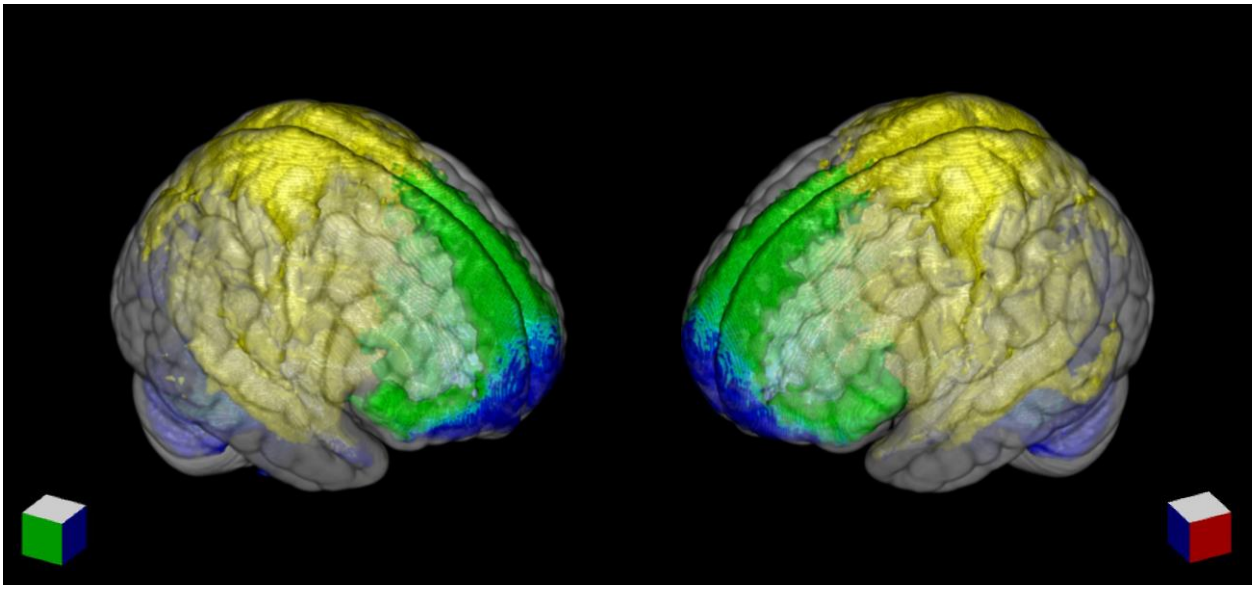

Anterior cluster is blue, middle cluster is green, and posterior cluster is yellow. The cube on the bottom of each image represents the following orientation views: white = superior, blue = anterior, green = left, red = right, purple = posterior.

Figure 2. Cortical and subcortical connectivity patterns of 3 GPe subregions

A. Radar display

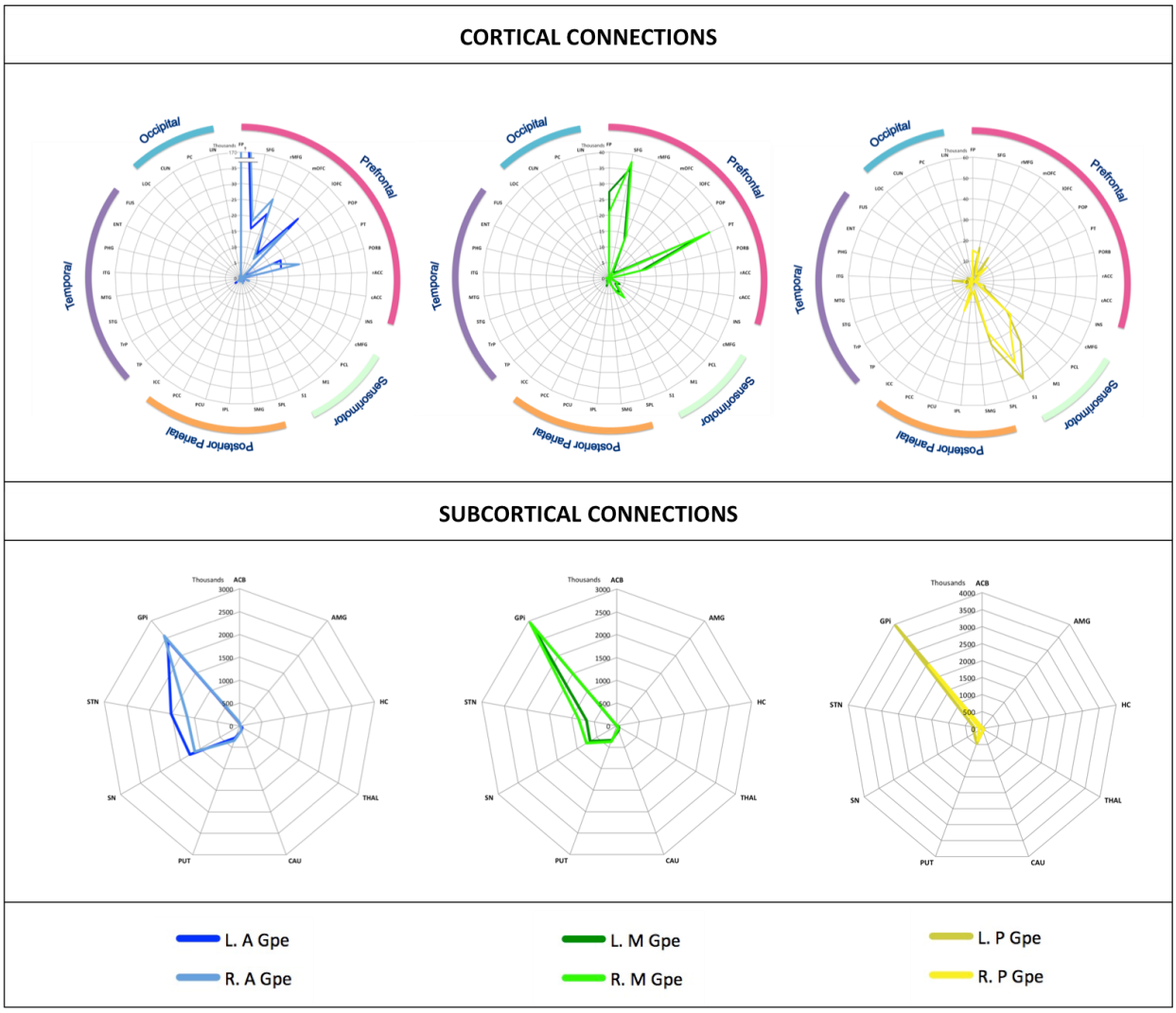

Total streamline counts between the 3 GPe seeds and cortical (top) and subcortical (bottom) targets are plotted.

B. Column Graph

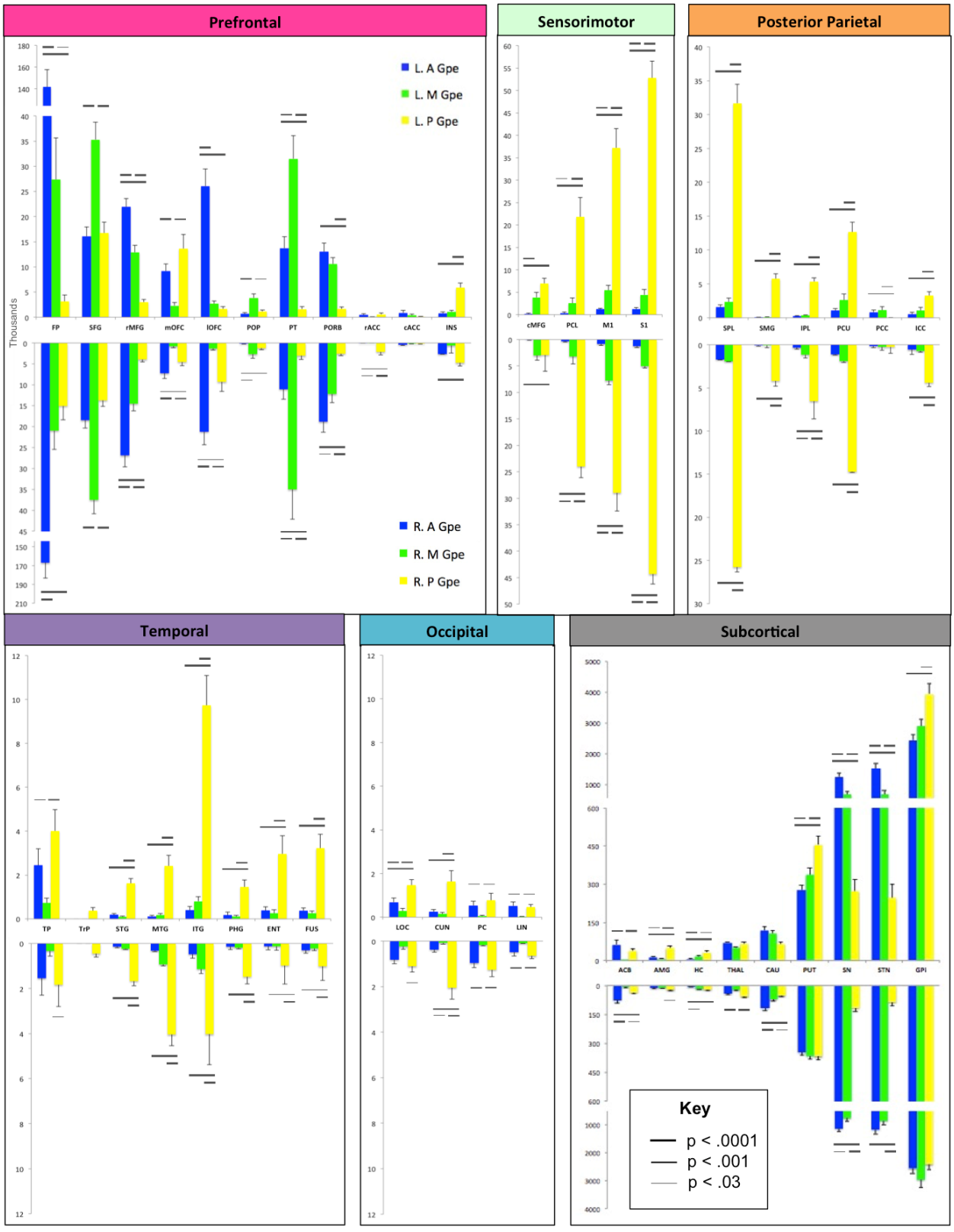

Y-axis = total streamline counts. X-axis = targets. Statistical comparisons between the 3 GPe seeds and their target connectivity are shown.

Abbreviations:

L = Left; R = Right; A = Anterior; M = Middle; P = Posterior; FP = Frontal Pole; SFG = Superior Frontal Gyrus; rMFG = Rostral Middle Frontal Gyrus; mOFC = Medial Orbitofrontal Cortex; lOFC = Lateral Orbitofrontal Gyrus; POP = Pars Opercularis; PT = Pars Triangularis; PORB = Pars Orbitalis; rACC = Rostral Anterior Cingulate Cortex; INS = Insula; cACC = Caudal Anterior Cingulate Cortex; cMFG = Caudal Middle Frontal Gyrus; PCL = Paracentral Lobule; M1 = Precentral Gyrus; S1 = Postcentral Gyrus; SPL = Superior Parietal Lobule; SMG = Supramarginal Gyrus; IPL = Inferior Parietal Lobule; PCU = Precuneus; PCC = Posterior Cingulate Cortex; ICC = Isthmus Cingulate Cortex; TP = Temporal Pole; TrP = Transverse Pole; STG = Superior Temporal Gyrus; MTG = Middle Temporal Gyrus; ITG = Inferior Temporal gyrus; PHG = Parahippocampal Gyrus; ENT = Entorhinal; FUS = Fusiform; LOC = Lateral Occipital Cortex; CUN = Cuneus; PCC = Pericalcarine Cortex; LIN = Lingual Gyrus; ACB = Accumbens; AMG = Amygdala; HC = Hippocampus; THAL = Thalamus; CAU = Caudate; PUT = Putamen; SN = Substantia Nigra; STN = Subthalamic Nucleus; GPi = Internal Globus Pallidus

Figure 3. Segmentation of BG and THAL based on connectivity with 3 GPe subregions

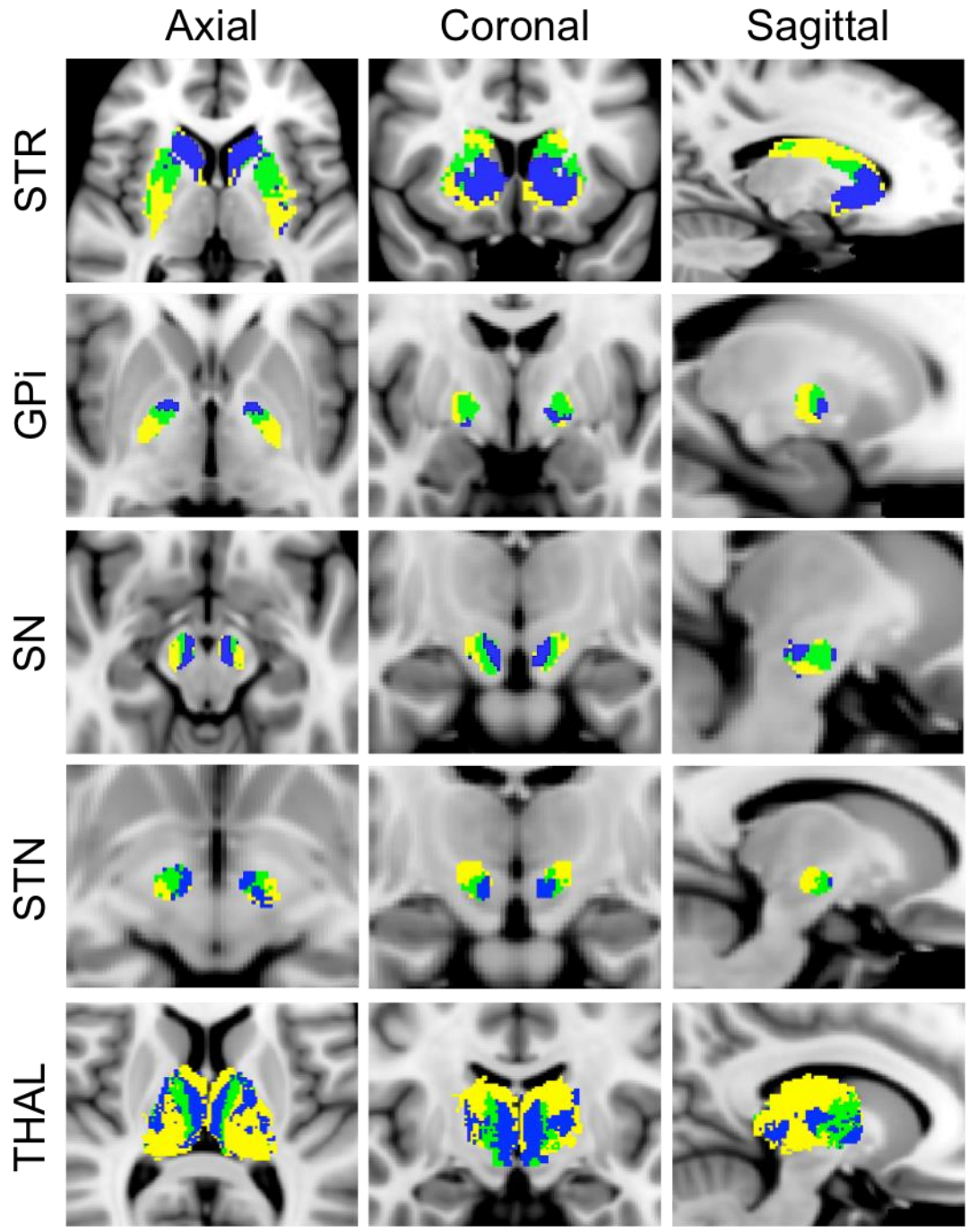

References

Alexander, G. E., DeLong, M. R., and Strick, P. L. (1986). Parallel organization of functionally segregated circuits linking basal ganglia and cortex. *Annu. Rev. Neurosci.* 9, 357–381. doi:10.1146/annurev.ne.09.030186.002041.

Behrens, T. E. J., Johansen-Berg, H., Woolrich, M. W., Smith, S. M., Wheeler-Kingshott, C. a. M., Boulby, P. A., et al. (2003). Non-invasive mapping of connections between human thalamus and cortex using diffusion imaging. *Nat. Neurosci.* 6, 750–757. doi:10.1038/nn1075.

Benjamini, Y., and Hochberg, Y. (1995). Controlling the False Discovery Rate: A Practical and Powerful Approach to Multiple Testing. *J. R. Stat. Soc. Ser. B Methodol.* 57, 289–300. doi:10.2307/2346101.

Berman, J. I., Lanza, M. R., Blaskey, L., Edgar, J. C., and Roberts, T. P. L. (2013). High angular resolution diffusion imaging probabilistic tractography of the auditory radiation. *AJNR Am. J. Neuroradiol.* 34, 1573–1578. doi:10.3174/ajnr.A3471.

Draganski, B., Kherif, F., Klöppel, S., Cook, P. A., Alexander, D. C., Parker, G. J. M., et al. (2008). Evidence for segregated and integrative connectivity patterns in the human Basal Ganglia. *J. Neurosci. Off. J. Soc. Neurosci.* 28, 7143–7152. doi:10.1523/JNEUROSCI.1486-08.2008.

Eickhoff, S. B., Jbabdi, S., Caspers, S., Laird, A. R., Fox, P. T., Zilles, K., et al. (2010). Anatomical and functional connectivity of cytoarchitectonic areas within the human parietal operculum. *J. Neurosci. Off. J. Soc. Neurosci.* 30, 6409–6421. doi:10.1523/JNEUROSCI.5664-09.2010.

François, C., Grabli, D., McCairn, K., Jan, C., Karachi, C., Hirsch, E.-C., et al. (2004). Behavioural disorders induced by external globus pallidus dysfunction in primates II. Anatomical study. *Brain J. Neurol.* 127, 2055–2070. doi:10.1093/brain/awh239.

Gabrieli, J. D. E., Poldrack, R. A., and Desmond, J. E. (1998). The role of left prefrontal cortex in language and memory. *Proc. Natl. Acad. Sci.* 95, 906–913. doi:10.1073/pnas.95.3.906.

Giguere, M., and Goldman-Rakic, P. S. (1988). Mediodorsal nucleus: areal, laminar, and tangential distribution of afferents and efferents in the frontal lobe of rhesus monkeys. *J. Comp. Neurol.* 277, 195–213. doi:10.1002/cne.902770204.

Gittis, A. H., Berke, J. D., Bevan, M. D., Chan, C. S., Mallet, N., Morrow, M. M., et al. (2014). New roles for the external globus pallidus in basal ganglia circuits and behavior. *J. Neurosci. Off. J. Soc. Neurosci.* 34, 15178–15183. doi:10.1523/JNEUROSCI.3252-14.2014.

Glasser, M. F., Sotiropoulos, S. N., Wilson, J. A., Coalson, T. S., Fischl, B., Andersson, J. L., et al. (2013). The minimal preprocessing pipelines for the Human Connectome Project. *NeuroImage* 80, 105–124. doi:10.1016/j.neuroimage.2013.04.127.

Goto, Y., and Grace, A. A. (2008). Limbic and cortical information processing in the nucleus accumbens. *Trends Neurosci.* 31, 552–558. doi:10.1016/j.tins.2008.08.002.

Grabli, D., McCairn, K., Hirsch, E. C., Agid, Y., Féger, J., François, C., et al. (2004). Behavioural disorders induced by external globus pallidus dysfunction in primates: I. Behavioural study. *Brain J. Neurol.* 127, 2039–2054. doi:10.1093/brain/awh220.

Haber, S. N. (2003). The primate basal ganglia: parallel and integrative networks. *J. Chem. Neuroanat.* 26, 317–330.

Haber, S. N., and Calzavara, R. (2009). The cortico-basal ganglia integrative network: the role of the thalamus. *Brain Res. Bull.* 78, 69–74. doi:10.1016/j.brainresbull.2008.09.013.

Haber, S. N., Fudge, J. L., and McFarland, N. R. (2000). Striatonigrostriatal pathways in primates form an ascending spiral from the shell to the dorsolateral striatum. *J. Neurosci. Off. J. Soc. Neurosci.* 20, 2369–2382.

Haber, S. N., Kunishio, K., Mizobuchi, M., and Lynd-Balta, E. (1995). The orbital and medial prefrontal circuit through the primate basal ganglia. *J. Neurosci.* 15, 4851–4867. doi:10.1523/JNEUROSCI.15-07-04851.1995.

Hamani, C., Saint-Cyr, J. A., Fraser, J., Kaplitt, M., and Lozano, A. M. (2004). The subthalamic nucleus in the context of movement disorders. *Brain J. Neurol.* 127, 4–20. doi:10.1093/brain/awh029.

Hoover, J. E., and Strick, P. L. (1993). Multiple output channels in the basal ganglia. *Science* 259, 819–821.

Hunnicutt, B. J., Jongbloets, B. C., Birdsong, W. T., Gertz, K. J., Zhong, H., and Mao, T. (2016). A comprehensive excitatory input map of the striatum reveals novel functional organization. *eLife* 5. doi:10.7554/eLife.19103.

Jbabdi, S., Sotiropoulos, S. N., Savio, A. M., Graña, M., and Behrens, T. E. J. (2012). Model-based analysis of multishell diffusion MR data for tractography: how to get over fitting problems. *Magn. Reson. Med.* 68, 1846–1855. doi:10.1002/mrm.24204.

Jones, D. K., Knösche, T. R., and Turner, R. (2013). White matter integrity, fiber count, and other fallacies: the do's and don'ts of diffusion MRI. *NeuroImage* 73, 239–254. doi:10.1016/j.neuroimage.2012.06.081.

Karachi, C., Yelnik, J., Tandé, D., Tremblay, L., Hirsch, E. C., and François, C. (2005). The pallidosubthalamic projection: an anatomical substrate for nonmotor functions of the subthalamic nucleus in primates. *Mov. Disord. Off. J. Mov. Disord. Soc.* 20, 172–180. doi:10.1002/mds.20302.

Kelly, R. M., and Strick, P. L. (2004). Macro-architecture of basal ganglia loops with the cerebral cortex: use of rabies virus to reveal multisynaptic circuits. *Prog. Brain Res.* 143, 449–459.

Keuken, M. C., and Forstmann, B. U. (2015). A probabilistic atlas of the basal ganglia using 7 T MRI. *Data Brief* 4, 577–582. doi:10.1016/j.dib.2015.07.028.

Kha, H. T., Finkelstein, D. I., Tomas, D., Drago, J., Pow, D. V., and Horne, M. K. (2001). Projections from the substantia nigra pars reticulata to the motor thalamus of the rat: single axon reconstructions and immunohistochemical study. *J. Comp. Neurol.* 440, 20–30.

Kikinis, Z., Fallon, J. H., Niznikiewicz, M., Nestor, P., Davidson, C., Bobrow, L., et al. (2010). GRAY MATTER VOLUME REDUCTION IN ROSTRAL MIDDLE FRONTAL GYRUS IN PATIENTS WITH CHRONIC SCHIZOPHRENIA. *Schizophr. Res.* 123, 153–159. doi:10.1016/j.schres.2010.07.027.

Koenigs, M., Barbey, A. K., Postle, B. R., and Grafman, J. (2009). Superior parietal cortex is critical for the manipulation of information in working memory. *J. Neurosci. Off. J. Soc. Neurosci.* 29, 14980–14986. doi:10.1523/JNEUROSCI.3706-09.2009.

Lambert, C., Zrinzo, L., Nagy, Z., Lutti, A., Hariz, M., Foltynie, T., et al. (2012). Confirmation of functional zones within the human subthalamic nucleus: patterns of connectivity and sub-parcellation using diffusion weighted imaging. *NeuroImage* 60, 83–94. doi:10.1016/j.neuroimage.2011.11.082.

Mastro, K. J., Bouchard, R. S., Holt, H. A. K., and Gittis, A. H. (2014). Transgenic mouse lines subdivide external segment of the globus pallidus (GPe) neurons and reveal distinct GPe output pathways. *J. Neurosci. Off. J. Soc. Neurosci.* 34, 2087–2099. doi:10.1523/JNEUROSCI.4646-13.2014.

Parent, A., and Hazrati, L. N. (1995). Functional anatomy of the basal ganglia. I. The cortico-basal ganglia-thalamo-cortical loop. *Brain Res. Brain Res. Rev.* 20, 91–127.

Pierpaoli, C., and Basser, P. J. (1996). Toward a quantitative assessment of diffusion anisotropy. *Magn. Reson. Med.* 36, 893–906.

Qiu, M. H., Chen, M. C., Wu, J., Nelson, D., and Lu, J. (2016). Deep brain stimulation in the globus pallidus externa promotes sleep. *Neuroscience* 322, 115–120. doi:10.1016/j.neuroscience.2016.02.032.

Reveley, C., Seth, A. K., Pierpaoli, C., Silva, A. C., Yu, D., Saunders, R. C., et al. (2015). Superficial white matter fiber systems impede detection of long-range cortical connections in diffusion MR tractography. *Proc. Natl. Acad. Sci. U. S. A.* 112, E2820–E2828. doi:10.1073/pnas.1418198112.

Saga, Y., Hoshi, E., and Tremblay, L. (2017). Roles of Multiple Globus Pallidus Territories of Monkeys and Humans in Motivation, Cognition and Action: An Anatomical, Physiological and Pathophysiological Review. *Front. Neuroanat.* 11, 30. doi:10.3389/fnana.2017.00030.

Thomas, C., Ye, F. Q., Irfanoglu, M. O., Modi, P., Saleem, K. S., Leopold, D. A., et al. (2014). Anatomical accuracy of brain connections derived from diffusion MRI tractography is inherently limited. *Proc. Natl. Acad. Sci. U. S. A.* 111, 16574–16579. doi:10.1073/pnas.1405672111.

Tremblay, L., Worbe, Y., Thobois, S., Sgambato-Faure, V., and Féger, J. (2015). Selective dysfunction of basal ganglia subterritories: From movement to behavioral disorders. *Mov. Disord. Off. J. Mov. Disord. Soc.* 30, 1155–1170. doi:10.1002/mds.26199.

Van Essen, D. C., Ugurbil, K., Auerbach, E., Barch, D., Behrens, T. E. J., Bucholz, R., et al. (2012). The Human Connectome Project: a data acquisition perspective. *NeuroImage* 62, 2222–2231. doi:10.1016/j.neuroimage.2012.02.018.

Vertes, R. P., Linley, S. B., and Hoover, W. B. (2015). Limbic circuitry of the midline thalamus. *Neurosci. Biobehav. Rev.* 54, 89–107. doi:10.1016/j.neubiorev.2015.01.014.

Xiao, D., Zikopoulos, B., and Barbas, H. (2009). Laminar and modular organization of prefrontal projections to multiple thalamic nuclei. *Neuroscience* 161, 1067–1081. doi:10.1016/j.neuroscience.2009.04.034.

Yelnik, J., Bardinet, E., Dormont, D., Malandain, G., Ourselin, S., Tandé, D., et al. (2007). A three-dimensional, histological and deformable atlas of the human basal ganglia. I. Atlas construction based on immunohistochemical and MRI data. *NeuroImage* 34, 618–638. doi:10.1016/j.neuroimage.2006.09.026.

Zhang, Y., Fan, L., Zhang, Y., Wang, J., Zhu, M., Zhang, Y., et al. (2014). Connectivity-based parcellation of the human posteromedial cortex. *Cereb. Cortex N. Y. N 1991* 24, 719–727. doi:10.1093/cercor/bhs353.

Zhang, Y., Larcher, K. M.-H., Misic, B., and Dagher, A. (2017). Anatomical and functional organization of the human substantia nigra and its connections. *eLife* 6. doi:10.7554/eLife.26653.

Study 4: Characterization of Direct Pallidofugal Connections with Cortex and Thalamus in Humans

Introduction

Arousal and awareness are two defining dimensions of consciousness in clinical neuroscience. As arousal, or wakefulness, pertains to the level of consciousness and is thought to be primarily supported by brainstem nuclei projecting to thalamic and cortical neurons, awareness concerns the content of consciousness and relies on the integrity of the cortex and its subcortical connections (Laureys et al., 2004). Current theories of disorders of consciousness (DOC) highlight the interplay between the thalamus, basal ganglia (BG), and cortex, in particular, the frontal cortex, to explain the mechanisms underlying loss and recovery of consciousness, whereby widespread neuronal death or deafferentation within the system following severe brain injury could result in down-regulation of frontal activity (Giacino et al., 2014; Schiff, 2010). Recent diffusion tensor imaging (DTI) studies have also revealed impaired structural connectivity in the cortico-thalamo-basal ganglia circuits in DOC patients (Lant et al., 2016; Weng et al., 2017).

While traditionally believed to be dedicated solely to the control of motor function, BG is now recognized to partake in a variety of cognitive and emotional processes (Alexander et al., 1986; Haber, 2003; Hazrati and Parent, 1991; Tremblay et al., 2015) as well as in the regulation of arousal and cortical activation (Qiu et al., 2010). Animal studies have offered direct evidence of sleep-wake disturbances following selective lesioning of structures within BG, namely, striatum and external globus pallidus (GPe). Ablating the dorsal striatum caused a reduction in wakefulness; in contrast, lesions of the GPe produced substantial increase in wakefulness and sleep-wake fragmentations

(Qiu et al., 2010). Moreover, deep brain stimulation (DBS) of GPe in rodents has been shown to induce natural sleep (Qiu et al., 2016). Although the striatum has been studied extensively, little attention has been given to the study of GPe, which is the second largest component of the BG and contains the most expansive efferent connections, connecting with not only structures within but also outside of BG, including direct projections to frontal cortex (Chen et al., 2015; Saunders et al., 2015) and thalamus (Chattopadhyaya and Pal, 2004; Hazrati and Parent, 1991; Mastro et al., 2014). The direct GABAergic output from GPe to the frontal cortex may be a pathway important for promoting sleep (Vetrivelan et al., 2010). On the other hand, promoting wakefulness may require the GPe to be inhibited by the dorsal striatum to lift GPe's suppression on frontal cortex (Vetrivelan et al., 2010). In the context of DOC after severe brain injury, reduced excitatory input from the frontal cortex and central thalamus to the striatum may yield a loss of active striatal inhibition on GPe and thereby allowing excessive inhibition on the frontal cortex, resulting in further decreased activity. This speculation may explain some of the paradoxical increase in arousal and awareness in DOC patients after administering the sedative, zolpidem. The direct GPe-frontal pathway has been identified in animals but not yet in humans. Moreover, direct connections between GPe and the thalamus have also been previously described in animal models but not in humans, and the functions of these pallido-thalamic pathways remain largely unknown. Verification of these direct GPe pathways in humans could thus potentially help shed light on the mechanism of arousal in the framework of DOC.

In this study, we aim to elucidate the pattern of "direct" GPe connectivity with the cortex and thalamus while employing the internal globus pallidus (GPi) as a control for

comparison. High angular resolution diffusion imaging (HARDI) data from the Human Connectome Project (HCP) were used to carry out the connectivity analyses. HARDI offers a main advantage over diffusion tensor imaging (DTI) by its ability to resolve intra-voxel fiber heterogeneity and may therefore, provide higher spatial and angular resolution (Tuch et al., 2002).

Methods

Data

We analyzed HARDI data provided by the HCP (Q3 Release), WU-Minn Consortium (http://www.humanconnectome.org) (Van Essen et al., 2012). 50 healthy subjects (26 females; 24 males; ages 22-35 years old) were included in the analysis. Imaging data were acquired on a modified 3T Siemens Skyra scanner. T1-weighted structural (TR = 2400 ms; TE = 2.14 ms; flip angle = 8°; FOV = 224x224 mm; voxel size = 0.7mm isotropic) and diffusion-weighted HARDI (TR = 5520 ms; TE = 89.5 ms; flip angle = 78°; FOV = 210x180 mm; voxel size = 1.25 mm isotropic; 3 shells of b = 1000, 2000, and 3000 s/mm^2 with 90 diffusion directions per shell) data were used. Basic diffusion preprocessing steps have been applied which included B0 image intensity normalization, EPI distortions correction, eddy current correction, motion correction, gradient-nonlinearities correction, and registration of diffusion data with structural (Glasser et al., 2013). Preprocessing was accomplished using FSL tools (http://fsl.fmrib.ox.ac.uk).

Regions of interest (ROIs).

For cortical and thalamic ROIs, segmented FreeSurfer labels supplied by HCP were used (http://surfer.nmr.mgh.harvard.edu). To create the five distinct cortical zones

(prefrontal [PFC], sensorimotor [SMC], posterior parietal [PPC], temporal [TEM], and occipital [OCC]), selected Desikan-Killiany atlas labels were combined together (See supplemental materials) (Desikan et al., 2006). Since many of the BG ROIs were not available through FreeSurfer, GPe, GPi, striatum (STR), substantia nigra (SN), and subthalamic nucleus (STN) masks were obtained from the standard (Keuken and Forstmann, 2015)probabilistic BG atlas and transformed into individual diffusion space. To refine the GPe and GPi masks, we used the individual whole pallidum FreeSurfer masks as a constraint to define the boundaries.

Probabilistic tractography

All imaging analyses were accomplished using FSL tools. First, the probability distribution function of fiber orientations at each voxel was estimated with the following parameters: 3 fibres per voxel, 1000 burn-ins, deconvolution model using zeppelins, and gradient nonlinearities considered. Next, probabilistic tractography was launched with 5000 samples drawn per voxel from each seed mask. For pallidocortical and pallidothalamic connectivity analysis, GPe and GPi each served as a seed mask with each of the five cortical targets and thalamus (THAL) as a waypoint mask, per hemisphere. A contralateral hemispheric mask was also included as an exclusion criterion to limit the connections ipsilaterally. This procedure generated ipsilateral pallidocortical and pallidothalalmic connections, though indirect connections arising from other nearby structures were also considered. For ease of referencing, we will refer to the results of this step as “indirect and direct” connections (IDC). To preclude the influence of indirect connections, we repeated probabilistic tractography with additional exclusion criteria, whereby streamlines entering any of the following masks were

discarded: the remainder of BG (STR, SN, STN, and GPe or GPi) and cortical ROIs, thalamus, brainstem, cerebellum, as well as the contralateral hemisphere. The results from this analysis will be referred to as “direct connections” (DC) only. As a final analysis to more precisely visualize the different subregions within thalamus that GPe and GPi may be directly connected with, the thalamus also served as a seed with GPe and GPi as targets, following similar exclusion criteria. Next, the number of streamlines (i.e. connectivity strengths) that successfully reached the cortical and thalamic targets from the pallidal seeds were computed after applying a threshold of 50 (1% of 5000 samples per voxel) (Zhang et al., 2014) to remove spurious connections for both IDC and DC. The results were then normalized and rescaled to account for individual differences in seed and target sizes (Eickhoff et al., 2010). Individual streamline counts were divided by the total number of samples sent (5000 x seed mask size) and then rescaled by multiplying by the average of all total number of samples sent across all seeds and targets. This step accounted for differences in seed sizes. Next, the resulting values were then divided by the size of the targets and then again multiplied by the average size of all targets. This accounted for the variability in target sizes. For display of the tractograms, a threshold of 0.01% of the total number of streamlines sent was applied with an additional threshold of least 10% of subjects sharing the tracks. Segmentation of the thalamus based on differential pallidal connectivity was achieved through a winner-take-all approach on the normalized average group connectivity.

Statistical analysis

Repeated-measures ANOVAs of normalized and rescaled pallidal connectivity values were carried out for IDC and DC with seed (GPe, GPi), target (PFC, SMC, PPC,

TEM, OCC, THAL), and hemisphere (left, right) as within-group factors. Upon finding significance, pairwise t-tests comparing GPe and GPi connections were performed along with multiple comparisons correction using the (Benjamini and Hochberg, 1995) method with false discovery rate = .05. The new significance cutoff value was established at $p < .02$. Moreover, percent change of total streamline counts from IDC to DC was calculated.

Results

Assessing pallidocortical and pallidothalamic connectivity strengths

The total number of streamlines (normalized and rescaled) that successfully reached the cortical and thalamic targets from the pallidal seeds for both IDC and DC are plotted in Fig. 1. Statistical results are reported below:

1. IDC: Significant main effects of seed ($F = 109.063$, $p < .0001$) and target ($F = 153.47$, $p < .0001$), as well as significant interactions of hemi. × seed × target ($F = 7.7$, $p < .01$), hemi. × seed ($F = 11.2$, $p < .01$), and seed × target ($F = 46.9$, $p < .0001$) were observed. Comparing GPe and GPi connectivity, post-hoc t-tests uncovered significantly higher connections for bilateral GPe-PFC, left GPe-THAL and GPe-TEM than GPi with these targets.

2. DC: Significant main effects of seed ($F = 59.6$, $p < .0001$), target ($F = 106.5$, $p < .0001$), and hemi. ($F = 15$, $p < .001$), along with significant interactions of hemi. × seed × target ($F = 15.8$, $p < .0001$), hemi. × seed ($F = 34.5$, $p<.0001$), hemi. × target ($F = 18.9$, $p < .0001$), and seed × target (51.7, $p < .0001$) were detected. Post-hoc comparisons revealed significantly greater connections for bilateral GPe-PFC and GPe-THAL, left GPe-SMC, GPe-PPC, and GPe-TEM than GPi with these targets.

Overall, while the general pattern of DC remained roughly the same as IDC after introducing comprehensive exclusion criteria to minimize the influence of indirect connections, the direct connectivity values reduced drastically, with up to 96% decrease from IDC to DC, with GPi appearing to suffer more than GPe for the most of the connections (Fig. 1). We evaluated relative residual direct connectivity strength by separating the total streamline counts (tSC) into 3 categories: high (tSC > 10,000), medium (5,000 – 10,000 tSC), and low (tSC < 5,000) probability of connection. THAL, SMC, and PPC all exhibited medium to high probability of direct connections with GPe and GPi, but only GPe, not GPi, demonstrated a high likelihood of direct connection with PFC. Additional low direct connectivities were noted for pallidal connections with TEM and OCC regions.

Topographical organization of GPe and GPi connections

Since our primary interest lies in direct connections, the descriptions hereafter will pertain only to DC. Group pallidal projections to the different cortical and thalamic targets as well as corresponding pallidal seed voxels with robust target connectivity are displayed in Fig. 2. Similar topographical connectivity patterns were identified for GPe and GPi, with the exception of PFC and THAL connections. While GPe-PFC connections covered the entire prefrontal target and originated from pallidal voxels concentrated mostly in the anterior subregion of GPe, GPi-PFC connections mainly projected to the posterior border of PFC (presumably, association motor cortices) and localized within the posterior subregion of GPi. Similar subregions of the GPe (anterior and a small posterior cluster) and GPi (posterior) corresponded to strong connections with THAL. Furthermore, SMC, PPC, TEM, and OCC connections resided primarily in

posterior portions of GPe and GPi. Given the difficulty of dissociating preferential targeting in the thalamus from individual pallidothalamic tracks, connectivity-based segmentation of THAL with respect to GPe and GPi revealed distinct patterns of disparate pallidal organization within thalamus (Fig. 3). Namely, GPe connections occupied more medial aspects of thalamus, predominantly including putative midline, mediodorsal (MD), intralaminar (IL), and ventral anterior (VA) nuclei, with the highest concentration in the central medial intralaminar nucleus (CeM); GPi connections, on the other hand, were found in more lateral and posterior portions of thalamus, reflecting primarily ventral lateral (VL), ventral posterior lateral (VPL), ventral posterior medial (VPM), lateral posterior (LP), pulvinar (PUL), as well as some IL nuclei, with peak connections in VL motor thalamus. While both pallidal connections within THAL covered intralaminar nuclei, comparatively, GPe was more connected with central lateral (CL), central medial (CeM), and parafasicular (pf) nuclei, and GPi with centromedian (CM).

Discussion

We used probabilistic tractography with comprehensive a priori exclusion criteria to characterize the pattern of direct pallidal connectivity with the cortex and thalamus. Direct connections between GPe and prefrontal cortex as well as thalamus have been previously established in animals (Chattopadhyaya and Pal, 2004; Chen et al., 2015; Hazrati and Parent, 1991; Mastro et al., 2014; Saunders et al., 2015). Our results not only confirmed the existence of these connections in humans, but also revealed additional probable direct pallidocortical connections. Furthermore, we uncovered varying patterns of prefrontal and thalamic connectivity between GPe and GPi.

The pattern of prefrontal connectivity with GPe differed from that of the control region, GPi. A strong, widespread coverage of GPe tracks into the PFC contrasted with the weak GPi tracks that were restricted to the posterior border of PFC (presumably, a partial association motor area). These pallido-PFC tracks also originated from different subregions of the pallidum, with anterior GPe corresponding to GPe-PFC projections, and posterior GPi representing GPi-PFC connections. Anterior GPe has been shown to connect with the prefrontal cortex (François et al., 2004; Grabli et al., 2004), whereas the posterior portion of GPi has been well established as a sensorimotor region (Visser-Vandewalle et al., 2009). While the strong, direct GPe-PFC would still survive a more stringent thresholding, the weak, direct GPi-PFC connectivity would most likely fail. The direct GPe-PFC connections are validated against animal tracer studies and are thus likely to exist, but direct GPi-PFC connections may be more limited and if present, perhaps, exclusive to sensorimotor regions. The functional role of the direct GPe-PFC pathway though cannot be clearly discerned from the current methodology.

Findings from animal studies have suggested that GPe may be involved in regulating sleep-wake (SW) behavior and cortical activity (Qiu et al., 2010, 2016; Vetrivelan et al., 2010). GPe lesions in rodents produced a 45% increase in wakefulness and significant slowing of cortical EEG (Qiu et al., 2010). DBS in GPe has been shown to directly promote sleep (Qiu et al., 2016). GPi lesions, however, did not significantly change SW activity. Considering the GABAergic nature of GPe, it has been proposed that GPe may directly suppress frontal cortex to promote sleep in the presence of dopamine binding to D2 receptors in the dorsal striatum to disinhibit the GPe (Vetrivelan et al., 2010). In the absence of D2 receptor activation, dorsal striatum

exerts inhibition on GPe, thereby promoting wakefulness. Lesioning of the dorsal striatum, not surprisingly, has been associated with a reduction in wakefulness.

In addition to the direct pathway from GPe to frontal cortex, a direct connection between GPe and thalamus may also have important implications in disorders of consciousness. The mesocircuit hypothesis of DOC posits that following structural damages, functional disruptions at the BG-THAL level may also occur, leading to a reduced excitation of the anterior forebrain (Schiff, 2010). Thalamo-prefrontal connections have been advocated to be necessary for sustaining organized behavior during wakefulness (Schiff, 2008) and consistently implicated in DOC (Laureys et al., 2000; Monti et al., 2015; Zheng et al., 2017). However, the current hypothesis fails to factor GPe into the model and attributes the reduced cortical excitation to the undertaking of the GPi through its excessive inhibition supposedly on the central thalamic nuclei (intralaminar complex and adjacent paralaminar portion of association nuclei—MD, VA, VL, and PUL) following insufficient inhibition from the striatum. According to our knowledge, no study to date has provided direct evidence indicating that GPi may be the pallidal structure responsible for the down-regulation of frontal activity. In fact, due to the difficulty of separating the pallidum into internal and external parts from limited resolution, studies investigating DOC have only reported the globus pallidus as whole to be involved. For example, DOC patients, compared to controls, showed reduced metabolisms in the striatum and central thalamus yet increased metabolism in the globus pallidus (Fridman et al., 2014). Moreover, Lutkenhoff and colleagues found arousal to be negatively correlated with atrophy in the dorsal striatum and globus pallidus in DOC patients (Lutkenhoff et al., 2015), and in another study,

identified globus pallidus shape changes to correlate with the Perturbational Complexity Index (PCI) (Lutkenhoff et al., in prep). A study examining proposal-induced loss of consciousness revealed effective connectivity between the globus pallidus and the posterior cingulate cortex to covary with the changing states of consciousness (Crone et al., 2017). These observations emphasize a critical role of the globus pallidus in supporting consciousness and do not preclude the possibility that GPe may be a vital contributor.

Nevertheless, our findings offer support for GPe as a potential influencer in the mesocircuitry. The direct connection between GPe and PFC, as shown in our results and prior animal studies, may serve to excessively suppress frontal activity when insufficient inhibitory input from the striatum extends to the GPe. Another indication of GPe being intimately involved with PFC is evident in the pallidal connectivity based segmentation of the thalamus, where GPe displayed a greater preference for medial thalamus, which contains the main prefrontal projecting thalamic nucleus—MD (Klein et al., 2010) and also a part of the central thalamus. Impairment in the mediodorsal nucleus stands as one of the most replicated findings in the DOC literature (Fernández-Espejo et al., 2010; Hannawi et al., 2015; He J.H. et al., 2014; Lutkenhoff et al., 2013, 2015; Monti et al., 2015; Zheng et al., 2017). Furthermore, the strongest thalamic connection with the GPe was detected in the central medial nucleus, a component of the anterior intralaminar complex. Receiving inputs from the brainstem and basal forebrain, the anterior intralaminar and mediodorsal thalamus have been postulated to assume a role in arousal regulation and possibly extending to awareness (Schiff, 2008). We hypothesize that GPe, in the absence of normal striatal inhibition, may also

excessively inhibit the medial thalamus in addition to directly inhibiting the PFC, leading to an amplified suppression of frontal activity. On the other hand, GPi was most connected with ventral lateral nucleus, implying a more motor-related function, consistent with the classic role of GPi. This is additionally reflected in GPi's projections to more motor parts of the frontal cortex.

Administration of zolpidem, a selective GABA-ω1 (a subunit of GABA-A receptor complex) agonist commonly used to treat insomnia, has produced paradoxical effects in DOC patients that have led to increased arousal and cognitive performance (Brefel-Courbon et al., 2007; Chatelle et al., 2014; Clauss et al., 2000; Clauss and Nel, 2006; Shames and Ring, 2008; Whyte et al., 2014). Although the mechanism of action of this paradoxical response is largely unknown, the notion that zolpidem could act on the GABA-A receptors found abundantly in the globus pallidus to shut down its inhibitory output has been considered. Seeing that both GPe and GPi may contain large numbers of GABA-A receptors (Xue et al., 2010), and that differing patterns of frontal and thalamic connectivity exist between the two pallidal structures, we propose that zolpidem's action on GPi may, if detectable, improve more motor-related aspects of behavior, whereas zolpidem's target on GPe may underlie the actual arousal and possibly cognitive increase observed in the DOC patients as GPe has been implicated in arousal regulation and is robustly connected with higher-order cognitive areas. Additional evidence alluding to a greater likelihood of GPe than GPi in contributing to the positive effects of zolpidem stems from findings that collectively demonstrate changes in prefrontal activity following administration of zolpidem in DOC patients who responded to the medication (Brefel-Courbon et al., 2007; Chatelle et al., 2014; Clauss

et al., 2000; Williams et al., 2013). Again, GPe's preferred connections with the PFC directly, and indirectly through the medial thalamus, strengthen our hypothesis. An update to the mesocircuit hypothesis with inclusion of the GPe is thus needed.

We found additional probable direct connections for both pallidal structures with SMC and PPC, although there currently lacks evidence from animal studies to validate these findings. We advise to interpret these results with caution. These pallido-cortical connections originated from the posterior portions of the pallidum, which is consistent with DTI findings in humans from (Draganski et al., 2008), but the authors did not use exclusion criteria to limit indirect connections. However, while quantitatively different, DC (direct connections) versus IDC (indirect + direct connections) may remain qualitatively similar, sharing the same topographical patterns of connectivity.

Using diffusion imaging to infer the existence of connections between regions presents many challenges, especially for determining "direct" connections. Currently, one of the only ways of approaching the delineation of "direct" connections relies on strategically implementing exclusion criteria based on some a priori knowledge. However, the selection of exclusion criteria proves to be difficult and presents a tradeoff. On the one hand, not adding enough exclusions may still be subjected to the influence of indirect connections, but on the other hand, including too many exclusions may be overly stringent and lead to false negatives. Because our primary goal was to demonstrate the existence of "direct" connections, we opted for extensive exclusion criteria, albeit overly stringent, in hopes of removing as much of the indirect connections as possible. Though there could still exist some indirect connections in our "direct" connectivity results, the majority of which are likely addressed. On a general note, the

inability to differentiate afferent and efferent connections remains a major limitation of diffusion tractography, although animal tracer studies suggest an output pathway from GPe to PFC and potentially bi-directional connections between GPe and thalamus.

Conclusion

We demonstrated with probabilistic tractography using HARDI data provided by the HCP that direct GPe connections with PFC and THAL are likely to exist in humans, concurrent with animal tracer studies. These direct GPe connections also exhibited differing patterns of frontal and thalamic connectivity when compared against GPi. Favoring connections with distributed prefrontal cortex and medial thalamus, GPe is situated in a position to influence key aspects of consciousness. Conversely, GPi, preferring connections with more motor-related regions, remains a central player in the regulation of motor control. The current findings urge for an update to the mesocircuit hypothesis with the incorporation of GPe to shed light on the mechanisms underlying disorders of consciousness.

Figures

Figure 1. Pallido-cortical and pallido-thalamic connectivity strengths

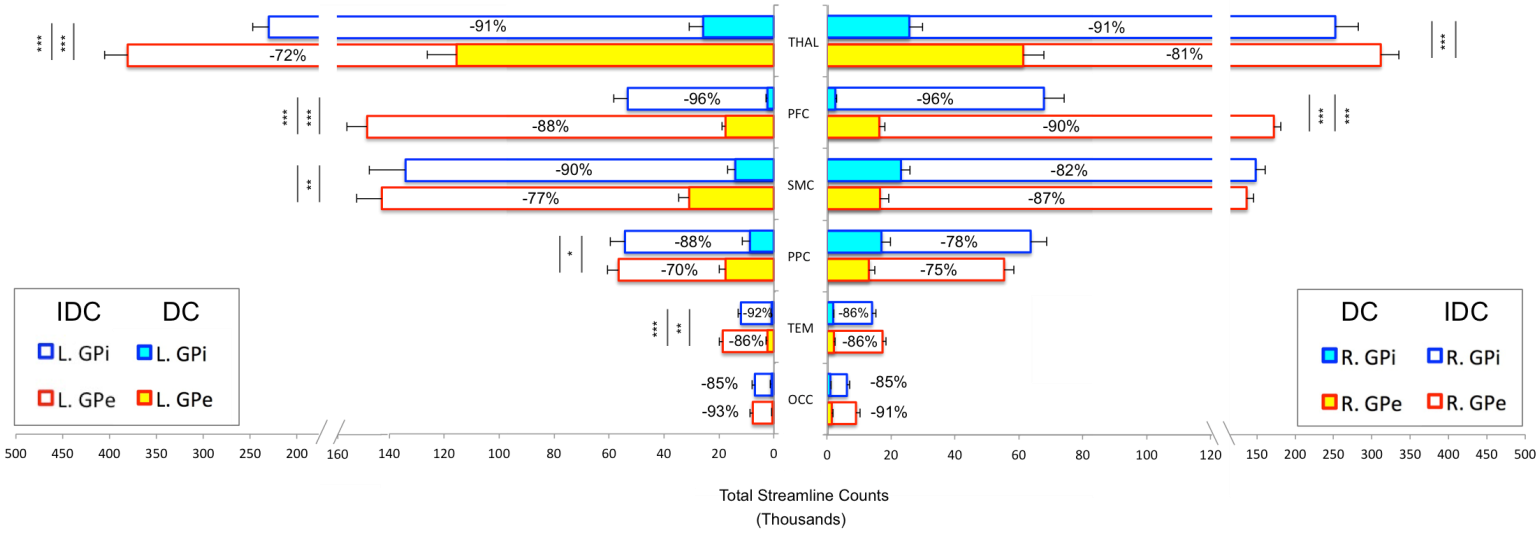

Connectivity strengths as assessed by the group averages of total streamline counts between each seed and target ROI (normalized and rescaled) are plotted. DC (direct connections) and IDC (indirect and direct connections) are overlapped to reflect a percent decrease going from IDC to DC. GPe and GPi connections are statistically compared, with significance denoted using inner asterisks to correspond to DC and outer asterisks to IDC.

Figure 2. Topographical patterns of direct pallidal connectivity

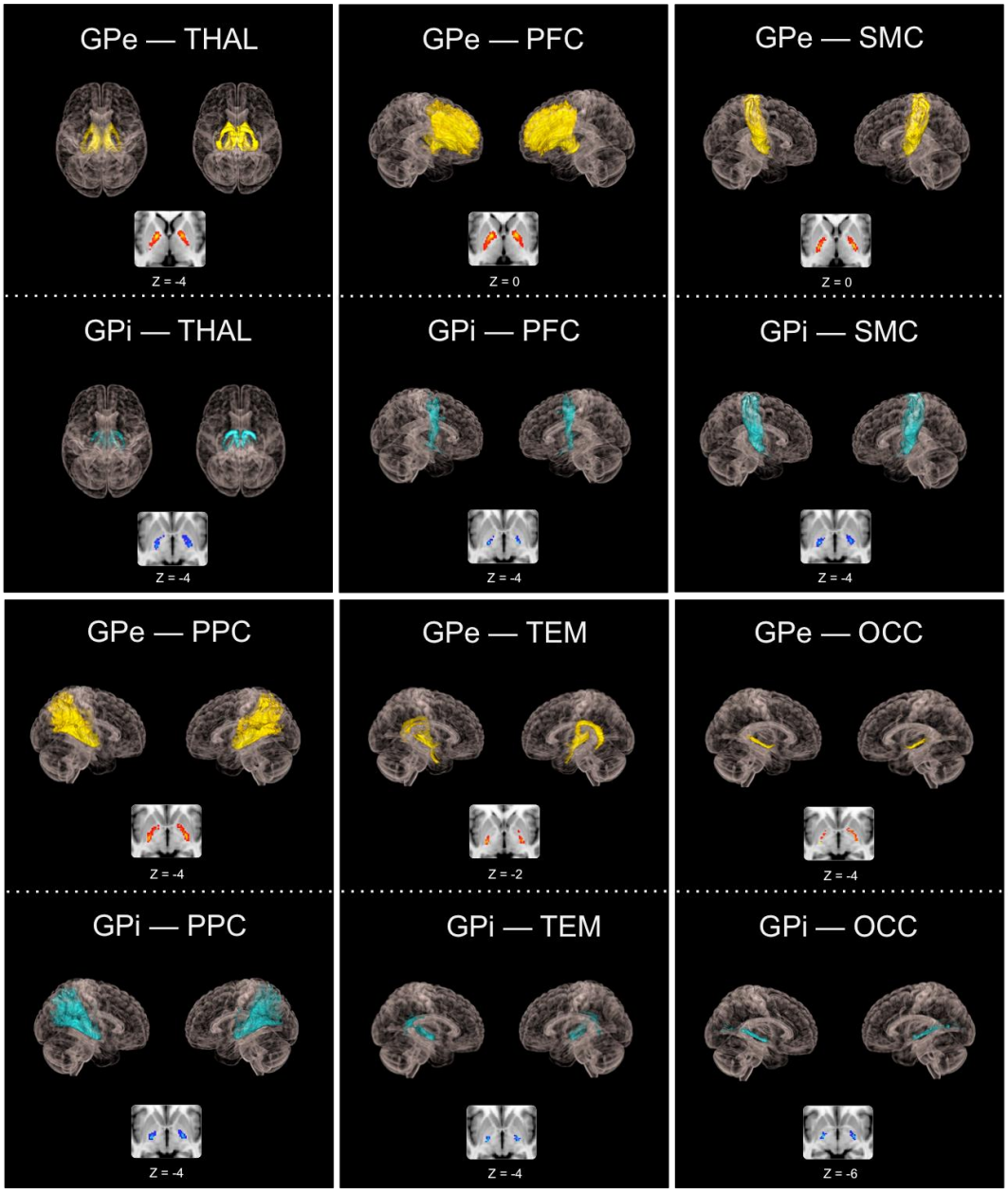

Top sections show reconstructed pallidal pathways, and cropped axial images below reflect preferred subregional connectivity originating from GPe or GPi.

Figure 3. Segmentation of thalamus based on connectivity with GPe and GPi

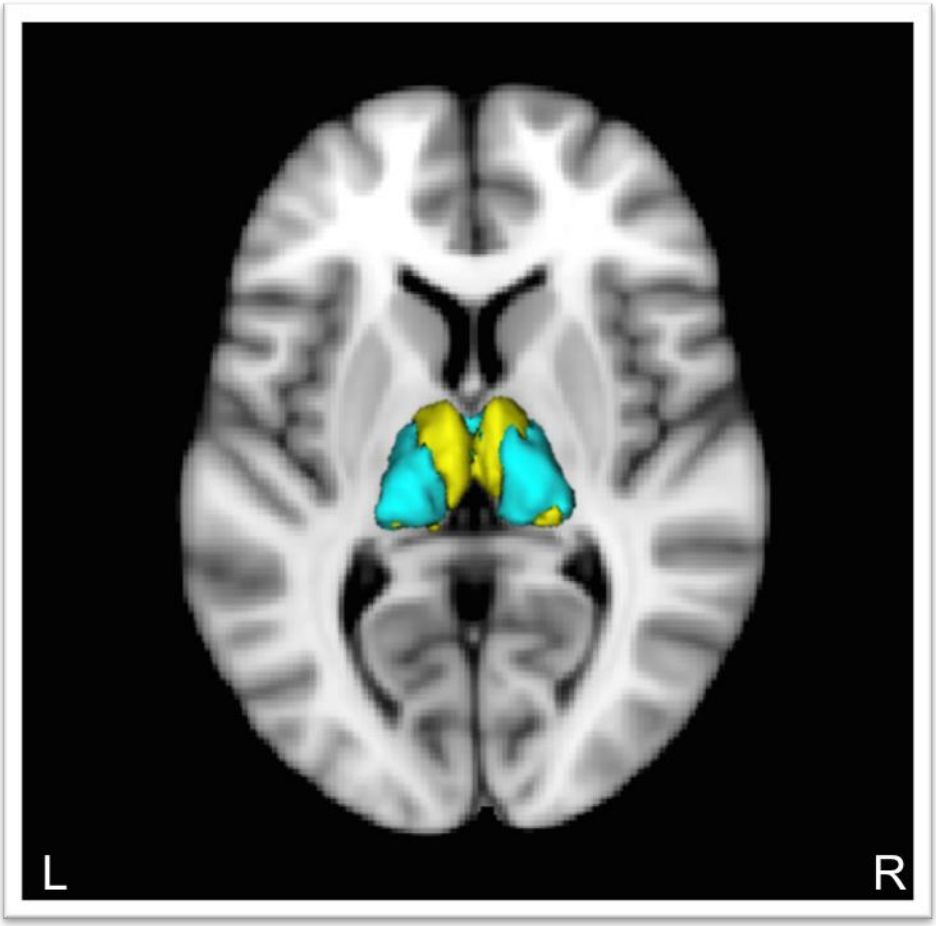

Yellow = GPe connections within thalamus. Blue = GPi connections within thalamus

References

Alexander, G. E., DeLong, M. R., and Strick, P. L. (1986). Parallel organization of functionally segregated circuits linking basal ganglia and cortex. *Annu. Rev. Neurosci.* 9, 357–381. doi:10.1146/annurev.ne.09.030186.002041.

Benjamini, Y., and Hochberg, Y. (1995). Controlling the False Discovery Rate: A Practical and Powerful Approach to Multiple Testing. *J. R. Stat. Soc. Ser. B Methodol.* 57, 289–300. doi:10.2307/2346101.

Brefel-Courbon, C., Payoux, P., Ory, F., Sommet, A., Slaoui, T., Raboyeau, G., et al. (2007). Clinical and imaging evidence of zolpidem effect in hypoxic encephalopathy. *Ann. Neurol.* 62, 102–105. doi:10.1002/ana.21110.

Chatelle, C., Thibaut, A., Gosseries, O., Bruno, M.-A., Demertzi, A., Bernard, C., et al. (2014). Changes in cerebral metabolism in patients with a minimally conscious state responding to zolpidem. *Front. Hum. Neurosci.* 8. doi:10.3389/fnhum.2014.00917.

Chattopadhyaya, R., and Pal, A. (2004). Improved model of a LexA repressor dimer bound to recA operator. *J. Biomol. Struct. Dyn.* 21, 681–689. doi:10.1080/07391102.2004.10506959.

Chen, M. C., Ferrari, L., Sacchet, M. D., Foland-Ross, L. C., Qiu, M.-H., Gotlib, I. H., et al. (2015). Identification of a direct GABAergic pallidocortical pathway in rodents. *Eur. J. Neurosci.* 41, 748–759. doi:10.1111/ejn.12822.

Clauss, R., and Nel, W. (2006). Drug induced arousal from the permanent vegetative state. *NeuroRehabilitation* 21, 23–28.

Clauss, R. P., Güldenpfennig, W. M., Nel, H. W., Sathekge, M. M., and Venkannagari, R. R. (2000). Extraordinary arousal from semi-comatose state on zolpidem. A case report. *South Afr. Med. J. Suid-Afr. Tydskr. Vir Geneeskd.* 90, 68–72.

Crone, J. S., Lutkenhoff, E. S., Bio, B. J., Laureys, S., and Monti, M. M. (2017). Testing Proposed Neuronal Models of Effective Connectivity Within the Cortico-basal Ganglia-thalamo-cortical Loop During Loss of Consciousness. *Cereb. Cortex N. Y. N 1991* 27, 2727–2738. doi:10.1093/cercor/bhw112.

Desikan, R. S., Ségonne, F., Fischl, B., Quinn, B. T., Dickerson, B. C., Blacker, D., et al. (2006). An automated labeling system for subdividing the human cerebral cortex on MRI scans into gyral based regions of interest. *NeuroImage* 31, 968–980. doi:10.1016/j.neuroimage.2006.01.021.

Draganski, B., Kherif, F., Klöppel, S., Cook, P. A., Alexander, D. C., Parker, G. J. M., et al. (2008). Evidence for segregated and integrative connectivity patterns in the human Basal Ganglia. *J. Neurosci. Off. J. Soc. Neurosci.* 28, 7143–7152. doi:10.1523/JNEUROSCI.1486-08.2008.

Eickhoff, S. B., Jbabdi, S., Caspers, S., Laird, A. R., Fox, P. T., Zilles, K., et al. (2010). Anatomical and functional connectivity of cytoarchitectonic areas within the human parietal operculum. *J. Neurosci. Off. J. Soc. Neurosci.* 30, 6409–6421. doi:10.1523/JNEUROSCI.5664-09.2010.

Fernández-Espejo, D., Junque, C., Bernabeu, M., Roig-Rovira, T., Vendrell, P., and Mercader, J. M. (2010). Reductions of thalamic volume and regional shape changes in the vegetative and the minimally conscious states. *J. Neurotrauma* 27, 1187–1193. doi:10.1089/neu.2010.1297.

François, C., Grabli, D., McCairn, K., Jan, C., Karachi, C., Hirsch, E.-C., et al. (2004). Behavioural disorders induced by external globus pallidus dysfunction in primates II. Anatomical study. *Brain J. Neurol.* 127, 2055–2070. doi:10.1093/brain/awh239.

Fridman, E. A., Beattie, B. J., Broft, A., Laureys, S., and Schiff, N. D. (2014). Regional cerebral metabolic patterns demonstrate the role of anterior forebrain mesocircuit dysfunction in the severely injured brain. *Proc. Natl. Acad. Sci.* 111, 6473–6478. doi:10.1073/pnas.1320969111.

Giacino, J. T., Fins, J. J., Laureys, S., and Schiff, N. D. (2014). Disorders of consciousness after acquired brain injury: the state of the science. *Nat. Rev. Neurol.* 10, 99–114. doi:10.1038/nrneurol.2013.279.

Glasser, M. F., Sotiropoulos, S. N., Wilson, J. A., Coalson, T. S., Fischl, B., Andersson, J. L., et al. (2013). The minimal preprocessing pipelines for the Human Connectome Project. *NeuroImage* 80, 105–124. doi:10.1016/j.neuroimage.2013.04.127.

Grabli, D., McCairn, K., Hirsch, E. C., Agid, Y., Féger, J., François, C., et al. (2004). Behavioural disorders induced by external globus pallidus dysfunction in primates: I. Behavioural study. *Brain J. Neurol.* 127, 2039–2054. doi:10.1093/brain/awh220.

Haber, S. N. (2003). The primate basal ganglia: parallel and integrative networks. *J. Chem. Neuroanat.* 26, 317–330.

Hannawi, Y., Lindquist, M. A., Caffo, B. S., Sair, H. I., and Stevens, R. D. (2015). Resting brain activity in disorders of consciousness. *Neurology* 84, 1272–1280. doi:10.1212/WNL.0000000000001404.

Hazrati, L. N., and Parent, A. (1991). Projection from the external pallidum to the reticular thalamic nucleus in the squirrel monkey. *Brain Res.* 550, 142–146.

He J.H., Cui Y., Song M., Yang Y., Dang Y.Y., Jiang T.Z., et al. (2014). Decreased functional connectivity between the mediodorsal thalamus and default mode network in patients with disorders of consciousness. *Acta Neurol. Scand.* 131, 145–151. doi:10.1111/ane.12299.

Keuken, M. C., and Forstmann, B. U. (2015). A probabilistic atlas of the basal ganglia using 7 T MRI. *Data Brief* 4, 577–582. doi:10.1016/j.dib.2015.07.028.

Klein, J. C., Rushworth, M. F. S., Behrens, T. E. J., Mackay, C. E., de Crespigny, A. J., D'Arceuil, H., et al. (2010). Topography of connections between human prefrontal cortex and mediodorsal thalamus studied with diffusion tractography. *Neuroimage* 51, 555–564. doi:10.1016/j.neuroimage.2010.02.062.

Lant, N. D., Gonzalez-Lara, L. E., Owen, A. M., and Fernández-Espejo, D. (2016). Relationship between the anterior forebrain mesocircuit and the default mode network in the structural bases of disorders of consciousness. *NeuroImage Clin.* 10, 27–35. doi:10.1016/j.nicl.2015.11.004.

Laureys, S., Faymonville, M., Luxen, A., Lamy, M., Franck, G., and Maquet, P. (2000). Restoration of thalamocortical connectivity after recovery from persistent vegetative state. *The Lancet* 355, 1790–1791. doi:10.1016/S0140-6736(00)02271-6.

Laureys, S., Owen, A. M., and Schiff, N. D. (2004). Brain function in coma, vegetative state, and related disorders. *Lancet Neurol.* 3, 537–546. doi:10.1016/S1474-4422(04)00852-X.

Lutkenhoff, E. S., Chiang, J., Tshibanda, L., Kamau, E., Kirsch, M., Pickard, J. D., et al. (2015). Thalamic and extrathalamic mechanisms of consciousness after severe brain injury. *Ann. Neurol.* 78, 68–76. doi:10.1002/ana.24423.

Lutkenhoff, E. S., McArthur, D. L., Hua, X., Thompson, P. M., Vespa, P. M., and Monti, M. M. (2013). Thalamic atrophy in antero-medial and dorsal nuclei correlates with six-month outcome after severe brain injury. *NeuroImage Clin.* 3, 396–404. doi:10.1016/j.nicl.2013.09.010.

Mastro, K. J., Bouchard, R. S., Holt, H. A. K., and Gittis, A. H. (2014). Transgenic mouse lines subdivide external segment of the globus pallidus (GPe) neurons and reveal distinct GPe output pathways. *J. Neurosci. Off. J. Soc. Neurosci.* 34, 2087–2099. doi:10.1523/JNEUROSCI.4646-13.2014.

Monti, M. M., Rosenberg, M., Finoia, P., Kamau, E., Pickard, J. D., and Owen, A. M. (2015). Thalamo-frontal connectivity mediates top-down cognitive functions in disorders of consciousness. *Neurology* 84, 167–173. doi:10.1212/WNL.0000000000001123.

Qiu, M. H., Chen, M. C., Wu, J., Nelson, D., and Lu, J. (2016). Deep brain stimulation in the globus pallidus externa promotes sleep. *Neuroscience* 322, 115–120. doi:10.1016/j.neuroscience.2016.02.032.

Qiu, M.-H., Vetrivelan, R., Fuller, P. M., and Lu, J. (2010). Basal ganglia control of sleep-wake behavior and cortical activation. *Eur. J. Neurosci.* 31, 499–507. doi:10.1111/j.1460-9568.2009.07062.x.

Saunders, A., Oldenburg, I. A., Berezovskii, V. K., Johnson, C. A., Kingery, N. D., Elliott, H. L., et al. (2015). A direct GABAergic output from the basal ganglia to frontal cortex. *Nature* 521, 85–89. doi:10.1038/nature14179.

Schiff, N. D. (2008). Central thalamic contributions to arousal regulation and neurological disorders of consciousness. *Ann. N. Y. Acad. Sci.* 1129, 105–118. doi:10.1196/annals.1417.029.

Schiff, N. D. (2010). Recovery of consciousness after brain injury: a mesocircuit hypothesis. *Trends Neurosci.* 33, 1–9. doi:10.1016/j.tins.2009.11.002.

Shames, J. L., and Ring, H. (2008). Transient reversal of anoxic brain injury-related minimally conscious state after zolpidem administration: a case report. *Arch. Phys. Med. Rehabil.* 89, 386–388. doi:10.1016/j.apmr.2007.08.137.

Tremblay, L., Worbe, Y., Thobois, S., Sgambato-Faure, V., and Féger, J. (2015). Selective dysfunction of basal ganglia subterritories: From movement to behavioral disorders. *Mov. Disord. Off. J. Mov. Disord. Soc.* 30, 1155–1170. doi:10.1002/mds.26199.

Tuch, D. S., Reese, T. G., Wiegell, M. R., Makris, N., Belliveau, J. W., and Wedeen, V. J. (2002). High angular resolution diffusion imaging reveals intravoxel white matter fiber heterogeneity. *Magn. Reson. Med.* 48, 577–582. doi:10.1002/mrm.10268.

Van Essen, D. C., Ugurbil, K., Auerbach, E., Barch, D., Behrens, T. E. J., Bucholz, R., et al. (2012). The Human Connectome Project: a data acquisition perspective. *NeuroImage* 62, 2222–2231. doi:10.1016/j.neuroimage.2012.02.018.

Vetrivelan, R., Qiu, M.-H., Chang, C., and Lu, J. (2010). Role of Basal Ganglia in sleep-wake regulation: neural circuitry and clinical significance. *Front. Neuroanat.* 4, 145. doi:10.3389/fnana.2010.00145.

Visser-Vandewalle, V., Temel, Y., and Ackermans, L. (2009). “Chapter 46 - Deep Brain Stimulation in Tourette’s Syndrome,” in *Neuromodulation*, eds. E. S. Krames, P. H. Peckham, and A. R. Rezai (San Diego: Academic Press), 579–586. doi:10.1016/B978-0-12-374248-3.00047-1.

Weng, L., Xie, Q., Zhao, L., Zhang, R., Ma, Q., Wang, J., et al. (2017). Abnormal structural connectivity between the basal ganglia, thalamus, and frontal cortex in patients with disorders of consciousness. *Cortex* 90, 71–87. doi:10.1016/j.cortex.2017.02.011.

Whyte, J., Rajan, R., Rosenbaum, A., Katz, D., Kalmar, K., Seel, R., et al. (2014). Zolpidem and restoration of consciousness. *Am. J. Phys. Med. Rehabil.* 93, 101–113. doi:10.1097/PHM.0000000000000069.

Williams, S. T., Conte, M. M., Goldfine, A. M., Noirhomme, Q., Gosseries, O., Thonnard, M., et al. (2013). Common resting brain dynamics indicate a possible mechanism underlying zolpidem response in severe brain injury. *eLife* 2, e01157. doi:10.7554/eLife.01157.

Xue, Y., Han, X.-H., and Chen, L. (2010). Effects of Pharmacological Block of GABAA Receptors on Pallidal Neurons in Normal and Parkinsonian State. *Front. Cell. Neurosci.* 4. doi:10.3389/neuro.03.002.2010.

Zhang, Y., Fan, L., Zhang, Y., Wang, J., Zhu, M., Zhang, Y., et al. (2014). Connectivity-based parcellation of the human posteromedial cortex. *Cereb. Cortex N. Y. N 1991* 24, 719–727. doi:10.1093/cercor/bhs353.

Zheng, Z. S., Reggente, N., Lutkenhoff, E., Owen, A. M., and Monti, M. M. (2017). Disentangling disorders of consciousness: Insights from diffusion tensor imaging and machine learning. *Hum. Brain Mapp.* 38, 431–443. doi:10.1002/hbm.23370.

Conclusions

This dissertation has investigated the mechanisms underlying disorders of consciousness (DOC) through exploring anatomical connectivity in clinical and healthy populations. In Study 1, we disentangled the varying states of consciousness impairment (VS, MCS-, and MCS+) by comparing univariate differences in their thalamo-cortical connectivity and revealed that the relative preservation of this system can generally account for the gradations of consciousness in DOC patients, with the exception of a paradoxical increase in thalamo-occipital connectivity in patients on the lower end of the consciousness spectrum compared to the higher end. Replicating and expanding upon Study 1, Study 2 introduced the EMCS group and additionally examined connections between the thalamus and basal ganglia in a separate cohort of patients. Again, a paradoxical increase in thalamo-occipital connectivity was observed in patients who were “less” conscious comparatively. The replication of this paradoxical finding may underscore the brain’s compensatory or recovery mechanism occurring in the spared occipital cortex following severe brain injury to higher-order cortices such as fronto-temporo-parietal regions. Moreover, increased thalamo-prefrontal connectivity in patients on the higher spectrum compared to the lower end was also replicated in Study 2, with a greater thalamo-striatal connectivity in EMCS compared to VS being further demonstrated. Prefrontal cortex and striatum both showed preferential connections with nuclei of the central thalamus, which has been consistently found to be selectively damaged in DOC and the extent of damage grades with the severity of outcome. In line with the mesocircuit hypothesis, these three regions likely form a shared circuitry and play important roles in the loss and recovery of consciousness.

In the second parts of Study 1 and 2, multivariate classification using a searchlight approach was implemented to distinguish among patients based on their whole-brain thalamic tractography patterns. In Study 1, pairwise 2-way classifications were carried out for VS, MCS-, and MCS+ to corroborate some of the univariate findings along with uncovering the most discriminative features in differentiating the patient groups. High classification accuracies in distributed thalamo-cortical networks were identified, with emphasis on thalamic connections with fronto-parietal and sensorimotor regions, all of which are common findings in DOC that may reflect impairments in areas proposed to be necessary for maintaining conscious behavior and for responding to behavioral stimulation to demonstrate residual awareness, respectively. High accuracies were also noted in the lateral occipital cortex (LOC), further supporting a possible role of thalamo-occipital connections in helping to differentiate patient groups. In Study 2, similar distributed networks were observed in the automatic 4-way classification of VS, MCS-, MCS+, and EMCS, with the addition of the cerebellum, which may highlight the differences in motor functioning across the patient groups.

Study 3 and 4 were dedicated to addressing the limitations of the mesocircuit hypothesis by introducing a new component, the external globus pallidus (GPe), to the model. First, we demonstrated that GPe is not just a homogenous motor relay structure and can be subdivided into an anteroventral, anterodorsal, and posterior zone, corresponding to limbic, associative, and sensorimotor functions, respectively. Then, in Study 4, we characterized the pattern of direct GPe connections with the cortex and thalamus using GPi as a control. Direct GPe connections outside of the basal ganglia have been previously shown in animals, but not yet in humans. Our results not only

confirmed the existence of direct GPe connections with prefrontal cortex and thalamus in humans, but also unveiled differential patterns of connectivity with these regions when compared against GPi. GPe showed robust connections with the whole prefrontal target and the medial aspect of thalamus, which contains nuclei of the central thalamus. GPi, on the other hand, was more restricted to motor-related cortical and thalamic regions. Our current understanding of the mesocircuit model that attributes the marked decrease in frontal activity after severe brain injury to the undertaking of the GPi may be inaccurate. Given the preferred connections, GPi may be more suited in influencing motor aspects of behavior, whereas GPe may additionally partake in non-motor related functions such as arousal regulation and cognition. Following severe brain injury and consequent lack of inhibition from the striatum, the GPe may be free to exert its inhibitory action directly on the prefrontal cortex and central thalamus, leading to a compounded reduction in anterior forebrain activity. Based on these findings, an update to the existing mesocircuit model is proposed (Figure 1).

Taken together, this dissertation has facilitated our understanding of the mechanisms underlying DOC through direct assessment of anatomical connectivity differences in the patient population and indirect inferences from the revelation of novel connectivity patterns in healthy participants. Future research should test the updated mesocircuit model using brain modulation techniques to verify the specific functions of the newly identified GPe pathways.

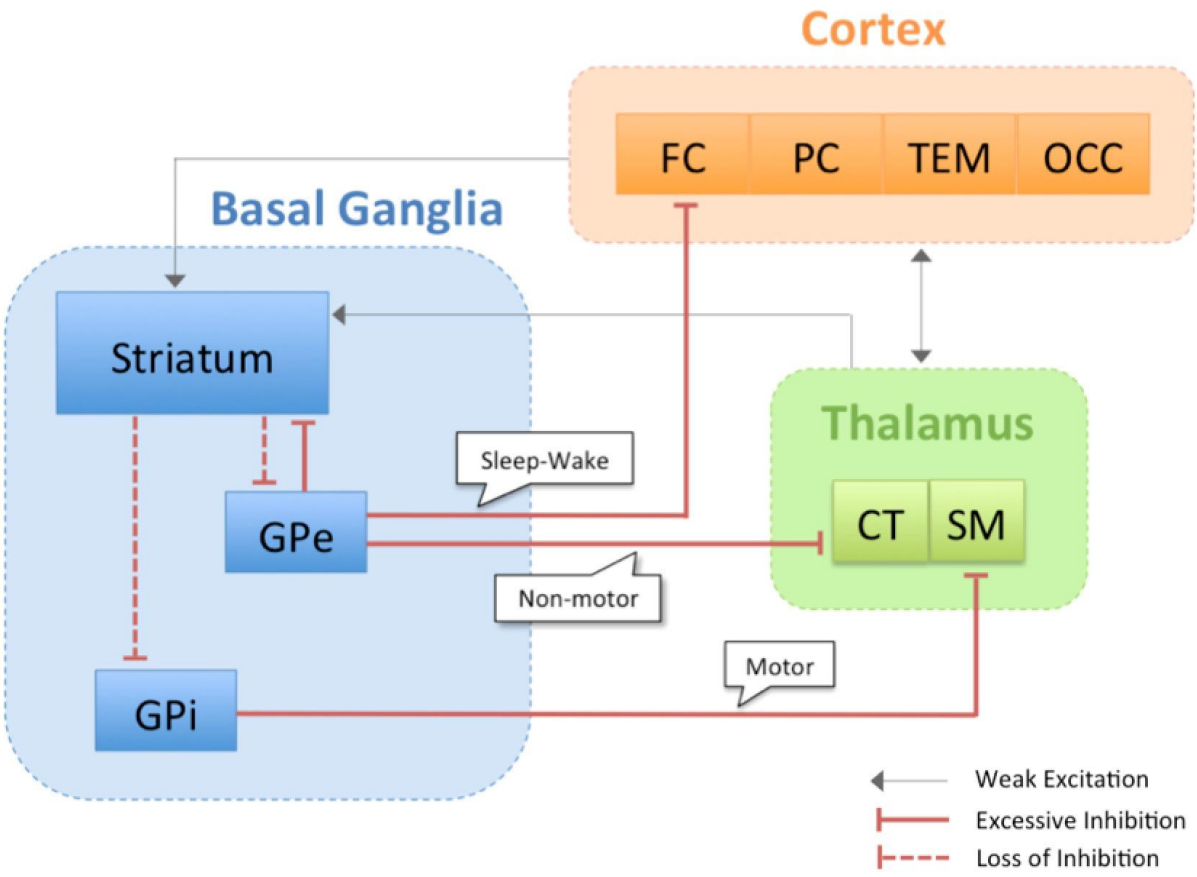

Figure 1. Updated mesocircuit model. GPe is incorporated into the updated model showing its direct connections and proposed functions with the frontal cortex and central thalamus. Abbreviations: CT = Central Thalamus; SM = Sensorimotor Thalamus; FC = Frontal Cortex; PC = Parietal Cortex; TEM = Temporal Cortex; OCC = Occipital Cortex